THE JOURNAL
OF
CHEMICAL PHYSICS

VOLUME 10 FEBRUARY, 1942 NUMBER 2

Raman Spectra of Compounds in the Gaseous and Liquid States*

J. RUD NIELSEN AND NEWTON E. WARD†
Department of Physics, University of Oklahoma, Norman, Oklahoma

(Received November 3, 1941)

An apparatus for exciting the Raman spectra of gases and liquids at temperatures up to 300°C is described. For phosphorus trichloride, methyl chloride, methyl bromide, methyl alcohol, methylene chloride, methylene bromide, chloroform, and carbon tetrachloride, the Raman spectra of the gas and the liquid at the same temperature have been photographed in juxtaposition with a liquid-prism spectrograph of speed f : 2.9 and linear dispersion 27A/mm at 4400A. The Raman spectra of gaseous *n*-pentane, *n*-hexane, and deuterium oxide have been photographed with 2537A excitation. The change in the Raman frequencies with the state of aggregation is different for different vibrations and varies greatly from compound to compound. In the absence of an adequate theory for this phenomenon, a search has been made for empirical regularities. The perpendicular bands of the symmetrical-top molecules are much less diffuse in the liquid than in the gas, showing that the intermolecular forces are effective in quenching the rotation of the molecules in the liquid. The other bands are about equally sharp in gas and liquid.

INTRODUCTION

LESS than one-half percent of the papers published on the Raman effect have reported observations on substances in the gaseous state. This is to be regretted, since the present theory of Raman spectra is strictly applicable only to free molecules. While data on compounds in the gaseous state are more difficult to obtain than data for liquids, they are of greater value. For some purposes, e.g., for testing Placzek and Teller's theory of the rotational structure of Raman bands,[1] data for the gaseous state are absolutely essential. In the present paper an apparatus for observing the Raman spectra of compounds in the gaseous and liquid states is described, and results are given for several compounds.

EXPERIMENTAL

The apparatus devised is shown schematically in Fig. 1. A Raman tube of the type used for vapors is shown in position, and a Raman tube for liquids is shown to the right of the figure. The tubes were mounted vertically in such a way that they could be interchanged without disturbing the alignment with the spectrograph. Each tube had a plane window at the upper end and a light trap at the bottom, and the necessary provisions

* This work was supported by grants to the senior author from the Penrose Fund of the American Philosophical Society and from the Faculty Research Fund of the University of Oklahoma.

† Present address: Magnolia Petroleum Company, Dallas, Texas. The present paper is based largely upon a thesis presented by Newton E. Ward to the faculty of the Graduate School of the University of Oklahoma in partial fulfillment of the requirements for the degree of Doctor of Philosophy.

[1] G. Placzek and E. Teller, Zeits. f. Physik **81**, 209 (1933); E. Teller, *Hand- und Jahrbuch der Chemishen Physik*, Vol. 9, II.

were made for preventing light from reaching the ends of the tubes. The effective length of the vapor tubes was 18 cm. The Raman tubes used for liquids were somewhat shorter and were constructed in such a manner that the surface of the liquid was above the plane window through which the scattered light was observed.

The Raman tubes were surrounded by a double-walled Pyrex tube and were heated to the desired temperature by hot air circulated by a centrifugal pump, the air entering at the top to keep the window free from condensed vapor. To reduce the temperature drop along the Raman tube, the space between the walls of the furnace tube was evacuated to below 10^{-4} mm of mercury. The top of the furnace tube was closed with a plane glass window held in place by a closely fitting brass cap. The temperatures of the air entering and leaving the furnace tube were read on the thermometers T_1 and T_2. From these temperatures it was possible, after securing the requisite data, to compute the temperatures at the ends of the Raman tube. The apparatus is suitable for temperatures up to 300°C and can be used also for very low temperatures.

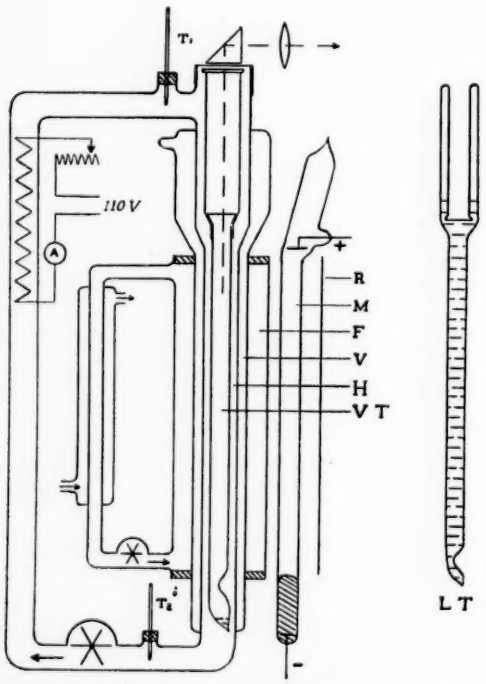

FIG. 1. Apparatus for observing the Raman spectra of vapors and liquids excited by Hg 4358A.
VT—Raman tube for vapors; *H*—hot air space; *V*—vacuum jacket; *F*—filter jacket; *M*—mercury lamp; *R*—reflector; T_1, T_2—thermometers; *LT*—Raman tube for liquids.

A Pyrex filter jacket surrounded the furnace tube. The filter was a solution of 100 g of *p*-nitrotoluene and 0.10 g of rhodamine 5 GDN Extra‡ in one liter of ethyl alcohol, as suggested by Edsall and Wilson.[2] In a thickness of 5 mm this filter transmits about 70 percent of the 4358A line but only a trace of 4047A. The filter decomposed slowly under the action of the light and had to be renewed every 15 or 20 hours.

Six symmetrically arranged mercury lamps surrounded by a six-section elliptical reflector of polished aluminum provided the irradiation. The lamps were made of Pyrex and had tungsten spiral anodes. The Raman spectra were photographed with a liquid-prism spectrograph built by the senior writer. When a camera lens of speed $f:2.9$ is used this instrument has a linear dispersion of 27A/mm at 4400A.

In most cases the Raman spectra of the vapor and of the liquid at the same temperature and pressure were photographed in juxtaposition through slightly overlapping holes in a Hartmann diaphragm. In this way any difference in frequency or intensity distribution between the two spectra is readily observed. The slit width was usually 0.05 mm. Agfa Super Plenachrome Press cut films were used. The exposure time ranged from 12 to 36 hours for the vapors and from 5 to 30 minutes for the liquids. Except for methyl chloride and methylene chloride, which were of a grade used for refrigeration, the purest commercially obtainable chemicals were used. With the exception of the volatile methyl chloride, which was placed directly into the Raman tube, all materials were redistilled before being distilled into the Raman tube under vacuum.

RESULTS

Results of varying degree of completeness have been obtained for phosphorus trichloride, methyl chloride, methyl bromide, methylene chloride, methylene bromide, chloroform, carbon tetrachloride, methyl alcohol, *n*-pentane, *n*-hexane, and deuterium oxide. Figure 2 shows a repro-

‡ This dye was presented to us by E. I. du Pont de Nemours and Company.

[2] J. T. Edsall and E. B. Wilson, J. Chem. Phys. **6**, 124 (1938).

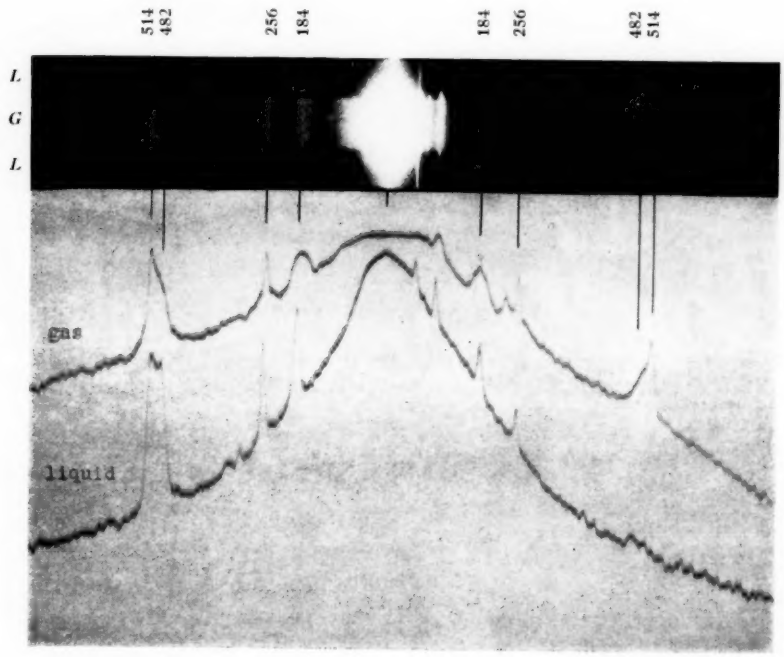

FIG. 2. Raman spectra of gaseous and liquid phosphorus trichloride.

duction of one of the films obtained with phosphorus trichloride together with microphotometer records of the spectra of the gas and the liquid. In Table I are listed the data obtained for the majority of the compounds studied. The pressure of the saturated vapor is given in the second column. In the third column are listed the differences $\Delta\nu$ between the frequencies of the Raman bands of the compound in the gaseous and liquid states. These frequency differences were determined directly from the distance between the adjacent Raman bands for gas and liquid and should be more accurate than values obtained by taking differences between frequencies for the gas and the liquid, measured separately. In the sixth column are given the Raman frequencies ν_l observed for the compound in the liquid state at a temperature roughly equal to the average temperature of the vapor during its exposure and at a pressure a little higher than that listed in column 2. Only such Raman bands are included in column 6 which were observed also for the vapor. Each value of $\Delta\nu$ and ν_l is the average of several independent measurements, all exposures and both Stokesian and anti-Stokesian bands having been considered. The Raman frequencies ν_g for the compound in the gaseous state, obtained by adding $\Delta\nu$ to ν_l, are listed in the fourth column. In columns 5 and 7 are given the visually estimated intensities of the Raman bands for the liquid and the gas as obtained from the most satisfactory exposure. The diffuse character of certain bands is indicated by the symbols *d* or *vd* (very diffuse).

Although four exposures were made with carbon tetrachloride vapor, no entirely satisfactory Raman spectrum was obtained. The Raman bands appeared with less intensity than expected and were partly masked by a continuous background. Within the experimental error $\Delta\nu$ was zero for all the bands. The two bands at 760 and 790 cm^{-1} were broadened to appear as a single diffuse band extending from about 740 to 810 cm^{-1}. In liquid carbon tetrachloride at the same temperature (140°C) these bands were barely resolved. No difference in the intensity distribution for gas and liquid could be observed for the other bands.

The work with *n*-pentane, *n*-hexane, and deuterium oxide was done with 2537A excitation, two Hanovia Sc-2537 lamps being used for irradiation and a medium-sized quartz spectro-

TABLE I. Raman bands of compounds in the gaseous and liquid states.

Compound	Pressure	$\Delta\nu$	ν_g	I_g	ν_l	I_l
PCl_3	5.8 atmos.	−4 cm^{-1}	184 cm^{-1}	8*vd*	188 cm^{-1}	5*d*
		−2	256	10	258	5
		0	482	3*d*	482	3*d*
		3	514	10	511	4
CH_3Cl	6.5	14	726	10	712	5
		10	2968	7	2958	7
CH_3Br	3.2	10	610	10	600	5
		14	2973	5	2959	5
$CHCl_3$	4.0	0	261	2*d*	261	10
		−3	363	3	366	10
		4	672	4	668	10
		0	760	1*vd*	760	6*d*
		0	1217	1	1217	2
		11	3030	1	3019	6
CH_3OH	3.2	0	1032	2*d*	1032	4*d*
		9	2945	4*d*	2836	10*d*
		10	2955	4*d*	2945	10*d*
CH_2Cl_2	3.2	−3	281	5	284	5
		12	712	10	700	10
		12	3002	5	2990	7
CH_2Br_2	3.5	−3	169	10	172	8
		6	584	10	578	10
		0	640	0*d*	640	1*d*
		12	1402	0	1390	2
		18	3008	1	2990	5

graph for photographing the spectra. The frequencies and intensities of the Raman bands obtained in the first exposure of *n*-pentane vapor at 5 atmos. and 124°C are given in Table II, columns 1 and 2. In the third and fourth columns are listed the corresponding data for liquid *n*-pentane at room temperature as given in Landolt-Börnstein, *Physikalisch-chemische Tabellen*. In addition to the Raman bands listed there appeared in the light scattered by the vapor several bands which are evidently due to fluorescence of a product formed by photochemical decomposition of *n*-pentane. The wavelengths and intensities of these bands are given in the last two columns of Table II. In a second exposure with the same Raman tube only the two Raman bands at 2890 and 2940 cm^{-1} appeared, a thin greenish-yellow deposit, which absorbed the 2537A strongly, having formed on the walls of the Raman tube. It may be of interest to mention that the Raman tube did not contain any mercury vapor. Normal hexane vapor, at 150°C and 5 atmos., also decomposed rapidly when illuminated by the Sc-2537 mercury lamps. Only two very diffuse Raman bands, at 2887 and 2947 cm^{-1}, were observed. Six exposures were made with deuterium oxide, but only the previously reported Raman band at 2666 cm^{-1} was observed.[3] The material fluoresced strongly even after prolonged treatment with potassium permanganate.

[3] Cf. D. H. Rank, K. D. Larsen, and E. R. Bordner, J. Chem. Phys. **2**, 464 (1934).

DISCUSSION OF RESULTS

(1) Completeness and Accuracy

All the fundamental Raman bands of phosphorus trichloride and chloroform were observed in the gaseous state. With the vapors of the other compounds, the observed Raman spectra were incomplete. Although a few additional Raman bands could undoubtedly have been observed with longer exposure times, especially for methylene chloride and methylene bromide, it would hardly have been possible to observe as complete Raman spectra for the vapors as for the compounds in the liquid state. This is mainly due to the fact that the Rayleigh scattering is more intense in the gas than in the liquid. Not only do the Rayleigh lines broaden more with long exposure, but more light is scattered in the prisms and lenses, thus increasing the fogging of the film.

The observed differences $\Delta\nu$ between the Raman frequencies for the gaseous and liquid states should be accurate to 1 cm^{-1} or better; in fact, only in one case did the values of $\Delta\nu$ as determined from Stokesian and anti-Stokesian bands differ by more than this amount. On the other hand, because of the inaccuracy in the observed Raman frequencies for the liquids, the frequencies $\nu_g = \nu_l + \Delta\nu$ for the gaseous state have inaccuracies ranging from ±1 cm^{-1} for sharp bands to ±5 cm^{-1} for very diffuse bands, the average inaccuracy being ±1.5 cm^{-1}. Somewhat more accurate values for the ν_g's can be obtained by adding the observed $\Delta\nu$'s to values for ν_l

TABLE II. Raman bands of gaseous and liquid *n*-pentane. Fluorescence band of decomposition product.

ν_g	I_g	ν_l	I_l	Fluorescence Bands λ	I
401 cm^{-1}	1	400	2*d*	2657.0A	1
850	1*vd*	838	5	2668.5	10
		865	4	2674.7	3
1073	0	1073	5*d*	2679.6	6
1142	0	1140	3	2686.0	4
				2691.5	5
1309	1	1300	5	2698.5	3
1455	2*vd*	1438	6*d*	2704.3	4
		1463	6*d*	2709.8	3
				2716.0	1
2890	4*vd*	2873	12	2744.9	4
		2906	8		
2940	10*vd*	2936	10*d*		
		2962	8		

TABLE III. Depression of vibration frequencies in liquid state.

Compound	$\Delta\nu$ in cm^{-1}									Dipole moment $\times 10^{18}$
	$\Delta\nu_1$		$\Delta\nu_3$		$\Delta\nu_2$		$\Delta\nu_4$			
CH_4	(5)		(0)		—		—			0
CCl_4	0		0		0		0			0
	$\Delta\nu_1\|\|$	$\Delta\nu_2\perp$	$\Delta\nu_3\|\|$		$\Delta\nu_4\perp$	$\Delta\nu_5\|\|$	$\Delta\nu_6\perp$			
CH_3Cl	10	(9)	14		(11)	(−2)	(7)			1.86
CH_3Br	14	—	10		—	—	—			1.45
CH_3OH	9, 10	—	—		—	0	—			1.68
$CHCl_3$	4	0	11		0	−3	0			1.05
	$\Delta\nu_1(s)$	$\Delta\nu_1(a)$	$\Delta\nu_2(a)$	$\Delta\nu_2(s)$	$\Delta\delta$	$\Delta\delta_1(s)$	$\Delta\delta_2(s)$	$\Delta\delta_1(a)$	$\Delta\delta_2(a)$	
CH_2Cl_2	12	—	—	12	—	−3	—	—	—	1.51
CH_2Br_2	6	0	—	18	12	−3	—	—	—	1.40

obtained with a spectrograph of greater linear dispersion.

There are few previous results with which to compare the present data. The single Raman frequency 523 cm^{-1} found by Braune and Engelbrecht[4] for gaseous PCl_3 is evidently not accurate. The Raman frequencies 726 and 2968 cm^{-1} for gaseous CH_3Cl and 610 and 2973 cm^{-1} for gaseous CH_3Br are, on the whole, in excellent agreement with the frequencies 732 and 2967 cm^{-1}, 610 and 2973 cm^{-1}, respectively, found by Bennett and Meyer[5] and Barker and Plyler[6] in the infra-red spectra of these vapors. The Raman frequencies 1032, 2845, and 2955 cm^{-1} for CH_3OH vapor agree fairly well with the values 1035, 2842, and 2850 cm^{-1} reported by Kastler.[7] The infra-red absorption spectrum of gaseous methyl alcohol has been investigated by Borden and Barker[8] who found, in part, the frequencies 1034.18, 2845, and 2978 cm^{-1}. The first two of these agree well with the Raman frequencies obtained by Kastler and by the present writers. The frequency 2978 cm^{-1} belongs to another band than 2957 cm^{-1}.

(2) Changes in Raman Frequencies with State of Aggregation

No complete theory exists at present for the effect of intermolecular forces upon molecular vibration frequencies. Breit and Salant[9] have pointed out that there should be three distinct effects: (1) a coupling of the molecules produced by the electric moments induced by the incident radiation field (Lorentz-Lorenz effect), (2) an effect of quantum-mechanical exchange forces between neighboring molecules upon the molecular force constants, and (3) a purely electrostatic effect. Breit and Salant evaluated the Lorentz-Lorenz effect but found that it accounts for only two percent of the frequency difference between gaseous and liquid hydrogen chloride. Cremer and Polanyi[10] found that the exchange effect could explain only ten percent of the frequency change observed for hydrogen chloride. Buchheim[11] estimated the effect of a uniform electric field upon molecular vibrations. Assuming that the large variable fields existing in the immediate neighborhood of molecules will have essentially the same effect as a constant, uniform field, he concluded that in the case of dipole substances the vibration frequencies should be shifted by an amount roughly of the observed order of magnitude and that the Raman bands should suffer a broadening depending upon the concentration of the scattering substance but not upon the temperature. Buchheim could not predict the direction of the shift. His formulas indicate that $\Delta\nu$ may have different signs for different vibrations. Kastler,[7] on the other hand, has given arguments which indicate that $\Delta\nu$ should usually be positive.

[4] H. Braune and G. Engelbrecht, Zeits. f. physik. Chemie **B19**, 303 (1932).
[5] W. H. Bennett and C. F. Meyer, Phys. Rev. **32**, 888 (1928).
[6] E. F. Barker and E. K. Plyler, J. Chem. Phys. **3**, 367 (1935).
[7] A. Kastler, Comptes rendus **194**, 858 (1932).
[8] A. Borden and E. F. Barker, J. Chem. Phys. **6**, 553 (1938).
[9] G. Breit and E. O. Salant, Phys. Rev. **36**, 871 (1930).
[10] E. Cremer and M. Polanyi, *Bodenstein-Festband* of Zeits. f. physik. Chemie (1930), p. 77.
[11] W. Buchheim, Physik. Zeits. **36**, 694 (1935).

Most of the observed vibration frequencies are greater for the gas than for the liquid, i.e., $\Delta\nu$ is predominantly positive. In the absence of an adequate theory, one may search for empirical regularities in the values of $\Delta\nu$ for different vibrational states and for a possible correlation with the dipole moment of the molecule.

For phosphorus trichloride $\Delta\nu$ is positive for one of the totally symmetrical vibrations and negative for the other. For one of the degenerate vibrations $\Delta\nu$ is zero and for the other it is negative. However, all the observed values are rather small, indicating that the molecular interaction is small. This is undoubtedly connected with the fact that the dipole moment is rather small (0.61×10^{-18} for PCl_3 dissolved in CCl_4).[12] The values of $\Delta\nu$ found for the methyl halides are listed in Table III, the symbols designating the various vibrations being those used by Wu.[13] Since methyl alcohol has approximately the same symmetry as CH_3Cl, the data for CH_3OH are included in the table. In order to make the table as complete as possible, two values for methane, obtained by subtracting the Raman frequencies for liquid methane from those for gaseous methane at room temperature,[14] and some values for methyl chloride, obtained by subtracting Raman frequencies for the liquid[15] from infra-red frequencies of the gas,[5] have been added, in parentheses. The dipole moments of the molecules are listed in the last column.

It is seen that $\Delta\nu$ varies from molecule to molecule and has widely different values for different vibrations. For CH_4 and CCl_4, which have no dipole moments, the $\Delta\nu$'s vanish or, at least, are very small. In the case of chloroform, which has a fairly small dipole moment, the average value of the $\Delta\nu$'s is rather low. For the remaining molecules the shifts are larger, but it is not possible to trace any simple dependence of $\Delta\nu$ upon the dipole moment. In fact, whereas $\Delta\nu_3$ is greater for CH_3Cl than for CH_3Br, which has the lower dipole moment, the opposite is true about $\Delta\nu_1$. Some regularity in the values of $\Delta\nu$ for different types of vibration is indicated by Table III. For the molecules of symmetry C_{3v} the totally-symmetrical energy levels $1\nu_1$ and $1\nu_3$ are greatly depressed relative to the ground level in the liquid, and the same is true about the corresponding levels $1\nu_1(s)$ and $1\nu_2(s)$ for the molecules of symmetry C_{2v}. On the other hand, the $1\nu_5$ level lies higher in the liquid than in the gas for the two compounds for which data are obtained. For the methyl derivatives the $1\nu_1$ state is strongly perturbed by the $2\nu_4$ state.[16] However, only for methyl alcohol could both of the levels, $(1\nu_1, 2\nu_4)$, be observed in the Raman spectrum of the gas. As might be expected, they are about equally depressed in the liquid. In the case of chloroform, the shift is zero for all three degenerate vibrations. However, that seems not to be the case for methyl chloride. For both CH_2Cl_2 and CH_2Br_2 $\Delta\delta_1(s)=-3$ cm^{-1}. On the other hand, $\Delta\nu_1(s)$ is greater for the chloride, while $\Delta\nu_2(s)$ is greater for the bromide.

Since no exposures were made of liquid *n*-pentane, less accurate values of the $\Delta\nu$'s have been obtained for this compound. However, a comparison of the observed frequency values for gaseous *n*-pentane at 125° with the frequencies reported for the liquid at room temperature shows that the values of $\Delta\nu$ are very small. This may be expected from the fact that the dipole moment is zero. The incomplete data for *n*-hexane permit no definite conclusions regarding the $\Delta\nu$'s. For deuterium oxide $\Delta\nu$ has the very large value 150 cm^{-1}, and, as in the case of ordinary water, the Raman band is extremely diffuse. These phenomena are undoubtedly connected with the formation of hydrogen bonds.

(3) Intensity Distribution. Quenching of Molecular Rotation in the Liquid State

When the visually estimated intensities of the Raman bands for the gas are compared with those for the liquid, the low frequency bands appear enhanced in the gas. However, this effect is probably an illusion caused by the continuous background which decreases in intensity with increasing distance from the Rayleigh line.

The two Raman bands observed for methyl chloride are slightly wider in the liquid than in

[12] E. Bergmann and L. Engel, Zeits. f. physik. Chemie **B13**, 232 (1931).
[13] Ta-You Wu, *Vibrational Spectra and Structure of Polyatomic Molecules* (Kun-Ming, China, 1939).
[14] Cf. Landolt-Börnstein, *Physikalisch-chemische Tabellen*.
[15] J. Wagner, Zeits. f. physik. Chemie **B40**, 36 (1938).
[16] A. Adel and E. F. Barker, J. Chem. Phys. **2**, 627 (1934).

the gas, in agreement with Buchheim's theoretical prediction[11] and with the findings of other observers.[17] For the other compounds investigated, such an effect could not be verified with certainty.

A striking result of the present investigation is the finding that the bands of phosphorus trichloride and chloroform corresponding to degenerate vibrations are much broader in the gas than in the liquid. The broadening of the 184 cm^{-1} band of PCl_3 in the gaseous state is clearly shown in Fig. 2. The other perpendicular band 482 cm^{-1} is also seen to be broadened. However, the diffuse character of this band in the gas is somewhat obscured by its proximity to the band at 514 cm^{-1} and perhaps also by the presence of an overtone $2\nu_3 \leqq 512$ cm^{-1}. The bands 256 and 514 cm^{-1}, which correspond to parallel, nondegenerate vibrations, seem to be as sharp in the gas as in the liquid.

In the case of chloroform, the perpendicular bands 261 and 760 cm^{-1} are definitely broader in the gas than in the liquid. The third perpendicular band 1217 cm^{-1} is so weak that its diffuse character in the gas could not be ascertained. The three parallel bands of chloroform, on the other hand, are about as sharp in the gas as in the liquid. For methyl chloride, methyl bromide, and methyl alcohol, only parallel bands were observed, and no bands were observed to be broadened in the gaseous state. No broadening was found for methylene chloride and methylene bromide which have only nondegenerate vibrations.

[17] Cf. K. W. F. Kohlrausch, *Der Smekal-Raman Effekt, Ergänzungsband* (Springer, 1938), Chapter V.

The fact that some Raman bands are much narrower in the liquid than in the gaseous state shows that the intermolecular forces in the liquid are effective in quenching the rotation of molecules. Although Bhagavantam[18] has reported that the 2611 cm^{-1} band of hydrogen sulfide is more diffuse in the gas than in the liquid, and Kirby-Smith and Bonner[19] that the perpendicular band, 1460 cm^{-1}, of gaseous methylamine is very diffuse, this quenching effect seems not to have been clearly recognized by previous workers on infra-red and Raman spectra.

The quenching is most readily observed for bands with strong rotational branches, such as the perpendicular bands of symmetrical-top-molecules. The diffuse character of such Raman bands, even in the liquid state, has been used, in the absence of polarization data, to differentiate them from parallel bands.[20] Our results indicate that this can be done with far greater safety when observations of the Raman spectrum for the gaseous state are available.

No accurate intensity measurements were made in the present work. However, Mr. D. K. Coles, in collaboration with the senior author, has recently made quantitative determinations of the intensity distribution in certain Raman bands of cyclopropane. These measurements not only throw further light on the quenching of the molecular rotation in liquids but furnish the first experimental test of Placzek and Teller's theory[1] for the rotational structure of Raman bands.

[18] S. Bhagavantam, Nature **126**, 502 (1930).
[19] J. S. Kirby-Smith and L. G. Bonner, J. Chem. Phys. **7**, 880 (1939).
[20] Cf. A. Langseth and E. Walles, Zeits. f. physik. Chemie **B27**, 214 (1934).

The Infra-Red Absorption Spectra of Ethylene and Tetra-Deutero-Ethylene under High Resolution

W. S. GALLAWAY AND E. F. BARKER
Harrison M. Randall Laboratory of Physics, University of Michigan, Ann Arbor, Michigan
(Received October 10, 1941)

The fine structure of several infra-red absorption bands of C_2H_4 and C_2D_4 have been resolved. From the rotational constants so found, the C−C and C−H distances in this molecule were calculated to be 1.353 and 1.071A, and the H−C−H angle to be 119°55′. An assignment of fundamental frequencies has been made which is consistent with the observed data.

INTRODUCTION

THE infra-red and Raman spectra of ethylene have been the subject of several investigations aiming to determine the molecular dimensions and fundamental frequencies of this molecule. Neither of these goals has been completely attained. From measurements in the photographic infra-red it has been possible to find the rotational constants of C_2H_4. However these do not provide sufficient information to permit the calculation of intermolecular distances without recourse to an estimation of at least one of the dimensions. Similarly, a unique assignment of fundamental frequencies is not possible with the available data.

By investigating the infra-red spectrum of C_2D_4 and re-examining parts of the spectrum of C_2H_4, new data have now been obtained which yield values for all the molecular dimensions, and also give a definite assignment of fundamental frequencies.

EXPERIMENTAL

The light ethylene (C_2H_4) used in these experiments was obtained from the Ohio Chemical Company. No information concerning the purity of the gas was available but only one region of absorption was found to indicate the presence of an impurity.

From a sample of $C_2D_4Br_2$, supplied by J. M. Delfosse from the University of Louvain, the heavy ethylene (C_2D_4) was prepared by a reaction of the ethylene dibromide with zinc in a solution of methyl alcohol. The gaseous yield was swept slowly through the purifying and collecting system by a stream of helium. A water condenser, a bulb containing $CaCl_2$ and one of dehydrite, and a dry ice trap effectively removed all traces of water and alcohol. Two liquid-air traps collected the desired product. No evidence of impurities was observed except for two regions of absorption which may be assigned to a hybrid molecule involving a mixture of deuterium and hydrogen.

Throughout the experiments, a grating spectrometer with a rocksalt foreprism was used. This instrument has been described by Barker and Meyer.[1] The addition of a divided circle on the tangent screw makes it possible to turn the grating by steps of 10 seconds of arc. A recent recalibration of the gratings (reported by Gillette and Eyster[2]) has reduced the absolute errors to the same order of magnitude as the relative errors in locating the line positions, which are about 5 seconds of arc or less. The individual points used for plotting were obtained as the result of several deflections of the galvanometer with and without the gas cell in the beam. The absorption of the NaCl windows has been subtracted. Table I lists the experimental conditions under which the various regions of absorption were studied.

The perpendicular type bands belonging to C_2H_4 at 3.22 and 10.55μ, which were resolved by Levin and Meyer,[3] have been reexamined to obtain the positions of the lines with greater precision so that the spacing, and thus the moment of inertia, could be calculated more certainly. Considerable improvement was gained by using finer gratings, narrower slits, smaller

[1] E. F. Barker and C. F. Meyer, Trans. Faraday Soc. **25**, 912 (1929).
[2] R. H. Gillette and E. H. Eyster, Phys. Rev. **56**, 1113 (1939).
[3] A. Levin and C. F. Meyer, J. Opt. Soc. Am. **16**, 137 (1928).

TABLE I. Experimental conditions used in examining the various regions of absorption.

Gas	Band (μ)	Center (cm^{-1})	Uncertainty (cm^{-1})	Grating (lines per inch)	Interval of reading* (cm^{-1})	Effective slit width (cm^{-1})	Pressure (cm Hg)	Cell length (cm)
C_2H_4	3.22	3105.5	0.2	4800	0.43	1.5	15	6
	3.35	2989.5	0.2	4800	0.22	1.0	15	6
	5.29	1889.6	0.1	4800	0.16	0.63	72	6
	5.66	1766	1.0	2400	0.46	1.5	75	80
	10.05	995	2	2400	0.28, 0.09	0.56	15	6
	10.55	949.20	0.05	2400	0.24, 0.08	0.49	5	6
C_2D_4	2.16	4628.0	0.3	7200	2.10, 0.7	3.2	70	11
	2.23	4478.6	0.9	7200	1.80	2.7	70	11
	2.26	4429.5	0.3	7200	1.80, 0.6	2.7	70	11
	2.59	3862.8	2.2	4800	2.20	2.6	70	11
	2.95	3387.8	0.6	4800	1.70	2.0	70	11
	2.98	3345.3	0.3	4800	1.70, 0.6	2.0	70	11
	3.12	3204.3	1.5	4800	1.5	1.7	70	11
	3.28	3049.0	0.2	4800	1.30, 0.4	1.5	70	11
	4.25	2345	1	4800	0.35	1.2	15	11
	4.54	2200.2	0.1	4800	0.31	0.90	15	11
	6.27	1595.1	0.1	2400	0.75, 0.25	1.05	70	11
	6.68	1495.7	0.1	2400	0.66, 0.22	1.10	35	11
	7.76	1289.1	0.1	2400	0.50, 0.16	0.70	70	11
	9.26	1077.9	0.1	2400	0.10	0.45	12	11
	10.88	919.0	0.1	1200	0.50	1.10	70	11
	13.88	720.00	0.03	2400	0.12	0.48, 0.68	5	11

* Where two values for the interval of readings are reported for the same region, it should be understood that the smaller steps were used only near sharp absorption maxima.

intervals of reading, and a better amplifier. The new results do not disagree seriously with the previous values but are much more consistent. However, due to the increased resolving power, much new detail was found at the longer wave-lengths, where several weak lines were observed between each strong one. In addition, an important band was found for the first time at 10.05μ. It has long been known that an infra-red active fundamental should appear near 1000 cm^{-1}. Therefore, for the double purpose of finding this frequency and obtaining more lines belonging to the observed band at 10.55μ, the region was examined with a higher gas pressure in the cell. Figure 1(e) shows definitely the presence of this new band.

In Fig. 1(a) and (b) the data taken at 3.35 and 5.29μ are plotted, each with well-resolved fine structure. Only the envelopes of these parallel bands were obtained by Levin and Meyer, but Smith[4] has resolved the band at 3.35μ. No atmospheric absorption was encountered except near 5μ, where a few lines due to water vapor were observed. The reported positions of the ethylene lines are quite reliable, though the intensities are not determined so certainly.

The curves for C_2H_4 reported by Coblentz[5] showed a small irregularity near 1725 cm^{-1}. Since a combination band involving the inactive torsional frequency of this molecule might appear here, the region was examined with a cell 80 cm long containing gas at a pressure of one atmosphere. The band shown in Fig. 1(f) was observed at 5.66μ (1766 cm^{-1}) but it must have been due to an impurity, since the line spacing is different from that appropriate to C_2H_4.

The spectrum of C_2D_4 was recorded from 2μ to 16μ with an evacuated prism spectrometer, using a cell 11 cm long containing gas at 70 cm pressure. The many regions of absorption so found were then examined under the conditions given in Table I. The detailed study showed sixteen distinct bands. Those lying above 3000 cm^{-1} were not resolved, due to insufficient dispersion. In this group atmospheric absorption was troublesome only in the neighborhood of the perpendicular type band at 2.59μ, of which even the envelope given in Fig. 2 is somewhat uncertain. The minimum at the center is very

[4] L. G. Smith, J. Chem. Phys. **8**, 798 (1940).

[5] W. W. Coblentz, *Investigations of Infra-Red Spectra*, (Carnegie Institution, 1905), p. 35.

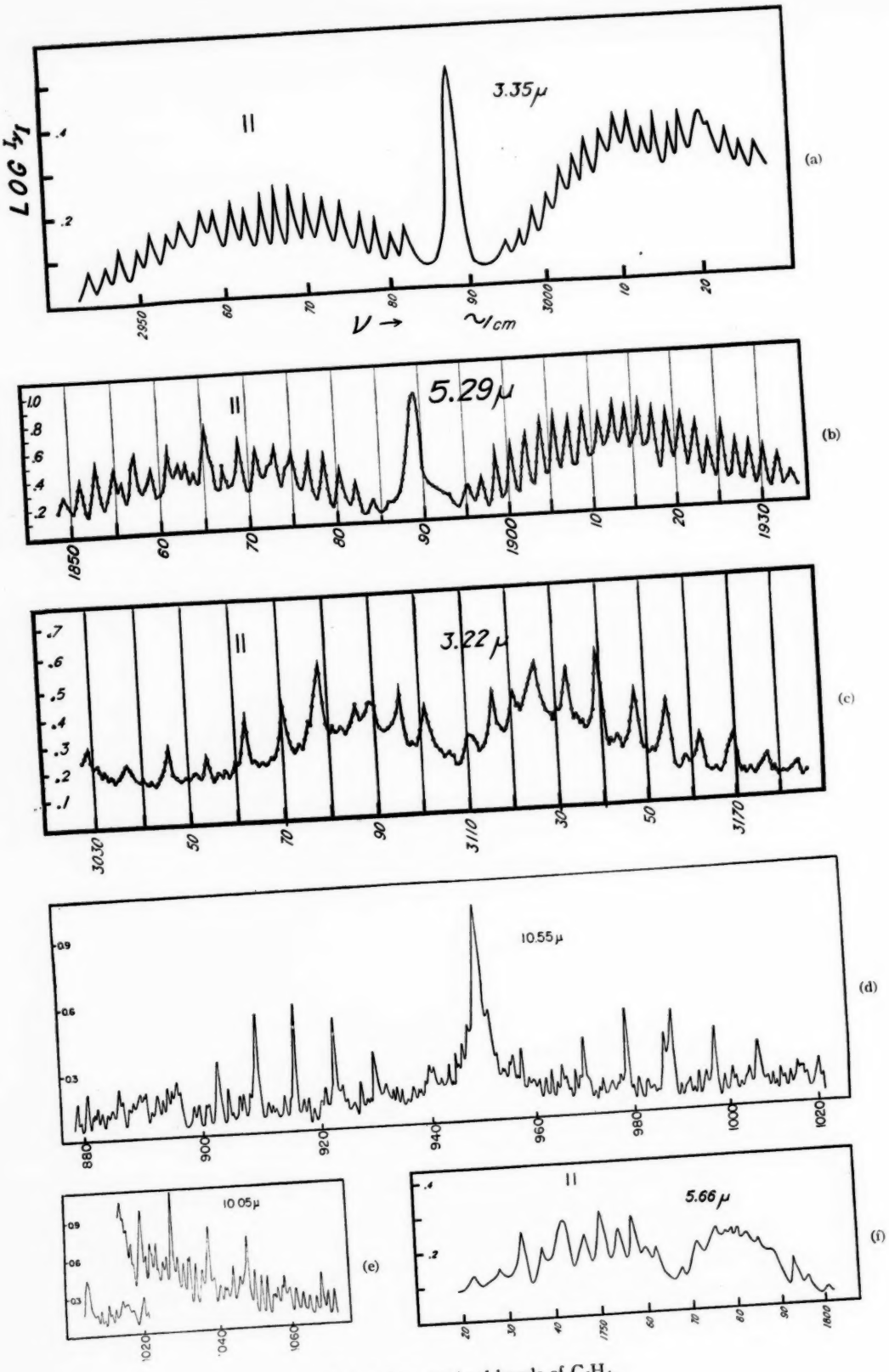

FIG. 1. The resolved bands of C_2H_4.

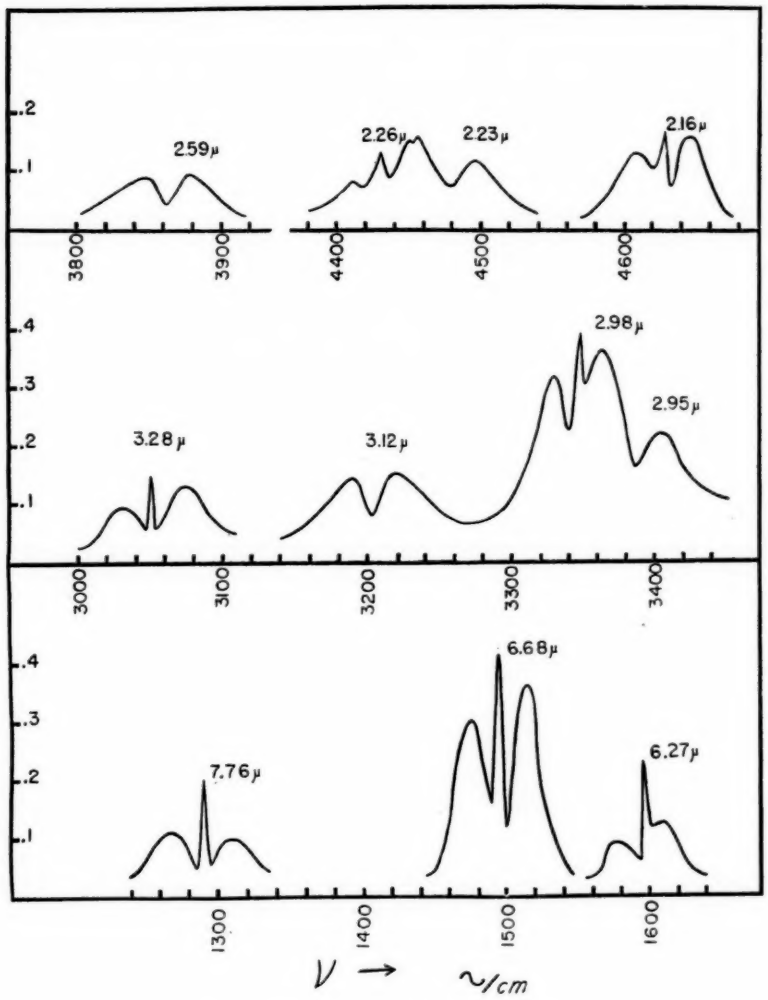

FIG. 2. The unresolved bands of C_2D_4.

reproducible however. It should also be noted that at 2.95 and 3.12μ there was some evidence of lines spaced about 4 cm^{-1} apart, but the variations in absorption were too small to be reliable.

The atmospheric absorption near 6μ prevented resolution of the two bands in this region, though the sharp central maxima were well determined. Figure 3 shows the five bands of C_2D_4 which were resolved. Only those at 9.26 and 10.88μ are in regions where the atmosphere is completely transparent. At 4.25μ the CO_2 absorption is so intense that the few lines shown in Fig. 3(d) are the only ones observable with certainty. It was impossible to locate the band center with the grating instrument, but the record from the evacuated prism spectrometer indicates that it lies 5 cm^{-1} below the center of the CO_2 band. Hence the value 2345 cm^{-1} is obtained. Fortunately the effect of the carbon dioxide is very small at 4.54μ. The parallel band in this position is more clearly resolved and has a more regular spacing than the one at 9.26μ, in spite of the use of relatively wider slits.

The rather complex band at 720.0 cm^{-1} was studied with extreme care, since two fundamentals should occur in this region corresponding to the frequencies 949.2 and 995 cm^{-1} of C_2H_4. Only the stronger one is definitely established, however, though the presence of a weaker band

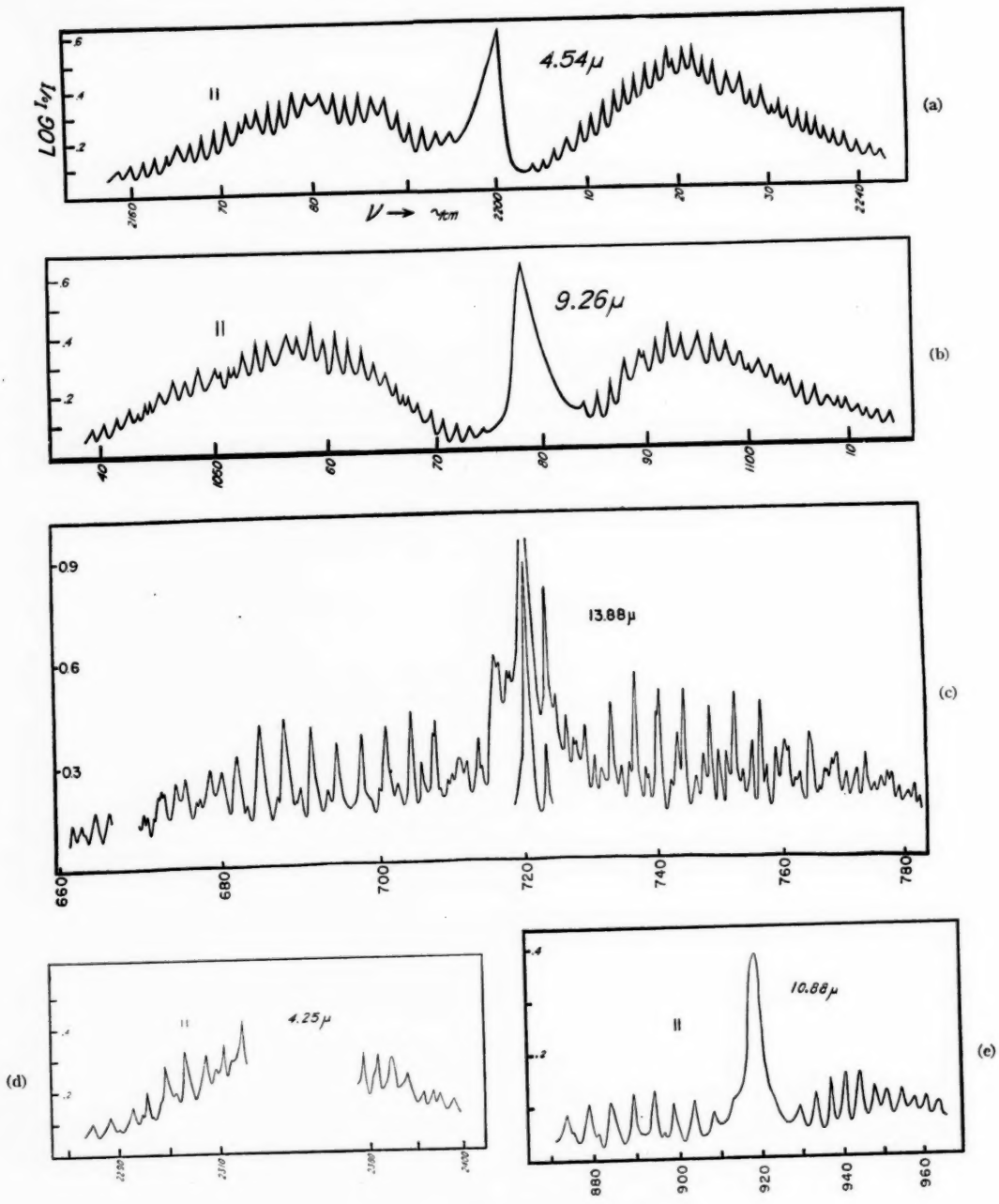

FIG. 3. The resolved bands of C_2D_4.

may account for some of the many observed lines. Here again carbon dioxide in the air caused some difficulty, though the CO_2 band structure is quite coarse. Fortunately none of the strong C_2D_4 lines was superimposed upon those of CO_2 except in a small interval near 668 cm^{-1}.

ASSIGNMENT OF FREQUENCIES

A reasonable assignment of seven of the twelve fundamental frequencies for C_2H_4 has been made by several authors.[6] The remaining five are

[6] A comprehensive bibliography is given by G. B. B. M. Sutherland and G. K. T. Conn, Proc. Roy. Soc. A172, 172 (1939).

ν_7, ν_9, ν_{10}, ν_{11}, and ν_{12} in Dennison's[7] notation. These vibrations are the torsional oscillations of the CH_2 groups. The frequency associated with the motions of these two groups about a common axis containing the carbon nuclei is designated by ν_7. When the axes are perpendicular to the plane of the molecule, the resulting oscillation is called ν_9 or ν_{10} depending on whether the motions of the two groups are in phase or out of phase. The frequencies ν_{11} and ν_{12} correspond to oscillations in and out of phase about axes in the plane of the molecule, and perpendicular to the axis of the carbon atoms. Of these, ν_7 is inactive, while ν_9 and ν_{11} are infra-red active, and ν_{10} and ν_{12} appear in Raman scattering. From data on similar molecules, the last four are known to be in the neighborhood of 1000 cm^{-1} while ν_7 should be somewhat lower. Table II shows the various assignments which have been made.

The frequency ν_{11} is the sole representative of the only group of fundamental vibrations which should yield infra-red bands having a coarse spacing and a central maximum. Since the very strong band at 10.55μ is the only one corresponding to this symmetry, the assignment of the value 949.2 cm^{-1} is very definite. The identification of the Raman line found at 950 cm^{-1} is not so immediate for the reason that it may be due to ν_{10} or ν_{12}. The latter choice is clearly indicated by the existence of a parallel band at 1889.6 cm^{-1}, due to the combination $\nu_{11}+\nu_{12}$. No other interpretation of this band is consistent with the selection rules and Boltzmann factors. The numerical agreement is satisfactory considering the fact that Bonner[8] estimates an uncertainty of 10 cm^{-1} in ν_{12}.

One of the contributions of this investigation was the discovery of a region of absorption at 10.05μ. Unfortunately, as seen by Fig. 1(e), it does not lie completely free of the strong 10.55μ band. The overlapping is just sufficient to prevent a direct observation of the minimum at the center. However, a reasonable assignment of ordinal numbers of the lines may be made by comparison with the band of similar type at 3.22μ. Then, by extrapolation, the center is found to lie at 995 cm^{-1}. Since ν_9 has the proper symmetry and should lie in this region, the correlation is quite convincing.

TABLE II. Various assignments of four of the fundamentals for C_2H_4

Author	Frequency of the fundamental in cm^{-1}			
	ν_9	ν_{10}	ν_{11}	ν_{12}
Mecke (1932)	1100	970	950	940
Teller and Topley (1935)	730	1160	950	1097
Bonner (1936)	950	950	940	1100
Thompson and Linnett (1937)	950	1160	—	—
Mannebach and Verleysen (1937)	950	950	—	—
Sutherland and Conn (1939)	1020	1030	950	943
Gallaway and Barker (1941)	995	1055	949	950

TABLE III. The fundamental frequencies of ethylene.

	C_2H_4	C_2D_4
ν_8	1623.3	1515
ν_2	3019.3	2251
ν_4	1342.4	981
ν_1	2989.5	2200.2
ν_3	1443.9	1077.9
ν_5	3105.5	2345
ν_9	995	740*
ν_6	3069	2304
ν_{10}	1055†	860*
ν_{11}	949.2	720.0
ν_{12}	950	780
ν_7	825‡	585‡

* Calculated from $\nu_9+\nu_{10}=1595$ for C_2D_4.
† Calculated from $\nu_9+\nu_{10}=2047$ for C_2H_4.
‡ Calculated from $2\nu_7=1654$ for C_2H_4 and from Eq. (1g) for C_2D_4.

The parallel band at 2047 cm^{-1} reported by Levin and Meyer can be explained only by a combination of ν_9 and ν_{10}. This bit of data permits us to assign the value of 1055 cm^{-1} to ν_{10}. This frequency has not yet been found in the Raman spectrum.

Various values for the torsional fundamental have previously been given which range from 700 to 850 cm^{-1}. If the small absorption found by Coblentz at 1725 cm^{-1} is taken as real, then ν_7 may be placed at either 670 or 775 depending on whether the band is a combination of ν_7 with ν_{10} or ν_{12}. Eucken and Parts[9] have estimated from specific heat data that this frequency should lie in the region 750–800 cm^{-1}. These authors used slightly different values than are given here for the other frequencies. Burcik, Eyster, and Yost[10] have recently recalculated the specific heat curve using both 700 and 825 cm^{-1} for ν_7 and the remaining fundamentals as here reported. Considerably better agreement is ob-

[7] D. M. Dennison and G. B. B. M. Sutherland, Proc. Roy. Soc. **A148**, 250 (1935).
[8] L. G. Bonner, J. Am. Chem. Soc. **58**, 34 (1936).
[9] A. Eucken and F. Parts, Zeits. f. physik. Chemie **B20**, 184 (1933).
[10] E. J. Burcik, E. H. Eyster, and D. M. Yost, J. Chem. Phys. **9**, 118 (1941).

TABLE IV. Calculated results for Eqs. (1).

Equation	Left Side	Right Side	% Difference
(1a)	1.922	1.988	3.3
(1b)	1.632	1.654	1.3
(1c)	1.820	1.869	2.6
(1d)	1.777	1.869	4.9
(1e)	1.318	1.322	0.3
(1f)	1.218	1.217	0.1

tained with the upper value though it seems slightly high. A convincing argument for a value near 825 cm^{-1} is provided by the observed Raman line at 1654 cm^{-1} which must represent the overtone of the torsional oscillation. No other combination could explain this line, since no other fundamentals have frequencies below 825 cm^{-1}. Combination tones are usually observable in Raman scattering only when accentuated by resonance with a Raman-active fundamental of the same symmetry; hence there must be interaction in this case with ν_8 at 1623 cm^{-1}. Therefore, the motion to which the line at 1654 cm^{-1} is due must be totally symmetric, and if it involves ν_7 at all it must be the harmonic $2\nu_7$, for ν_7 is the only representative of its symmetry class, and could combine in a totally symmetric way with no other fundamental.

In a very similar manner, the fundamentals of C_2D_4 may be determined. It is also possible to estimate the values for the frequencies of the heavier molecule from those of the lighter one by use of an approximate value for the reduced mass. A reasonably accurate check on the data listed in Table III may be obtained from the product rule, which gives the ratio of the products of the normal frequencies in the same symmetry class for the light molecule to the corresponding products for the heavy molecule. According to Sutherland,[6] these relations are

$$\frac{(\omega_2\omega_4\omega_8)_H}{(\omega_2\omega_4\omega_8)_D}=\frac{m_D}{m_H} \tag{1a}$$

$$\frac{(\omega_6\omega_{10})_H}{(\omega_6\omega_{10})_D}=\left(\frac{m_D\mu'_D}{m_H\mu'_H}\right)^{\frac{1}{2}} \tag{1b}$$

$$\frac{(\omega_1\omega_3)_H}{(\omega_1\omega_3)_D}=\left(\frac{m_D\mu_D}{m_H\mu_H}\right)^{\frac{1}{2}} \tag{1c}$$

$$\frac{(\omega_5\omega_9)_H}{(\omega_5\omega_9)_D}=\left(\frac{m_D\mu_D}{m_H\mu_H}\right)^{\frac{1}{2}} \tag{1d}$$

$$\frac{(\omega_{11})_H}{(\omega_{11})_D}=\left(\frac{\mu_D}{\mu_H}\right)^{\frac{1}{2}} \tag{1e}$$

$$\frac{(\omega_{12})_H}{(\omega_{12})_D}=\left(\frac{\mu''_D}{\mu''_H}\right)^{\frac{1}{2}} \tag{1f}$$

$$\frac{(\omega_7)_H}{(\omega_7)_D}=\left(\frac{m_D}{m_H}\right)^{\frac{1}{2}} \tag{1g}$$

where the subscripts H and D refer to hydrogen and deuterium and

$$1/\mu=1/m+2/M$$

$$\frac{1}{\mu'}=\frac{1}{m}+\frac{2}{M}\left(1+\frac{4l^2}{L^2}+\frac{4l}{L}\cos\frac{\theta}{2}\right)$$

$$\frac{1}{\mu''}=\frac{1}{m}+\frac{2}{M}\left(1+\frac{2l}{L}\cos\frac{\theta}{2}\right)^2$$

M = mass of the carbon nucleus
m = mass of the H or D nucleus
l = C−H distance
L = C−C distance
θ = H−C−H angle.

The agreement shown in Table IV is sufficient to insure that the correct assignment of frequencies has been made. The discrepancies lie in the difference between the normal frequencies with infinitesimal amplitudes, designated by ω_i,

TABLE V. The infra-red combination frequencies for ethylene.

Gas	Frequency (cm^{-1})	Assignment	Calculated frequency (cm^{-1})	Observed in both Molecules
C_2H_4	4729.0	$\nu_5+\nu_8$	4729	Yes
	4515.5	$\nu_3+\nu_6$	4513	Yes
	4324.3	$\nu_4+3\nu_9$	4327	Yes
	4207.9	$2\nu_{11}+\nu_9+\nu_4$	4236	No
	2047.0	$\nu_9+\nu_{10}$	2050*	Yes
	1889.6	$\nu_{11}+\nu_{12}$	1899	Yes
C_2D_4	4628.0	$\nu_5+\nu_6$	4654	No
	4478.6	$\nu_1+\nu_6$	4504	No
	4429.5	$\nu_2+3\nu_{11}$	4411	No
	3862.8	$\nu_5+\nu_8$	3860	Yes
	3387.8	$\nu_3+\nu_6$	3382	Yes
	3345.3	$\nu_2+\nu_3$	3329	?
	3204.3	$\nu_4+3\nu_9$	3201	Yes
	3049.0	$\nu_9+\nu_6$	3044	No
	1595.1	$\nu_9+\nu_{10}$	1600†	Yes
	1495.7	$\nu_{11}+\nu_{12}$	1500	Yes

* Used to determine ν_{10} for C_2H_4.
† Used to determine ν_9 and ν_{10} for C_2D_4.

for which the equations were derived, and the fundamentals which were used to calculate the left members. Only a small percent anharmonicity need be assumed to obtain exact agreement in Table IV. The frequency 585 cm^{-1} calculated for ν_7 of C_2D_4 cannot be checked by any available observations. In this case its harmonic does not appear in Raman scattering, since there is no totally symmetric fundamental near 1170 cm^{-1} with which it might interact.

The high resolving power obtainable beyond 10μ made it possible to observe many weak lines between the strong ones shown in Fig. 1(d). The latter group is identified with transitions in which $K=\pm1$ and $J=0$ and the former with $K=\pm1$ and $J=\pm1$. By a trial and error method, one can associate nearly all the observed lines with some transition. However, since the convergence of these weak P and R branches is not known and there is a lack of uniqueness, a definite assignment is not given. The presence of the fundamental at 10.05μ also complicates the short wave-length side of the 10.55μ band. A similar effect in C_2D_4 is observed at 13.88μ where it appears that the less intense band lies even closer to the more intense one. In addition, the strong peak at 723.4 cm^{-1} may be identified with the transition ν_{11} to $2\nu_{11}$.

The assignments for the combination bands given in Table V are probable ones chosen to fit

TABLE VI. The line positions in the parallel type bands of C_2H_4

	The 5.29μ band				The 3.35μ band†		
J	P branch (cm^{-1})	J	R branch (cm^{-1})	J	P branch (cm^{-1})	J	R branch (cm^{-1})
4	1882.10	3	1896.77	4	2982.15	2	2994.81
5	1880.32	4	1898.50	5	2980.38	3	2996.68
6	1878.52	5	1900.28	6	2978.58	4	2998.51
7	1876.71	6	1902.08	7	2976.77	5	3000.61
8	1874.85	7	1903.87	8	2974.41	6	3002.10
9	1872.98	8	1905.55	9	2972.39	7	3003.85
10	1870.79	9	1907.22	10	2970.25	8	3005.60
11	1868.97	10	1908.95	11	2968.37	9	3007.54
12	1867.02	11	1910.87	12	2966.49	10	3009.34
13	1865.18	12	1912.54	13	2964.78	11	3011.19
	1863.80	13	1914.02	14	2962.70	12	3012.77
14	1862.88	14	1915.68	15	2961.16	13	3014.27
	1862.07	15	1917.28	16	2959.25	14	3016.13
15	1860.96	16	1918.92	17	2957.64	15	3017.54
16	1859.00	17	1920.73	18	2955.14		3020.07*
17	1857.09	18	1922.43	19	2953.40	17	3021.18
	1855.57	19	1923.84	20	2951.50	18	3023.31
18	1854.85	20	1925.54	21	2949.73	19	3024.95
19	1852.87	21	1927.12	22	2947.50	20	3026.86
20	1851.05	22	1928.72	23	2945.94		
21	1849.29	23	1930.35	24	2943.72		
		24	1932.13				

Maxima of Q Branches at 1889.23 and 2988.51 cm^{-1}

* $^PQ(11)$ of the 3.22μ perpendicular band of C_2H_4.
† These values are in essential agreement with those recently reported by L. G. Smith, J. Chem. Phys. **8**, 798 (1940).

TABLE VII. The line positions in the perpendicular type bands of C_2H_4.

	The 3.22μ band			The 10.55μ band		
K	P branch (cm^{-1})	R branch (cm^{-1})	K	P branch (cm^{-1})	K	R branch (cm^{-1})
0		3110.38	3	929.74	2	970.13
1	3100.74	3116.00	4	922.63	3	978.83
2	3095.35	3125.66	5	915.63		986.44
3	3085.78	3132.73	6	909.03	4	988.08
4	3078.22	3139.54	7	902.57	5	997.31
5	3069.79	3147.74	8	896.61	6	1006.55
6	3061.32	3155.24		890.81		1014.98
7	3053.27	3162.69	9	890.04	7	1015.92
8	3045.60	3170.36		886.47		1020.22
9	3036.87	3177.52		880.80		
10	3028.78	3184.66		878.89		
11	3020.07*					
	Central minimum at 3170.39 cm^{-1}			Central maximum at 949.85 cm^{-1}		

* Lies in 3.35μ parallel band.

the data from both light and heavy molecules as well as possible. In a few cases other allowed combinations would not be excluded. It is noted immediately that the lower frequencies characteristic of the heavy molecule permit the observation of additional combinations below 5000 cm^{-1}. These are assigned so that the fewest number of frequencies are involved. The combinations $\nu_2+\nu_3$ and $\nu_9+\nu_6$ have not been definitely observed for C_2H_4, although the former may explain a weak peak at 4461 cm^{-1}, observed by Levin and Meyer. The analogue of the doublet combination band at 4207.9 cm^{-1} has not been found in the spectrum of C_2D_4. It may be present but masked by other absorptions.

The two frequencies observed at 919.0 and 1289.1 cm^{-1} which were not included in the above classification are assigned to a hybrid molecule involving a mixture of hydrogen and deuterium. The intensities and positions are such that the bands may be identified as ν_{11} and ν_3 of C_2HD_3. The spacing of the lines in the band at the longer wave-length supports this assignment.

THE MOMENTS OF INERTIA AND MOLECULAR DIMENSIONS

It is well known that the ethylene molecule is very nearly a symmetric top. Hence the rotational energy F may be expressed in the form

$$F=DJ(J+1)+\alpha J^2(J+1)^2 +(C-D)K^2+\beta K^4+\cdots$$

and used to calculate the following relations

TABLE VIII. The line positions in the parallel type bands of C_2D_4.

J	The 4.54μ band P branch (cm^{-1})	R branch (cm^{-1})	J	The 9.26μ band P branch (cm^{-1})	J	R branch (cm^{-1})
2		2203.97	3	1074.59	4	1084.31
3		2205.10	4	1073.37	5	1085.57
4	2195.04	2206.49	5	1072.17	6	1086.85
5	2193.37	2207.91	6	1070.91	7	1088.13
6	2191.86	2209.37	7	1069.75	8	1089.76
7	2190.51	2210.62	8	1068.49		1090.26
8	2189.25	2211.97		1067.60	9	1091.38
9	2187.79	2213.17	9	1067.15	10	1092.56
10	2186.36	2214.28		1066.50	11	1093.78
11	2185.01	2215.42	10	1065.56	12	1095.34
12	2183.60	2216.62	11	1064.41	13	1096.82
13	2182.31	2217.83	12	1063.34	14	1098.24
14	2180.80	2219.01	13	1062.09	15	1099.53
15	2179.24	2219.65	14	1060.90		1100.34
16	2177.84	2220.79	15	1059.85	16	1101.33
17	2176.53	2221.87	16	1058.74	17	1102.50
18	2175.18	2223.05	17	1057.48	18	1103.55
19	2173.89	2224.27	18	1056.31		1104.23
20	2172.78	2225.53	19	1054.60	19	1104.51
21	2171.96	2227.09	20	1053.60	20	1105.72
22	2170.59	2228.17	21	1052.43	21	1106.91
23	2169.38	2229.39		1051.67	22	1108.23
24	2167.99	2230.47	22	1051.16		1109.22
25	2166.76	2231.32		1050.40	23	1110.00
26	2165.46	2232.27	23	1049.90	24	1111.23
27	2164.28	2233.43	24	1048.51	25	1112.11
28	2163.03	2234.40	25	1047.42	26	1113.18
29	2161.84	2235.42	26	1046.30	27	1114.53
30	2160.45	2236.20	27	1045.13		
31	2159.12	2237.34		1044.27		
32		2238.52	28	1043.82		
33		2239.97		1043.22		
34		2241.48	29	1042.68		
35		2242.53	30	1041.61		
			31	1040.51		
			32	1039.51		

Maxima of Q branches at 2200.39 and 1078.10 cm^{-1}.

involving the line positions of the fine structure in the bands.

$$\frac{R(J)-P(J)}{2(2J+1)}=(D'+\tfrac{3}{2}\alpha')+2\alpha'(J+\tfrac{1}{2})^2+\cdots, \quad (2a)$$

$$\frac{R(J-1)-P(J+1)}{2(2J+1)}=(D''+\tfrac{3}{2}\alpha'')+2\alpha''(J+\tfrac{1}{2})^2+\cdots, \quad (2b)$$

$$\frac{{}^RQ(K)-{}^PQ(K)}{4K}=(C'-D'+2\beta')+2\beta'K^2+\cdots, \quad (2c)$$

$$\frac{{}^RQ(K-1)-{}^PQ(K+1)}{4K}=(C''-D''+2\beta'')+2\beta''K^2+\cdots, \quad (2d)$$

$$\frac{R(J-1)+P(J)}{2}=\nu_0+(D'-D''+\alpha'-\alpha'')J^2+\cdots, \quad (2e)$$

$$\frac{{}^RQ(K)+{}^PQ(K)}{2}=\nu_0+(C'-D'+\beta')+(C'-D'-C''+D''+6\beta')K^2+\cdots. \quad (2f)$$

The values of the constants A, B, C and D are

$$A=\frac{h}{8\pi^2cI_a}, \quad B=\frac{h}{8\pi^2cI_b}, \quad C=\frac{h}{8\pi^2cI_c}$$

and

$$D=\frac{A+B}{2}$$

if the frequencies are measured in cm^{-1}, a, b, and c designating the axes of greatest, middle and least moments of inertia. The values of J and K refer to the lower (double primed) state.

It is interesting to note that the positions of the lines in the bands of C_2H_4 fit quite well with the symmetric rotator formulae yet the intensities are definitely those of an asymmetric molecule. Solutions of the Wang equation for the energy levels of an asymmetric top show that, for C_2H_4, Eqs. (2) are correct up to $J=K=20$ within the experimental error. The deviations are greatest for low K and high J. In general, the results indicate that the lines are broadened but not shifted appreciably. Similar calculations for C_2D_4 were not made. However, the greater asymmetry of the heavy molecule would predict a more pronounced broadening of the lines and an observable shift. These conclusions are verified in the parallel bands. The broadening is shown by the fact that the troughs between the lines are filled in thus making resolution difficult. The shift in position is noted when a Fortrat plot is made. A smooth curve could not be drawn except for low J. However, the perpendicular band for C_2D_4 follows the symmetric rotator formula. This is understandable in view of the fact that, while more lines are observed than for the light molecule, the deviations due to asymmetry are smaller for the high K levels.

Since Eqs. (2) may be put into linear form, the data given in Tables VI to IX were fitted by least squares to a straight line. This procedure yielded, for the ground state,

$$D_H=0.9116 \text{ cm}^{-1},$$
$$C_H-D_H=3.955,$$
$$D_D=0.6522,$$
$$C_D-D_D=1.785.$$

In order to estimate the reliability of these values, the coefficients found for the right sides

of Eqs. (2) were used to calculate the left sides. The deviations from the observed results were taken as a measure of the reliability of the above constants. The average deviations were 0.5 percent or less except for D_D. In this case, not only were the deviations larger, but the values found from the two parallel type bands differed by a few percent. A simple average yields 0.6522 cm^{-1}. The remaining results given are averages weighted according to the average deviations, which were of the same order of magnitude as the differences of the values found from different bands.

A check may be made between these constants. From the first two, C_H can be found. Then, since the relation

$$C_H/C_D = m_D/m_H$$

should hold, one may calculate C_D. The value thus obtained for $C_D - D_D$ may then be used to find $D_D = 0.652$ which agrees remarkably well.

The positions of the lines in the resolved bands were also used to determine the band centers. These results are given in Table I. The uncertainties indicated are estimated from the upper limit of the absolute errors in calibration.

Since the ethylene molecule is planar, it follows that

$$I_a = I_b + I_c$$

or

$$1/A = 1/B + 1/C$$

also

$$A = D\left(1 - \frac{D}{2C} + \frac{1\cdot 3\cdot D^3}{2!2^2C^3} - \frac{1\cdot 3\cdot 5D^5}{3!2^3C^5} + \cdots\right)$$

and

$$B = D\left(1 + \frac{D}{2C} - \frac{1\cdot 3\cdot D^3}{2!2^2C^3} + \frac{1\cdot 3\cdot 5D^5}{3!2^3C^5} - \cdots\right).$$

The moments of inertia may now be calculated. For C_2H_4 they are

$$I_a = 33.84\times 10^{-40} \text{ g cm}^2,$$

$$I_b = 28.09,$$

$$I_c = 5.750,$$

and for C_2D_4

$$I_a = 49.41,$$

$$I_b = 37.92,$$

$$I_c = 11.49.$$

From these values, it is found that the C−H and C−C distances are 1.071 and 1.353A ±0.01, respectively, while the H−C−H angle is 119° 55′±30′.

It is a pleasure to acknowledge our indebtedness to Dr. E. H. Eyster for helpful discussion and suggestions.

TABLE IX. The line positions in the perpendicular type bands of C_2D_4.

	The 13.88μ band			The 4.54μ band	
K	P branch (cm^{-1})	K	R branch (cm^{-1})	P branch (cm^{-1})	R branch (cm^{-1})
	715.58		723.38	2285.30	2378.69
2?	713.48	1?	726.26	2289.02	2381.72
3?	710.85	2	728.90	2292.72	2384.57
4	707.58	3	732.92	2295.94	2387.92
5	704.39	4	736.63	2299.67	2391.73
6	701.03	5	740.52	2303.41	2395.17
7	697.81	6	744.43	2307.67	2398.02
8	694.58	7	748.43	2311.35	
9	691.46	8	752.34	2315.16	
10	688.19	9	756.28		
11	685.27	10	760.18		
12	682.22	11	764.27		
	680.09	12	768.68		
13	678.85		769.62		
14	676.28	13	772.05		
	675.38		773.51		
15	673.81	14	776.71		
16	671.02		777.67		
	667.18		781.89		
18	665.58				
	664.20				
19	663.00				

Central maximum at 720.30 cm^{-1}

Dispersion and Absorption in Dielectrics

II. Direct Current Characteristics*

KENNETH S. COLE,
Department of Physiology, Columbia University, New York, New York

AND

ROBERT H. COLE,
Research Laboratory of Physics, Harvard University, Cambridge, Massachusetts

(Received October 30, 1941)

In the first paper of this series [J. Chem. Phys. 9, 341 (1941)], it was shown that the complex dielectric constant, ϵ^*, of many liquid and solid dielectrics is given by a single very general formula

$$\epsilon^*=\epsilon_\infty+(\epsilon_0-\epsilon_\infty)/[1+(i\omega\tau_0)^{1-\alpha}].$$

In this equation ϵ_0 and ϵ_∞ are the "static" and "infinite frequency" dielectric constants, $\omega=2\pi$ times the frequency, τ_0 is a generalized relaxation time and α is a constant, $0<\alpha<1$. The transient current as a function of the time, t, after application of a unit constant potential difference has been calculated from this expression in series form. For times much less than τ_0, the time dependence is of the form $(t/\tau_0)^{-\alpha}$, and for times much greater than τ_0, it is of the form $(t/\tau_0)^{-(2-\alpha)}$. The transition between these extremes occurs for the range in which t is comparable with τ_0. The total absorption charge, which is the integral of the exact expression, is always finite. Although many transient data for dielectrics are of the predicted form, none have been taken over a sufficiently wide range of times adequately to test the result, nor is it yet possible to determine either the relaxation time or the static dielectric constant from available data.

I. INTRODUCTION

THE Debye theory of dispersion and absorption in dielectrics[1] leads to the formula

$$\epsilon^*=\epsilon'-i\epsilon''=\epsilon_\infty+(\epsilon_0-\epsilon_\infty)/(1+i\omega\tau_0) \qquad (1)$$

for the complex dielectric constant ϵ^* as a function of frequency $\nu(=\omega/2\pi)$, where ϵ' and ϵ'' are the real and imaginary parts of ϵ^*, ϵ_0 and ϵ_∞ are the limiting (real) values of ϵ^* at very low and high frequencies, and τ_0 is the relaxation time. A result of this same form is predicted by other simple dispersion theories, as was discussed in the preceding paper under the same title[2] (hereafter referred to as I).

It has been shown that the transient current $I(t)$ following application of unit potential difference across the dielectric at time $t=0$ is given by

$$I(t)=(1/\tau_0)(\epsilon_0-\epsilon_\infty)e^{-t/\tau_0}, \qquad (2)$$

if Eq. (1) is a correct description of the alternating current characteristics.[3] The result (2) is apparent by inspection of the equivalent circuit of the dielectric (cf. Fig. 2 of I) and may be derived by the Fourier integral theorem.[4]

It has long been known that Eq. (2) is not a satisfactory expression for the transient absorption current in dielectrics. In a considerable number of cases the experimental results are well fitted by the formula

$$I(t)=At^{-n}, \qquad (3)$$

where A is a constant and the exponent n usually but not always has a value between 0 and 1. The result (1) predicted by the Debye and other theories cannot, therefore, represent the alternating-current characteristics of these dielectrics. It is well known that Eq. (1) is in fact a poor

* Publication assisted by the Ernest Kempton Adams Fund for Physical Research of Columbia University.

[1] P. Debye, *Polar Molecules* (Chemical Catalog Company, New York, 1929).

[2] K. S. Cole and R. H. Cole, J. Chem. Phys. 9, 341 (1941).

[3] See reference 1, p. 88. The current involved in setting up the high frequency polarization represented by ϵ_∞ has been omitted in Eq. (2). This is justified as this current flows for an extremely short time and is not ordinarily measured.

[4] J. R. Carson, *Electric Circuit Theory and Operational Calculus* (McGraw-Hill Book Company, New York, 1926).

approximation for many dielectrics. As the writers have shown in I, the complex dielectric constant is in many cases given by the formula

$$\epsilon^* = \epsilon_\infty + (\epsilon_0 - \epsilon_\infty)/[1+(i\omega\tau_0)^{1-\alpha}], \quad (4)$$

the parameter α having values between 0 and 1.

If the principle of superposition[5] holds, it is possible to calculate the transient current corresponding to Eq. (4). The present paper describes the results of these calculations and the interpretation of transient current data in terms of them.

II. MATHEMATICAL DETAILS

The complex admittance $Y(i\omega)$ of a dielectric described by Eq. (4) is given by

$$Y(i\omega) = i\omega\epsilon^* = i\omega\{\epsilon_\infty + (\epsilon_0-\epsilon_\infty)/[1+(i\omega\tau_0)^{1-\alpha}]\}, \quad (5)$$

if a condenser of unit geometrical capacity is assumed. The transient current $I(t)$ following application of unit potential difference at time $t=0$ may be written as

$$I(t) = \frac{1}{\pi}\int_0^\infty \epsilon^*(i\omega)e^{i\omega t}d\omega. \quad (6)$$

The direct-current transient may also be written as either a Fourier sine or cosine integral involving ϵ'' or ϵ', respectively, the formulas being[6]

$$I(t) = \frac{2}{\pi}\int_0^\infty \epsilon''(\omega)\sin\omega t d\omega, \qquad I(t) = \frac{2}{\pi}\int_0^\infty \epsilon'(\omega)\cos\omega t d\omega, \quad (7)$$

the initial current involved in charging ϵ_∞ being omitted as before.

The direct-current transient is therefore determined by the frequency dependence of either ϵ' or ϵ''. Thus the behavior of the dielectric is completely determined if any one of the three functions $I(t)$, $\epsilon'(\omega)$, $\epsilon''(\omega)$ is known over the *complete* range of time or frequency. As a corrollary, it is possible to calculate any one of these functions from any other. The expressions for $\epsilon'(\omega)$ and $\epsilon''(\omega)$ in terms of $I(t)$ are well known[7] and follow directly from Eqs. (7) by use of Fourier sine or cosine transforms. The mutual integral relations between ϵ' and ϵ'' are less familiar. They were originally given by Kramers[8] for the case of optical dispersion (i.e., for the frequency variation of ϵ_∞ in terms of the optical absorption and vice versa). The Kramers' relations are readily derived from Eqs. (7) by use of Fourier transforms as has been pointed out by Gross[9] and independently by one of the writers.[10]

The solution of Eq. (6) is easily obtained in series form by the Heaviside operational calculus.[4] Rewriting Eq. (6) as a series in descending powers of the Heaviside operator p and using the operational formula $p^{-n}\rightarrow t^n/\Gamma(1+n)$, one obtains

$$I(t) = \frac{\epsilon_0-\epsilon_\infty}{\tau_0}(1-\alpha)\left(\frac{t}{\tau_0}\right)^{-\alpha} \times\sum_{n=1}^{\infty}\frac{(-1)^{n-1}n}{\Gamma[1+n(1-\alpha)]}\left(\frac{t}{\tau_0}\right)^{(n-1)(1-\alpha)}. \quad (8)$$

In the case $\alpha=0$, Eq. (8) reduces, as it should, to the exponential form (2). For $t/\tau_0 \ll 1$, the current is given with sufficient accuracy by the leading term of the series:

$$I(t) = \frac{\epsilon_0-\epsilon_\infty}{\tau_0}\cdot\frac{1}{\Gamma(1-\alpha)}\left(\frac{t}{\tau_0}\right)^{-\alpha}, \quad t\ll\tau_0. \quad (9)$$

It is also possible to obtain an asymptotic expansion in negative powers of t/τ_0:

$$I(t) = \frac{\epsilon_0-\epsilon_\infty}{\tau_0}(1-\alpha)\left(\frac{t}{\tau_0}\right)^{-(2-\alpha)} \times\sum_{n=1}^{\infty}\frac{(-1)^{n-1}n}{\Gamma[1-n(1-\alpha)]}\left(\frac{t}{\tau_0}\right)^{-(n-1)(1-\alpha)}. \quad (10)$$

For sufficiently large values of t/τ_0 the current is given by

$$I(t) = \frac{\epsilon_0-\epsilon_\infty}{\tau_0}\cdot\frac{(1-\alpha)}{\Gamma(\alpha)}\left(\frac{t}{\tau_0}\right)^{-(2-\alpha)}, \quad t\gg\tau_0. \quad (11)$$

The time dependence of the absorption current $I(t)$ is most conveniently represented on a double logarithmic scale. From Eqs. (9), (11) the log I, log t characteristic is a curve with limiting slopes $-\alpha$ for $t\ll\tau_0$ and $-(2-\alpha)$ for $t\gg\tau_0$. The Fourier mate[11] $\mathfrak{M}(1+p^{1-\alpha})^{-1}$, to which the transient

[5] For a discussion of the superposition principle, see M. F. Manning and M. E. Bell, Rev. Mod. Phys. **12**, 215 (1940).

[6] See reference 4, p. 180.

[7] E. Von Schweidler, Ann. d. Physik **24**, 711 (1907). See also reference 5.

[8] H. A. Kramers, Atti Congr. dei Fisici Como, 545 (1927). See also reference 2.

[9] B. Gross, Phys. Rev. **59**, 748 (1941).

[10] R. H. Cole, Phys. Rev. **60**, 172A (1941); see also reference 2.

[11] G. A. Campbell and R. M. Foster, *Fourier Integrals for Practical Applications*, Bell Telephone Monograph B-584 (1931). The writers are very much indebted to Dr. Foster of the Bell Telephone Laboratories for making his calculations of the Fourier mate available to them.

current is proportional, has been calculated from the appropriate expansions over the range 10^{-6} to 10^{5} for t/τ_0 and for values 0.1, 0.3, 0.5, 0.7, 0.9 of α. Wilbur[12] has calculated the integral of the series (8) in the range $10^{-3}<t/\tau_0<10^{2}$ for $\alpha=0.1$, 0.2, 0.3, 0.4, 0.5. These values thus give the absorption charge as a function of time after application of unit potential difference. The absorption currents have been obtained from these results by graphical differentiation and

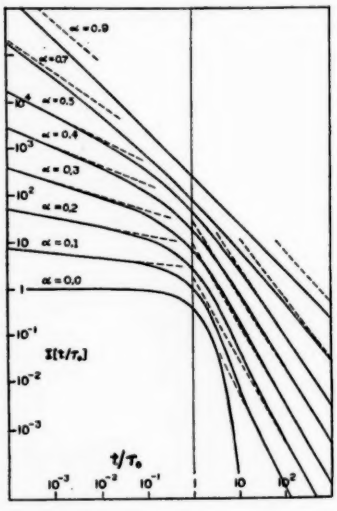

FIG. 1. Calculated transient currents as a function of time. The curves for increasing values of the parameter α have been successively displaced vertically upward by half-decade intervals for greater clarity.

these independent values agree within their limit of accuracy with the directly calculated values.

The transient currents for several values of α are shown graphically in Fig. 1. The limiting straight lines as predicted by Eqs. (8), (10) are also drawn in as dashed lines. Some of the numerical data from which Fig. 1 was drawn are given in Table I in which values of the current $I(t/\tau_0)$ are given for values of t/τ_0 at approximately equal logarithmic intervals. It has been found very useful in drawing curves such as those of Fig. 1 to draw in the limiting straight lines of slope $-\alpha$ and $-(2-\alpha)$. The intercepts of these lines on the axis $t/\tau_0=1$ as calculated from Eqs. (8), (10) are listed in Table II, together with the value of the intercept: $I(t/\tau_0=1)$. These data are also useful in matching experimental results to the predicted curves.

[12] The writers are indebted to Dr. D. T. Wilbur of Cornell University for use of his results.

III. SIGNIFICANCE OF THE RESULTS

It is apparent from Fig. 1 and Eqs. (9), (11) that experimental data requiring a time dependence of the form t^{-n} are consistent with the alternating-current characteristic expressed by Eq. (4) and discussed in I. It is further evident that data for which a slope of value less than unity is found over the entire time interval of measurement have not been taken at sufficiently long times to reveal the departures shown in Fig. 1. This situation has an exact counterpart in the complex plane locus (ϵ'' *versus* ϵ') of the dielectric constant. This may be seen by calculating the steady state relations for $\epsilon'(\omega)$, $\epsilon''(\omega)$ required by Eq. (9) if the superposition principle is valid. It is well known that in this limiting case one obtains[13]

$$\epsilon'(\omega)=(\epsilon_0-\epsilon_\infty)(\omega\tau_0)^{-(1-\alpha)}\sin\tfrac{1}{2}\alpha\pi,$$
$$\epsilon''(\omega)=(\epsilon_0-\epsilon_\infty)(\omega\tau_0)^{-(1-\alpha)}\cos\tfrac{1}{2}\alpha\pi. \qquad (12)$$

The complex plane locus defined by Eq. (12) is a straight line of slope $\tan(1-\alpha)\pi/2$. This is simply the limiting slope of the circular arc locus for $\omega\tau_0\gg1$, as discussed in I. As pointed out there, one has from this limiting behavior no estimate of either the relaxation time or the static dielectric constant for the reason that the measurements do not extend to sufficiently low frequencies. In the present direct-current case one has no information about either of these quantities for the reason that the measurements do not extend to sufficiently long times.

A similar argument applies to data for which values of α greater than unity are found, the time intervals of measurement being in this case considerably greater than the relaxation time τ_0. In these cases then, the measurements do not extend to sufficiently short times to determine $\epsilon_0-\epsilon_\infty$ or τ_0 and the situation corresponds to the limiting slope $-\tan(1-\alpha)\pi/2$ of the circular arc locus at low frequencies ($\omega\tau_0\ll1$).

For times comparable with the relaxation time a transition between the limiting behaviors outlined above is to be expected; that is, the locus is a curve of increasing negative slope as shown in Fig. 1 and corresponds to the major part of the circular arc locus for the alternating-current

[13] See reference 5 for details of the calculation.

TABLE I. Transient currents for various values of the parameter α.

t/τ_0 \ α	0.0	0.1	0.3	0.5	0.7	0.9
1×10^{-4}	0.9999	2.350	12.18	55.43	184.4	209.0
2	0.9998	2.192	9.880	38.92	111.6	107.4
5	0.9995	1.999	7.480	24.26	56.13	44.41
1×10^{-3}	0.9990	1.867	6.049	16.88	33.07	22.71
2	0.9980	1.742	4.878	11.66	19.31	11.59
5	0.9950	1.574	3.643	7.054	9.328	4.747
1×10^{-2}	0.9900	1.456	2.894	4.745	5.300	2.410
2	0.9802	1.338	2.268	3.131	2.966	1.220
5	0.9512	1.169	1.585	1.733	1.341	
1×10^{-1}	0.9048	1.020	1.156	1.061	0.719	
2	0.8187	0.8410	0.791	0.618		
5	0.6065	0.5478	0.411	0.275		
1	0.3679	0.2996	0.211	0.137	0.073	0.025
2	0.1353			0.0627		
5	0.00674			0.0200		
10	0.000045	0.00212	0.00605	0.00794		
20		0.000413	0.00172	0.00294	0.0029	
50		0.000062	0.000335	0.000775	0.00101	0.00048
1×10^{2}		0.000016	0.000099	0.000278	0.000430	0.000235
2			0.000030	0.000099	0.000185	0.000115
5				0.000025	0.000059	0.000045

characteristic. This correlation of the direct-current and alternating-current characteristics is shown in Fig. 2 in which the log I, log t curve and the complex plane locus are shown, one above the other with corresponding quantities indicated. The figure is drawn for the case $\alpha=0.5$, but a similar situation holds for other values in the range $0<\alpha<1$.

Two objections have often been raised to the empirical expression (3) or its equivalent (9) for the absorption current. The first of these is that Eq. (2) predicts an infinite current for $t=0$. It should, however, be realized that the same thing is true of a perfect capacity on applying a discontinuous change in potential and that the constant phase angle impedance element in the equivalent circuit (see Fig. 2 of I) has the characteristics of both resistance and capacity. The significant quantity is the total charge stored in the dielectric. This total charge is finite for any finite time, being the time integral of Eq. (9).

TABLE II. Values of $I(t/\tau_0)$ for $t/\tau_0=1$; intercepts with axis $t/\tau_0=1$ of asymptotic functions valid for $t/\tau_0\ll1$ and for $t/\tau_0\gg1$.

α	$I(t/\tau_0)$	$I(t/\tau_0\ll1)$	$I(t/\tau_0\gg1)$
0.0	0.3679	1.000	0.000
0.1	0.2996	0.936	0.0946
0.2	0.254	0.859	0.174
0.3	0.211	0.770	0.234
0.4	0.172	0.672	0.271
0.5	0.137	0.564	0.282
0.7	0.073	0.334	0.231
0.9	0.025	0.105	0.0936

The second objection is that the total charge $Q(t)$ is not finite for an infinite time of charging, as this is given by

$$Q(t)=A\int_0^t t^{-\alpha}dt,$$

which does not converge for $\alpha<1$ as $t\to\infty$. This cannot be the case for the true reversible absorption current, as it would require that the dielectric be capable of storing an infinite amount of charge, all of which could be recovered on discharge. The answer is of course that Eq. (9) is valid only for short times ($t\ll\tau_0$) and does not account for the approach to equilibrium or "saturation." The integral of Eq. (6), which is the general expression for a dielectric, does converge to the proper limiting value ($\epsilon_0-\epsilon_\infty$), as can be seen intuitively from the equivalent circuit of Fig. 2b in I.

IV. EXPERIMENTAL EVIDENCE

It must be realized that the discussion above is concerned only with the reversible absorption current. If any comparison is to be made with experimental data, it is necessary that the effect of any irreversible "Joule" conductivity be taken into account. The charging current in a dielectric after application of a constant potential difference must ultimately reach a steady value if such a conductivity exists. This steady value may well be sufficiently large to mask completely the absorption current at large times and so make difficult or impossible any comparison with the predicted curves of Fig. 1 for large values of time.

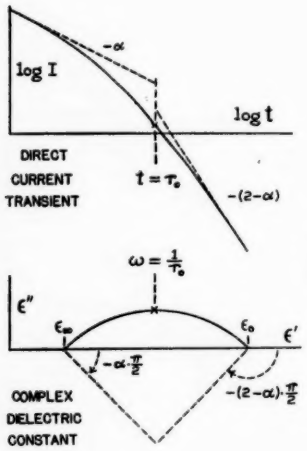

FIG. 2. Comparison of transient direct-current and steady-state alternating-current characteristics of dielectrics exhibiting dispersion.

This difficulty in determining the true absorption current can be avoided by measuring the discharge current when the dielectric is short-circuited. In this case, the Joule conductivity is negligible and the absorption current, because of its reversibility, is given by Eqs. (8), (10) except for sign. This is, however, strictly true only if the dielectric has been kept at a constant potential for an infinite time before short-circuiting to measure the discharge current. In practice, this means that the time of charging must be long in comparison with the relaxation time τ_0. If τ_0 is of the order of days or weeks, as the discussion below indicates may often be the case, this condition has been not at all satisfied in many experiments.

If the charging time is comparable with the relaxation time, one has to consider the response of the dielectric to a potential difference in the form of a rectangular pulse rather than a unit function. Such a pulse can be regarded as the sum of two equal and opposite unit functions with the discontinuities separated by the charging interval. Because of the superposition principle, the resulting absorption current is then the algebraic sum of the currents due to these two unit functions applied separately.

It should perhaps be mentioned that it is formally possible to calculate the variation of potential difference across a dielectric with time if the transient current expression is known and the superposition principle is valid. Gross[14] has considered the problem in detail for various conditions of charging and the reader is referred to his papers for a more detailed discussion.

The analysis of dielectric phenomena in terms of potential rather than current variations does not appear to be very useful experimentally as the mathematical expressions involved are difficult to handle in numerical form. Gross has considered the case in which the transient current is given by a formula of the form (9). He obtains an approximate expression for the variation of potential across an open-circuited dielectric as a series of functions involving Mittag-Leffler functions.[15] The complications involved in any attempt to evaluate explicitly the potential variations required by a more general formula such as Eq. (8) for the transient current can readily be appreciated.

The additive property of absorption currents is not particularly useful in practice for the reason that one does not know the value τ_0 in advance. If, however, the charging time is small compared with τ_0, the current is essentially that for a unit impulse and is given by the derivative of Eqs. (8), (10) with respect to t/τ_0. In this case one should expect limiting slopes $-(1+\alpha)$ and $-(3-\alpha)$ on the log I *vs.* log t plot for t small and large, respectively. One cannot expect to evade the difficulties in determining the long time behavior by any such simple expedient as this. The reason is simply that the long time response of the dielectric does not come into play for a very short charging time. As a consequence, the current for large values of time will be extremely small and correspondingly difficult to measure.

---

[14] B. Gross, Zeits. f. Physik **107**, 217 (1937); *ibid.* **108**, 598 (1938).

[15] The Mittag-Leffler function encountered is similar to, but not to be confused with, Eq. (8). The series (8) can be written in terms of the derivative of this function of order $1-\alpha$. For a discussion of the Mittag-Leffler function, see H. T. Davis, *The Theory of Linear Operators* (Principia Press, Bloomington, Indiana, 1936).

Because of the complications discussed above, it is necessary to be circumspect in analyzing experimental results. With these difficulties in mind, representative examples of transient current data in the literature will now be considered.

Experiments showing the existence of "anomalous" discharge in dielectrics were made by R. Kohlrausch in 1854.[16] This observer measured the decay of charge on the plates of glass condensers after removal of the charging potential. His values for the loss of charge $Q_0-Q(t)$, where $Q(t)$ is the charge at time t and Q_0 is the initial charge, are shown in Fig. 3 plotted against time. The data on a double logarithmic plot are well fitted by a straight line of slope 0.3. As the loss of charge is the integral of the discharge current, the expression for the discharge current is of the form $I(t)=At^{-0.7}$. The point already emphasized, that a formula of this kind can be true only for times small compared to the relaxation time of the dielectric, is brought out in another way in Fig. 3, as the curve for $Q_0-Q(t)$ must approach the value Q_0 indicated by the dashed line for very large values of time. It is seen that, while there is some evidence of this flattening out, a time of $5\cdot10^3$ seconds is still small compared with the relaxation time.

It should be pointed out that these data are not strictly comparable to the results of Section II, as Kohlrausch measured the charge on open circuit. The discharge current was thus maintained by leakage and the potential difference across the dielectric was not constant as assumed in the derivation above.[17]

Most of the available results on absorption currents *versus* time are for practically important insulators such as quartz, amber, hard rubber. It is unfortunate that there are few direct-current

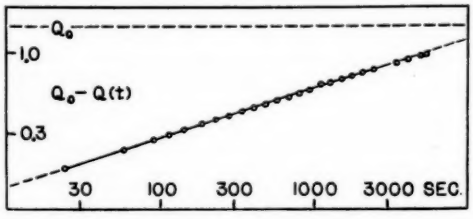

FIG. 3. Loss of absorption charge from glass as a function of time (from data of R. Kohlrausch).

[16] R. Kohlrausch, Pogg. Ann. **91**, 56 (1854).
[17] For a detailed discussion of such cases, see reference 14.

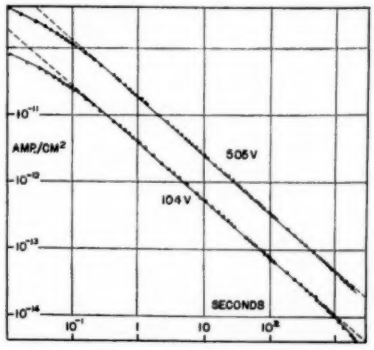

FIG. 4. Discharge currents in mica for two values of original potential difference across the dielectric (from data of Voglis).

data for dielectrics similar to the ones considered in I for which there are alternating-current data available as well.

A. Mica

One example for which both kinds of data are available is mica. The results of Voglis[18] for the discharge current over a time range 10^{-2} to 10^3 seconds are shown in Fig. 4. Over most of this range the curve is a straight line of slope -0.87 and hence $\alpha=0.87$. MacLeod[19] has measured the resistance and capacity over the frequency range $500-10^6$ cycles and his results give a value $\alpha=0.88$.

The departure from the $t^{-\alpha}$ formula for large values of time is, as mentioned by Manning and Bell,[5] in the necessary direction that the total charge recovered be finite. Voglis suggested that the flattening of the $\log I-\log t$ characteristic for t small is evidence that the $t^{-\alpha}$ formula breaks down for sufficiently small times. It is interesting to note that this conclusion is contradicted by MacLeod's results which correspond to times as small as 10^{-6} second and require the value $\alpha=0.88$.

Hippauf and Stein[20] have also made measurements on mica in the time range $4\cdot10^{-3}-2\cdot10^{-1}$ second and they found a value $\alpha=0.24$, which is not at all in agreement with Voglis and MacLeod. Some unpublished measurements of R. F. Field are interesting in this connection. Field has made alternating-current measurements on stained

[18] G. M. Voglis, Zeits. f. Physik **109**, 52 (1938).
[19] H. J. MacLeod, Phys. Rev. **21**, 53 (1923).
[20] E. Hippauf and R. Stein, Physik. Zeits. **39**, 90 (1938).

samples of mica over the frequency range $25-10^4$ cycles. He finds in one case that the data for loss factor *versus* capacity plot into a circular arc for which $\alpha=0.46$, and the relaxation time $\tau_0=0.016$ sec. His measurements of the absorption current for the time range 1.5–100 seconds give a straight line of slope -0.92 on the $\log I-\log t$ plot. The natural conclusion is that one is dealing here with two more or less distinct dispersion regions characterized by separate values of τ_0, α. It is quite possible that the higher frequency dispersion is not a true characteristic of the mica itself but arises from imperfections in the sample. Whatever the cause, it is evident that the question can be resolved only when data over a wide range of frequency and time are available.

The existence of more than one region of dispersion is a possibility which may very well have to be considered in other dielectrics as well. For example, the data of Yager[21] on polyvinyl chloride and chloroprene in the frequency range $10^3-3\cdot10^7$ cycles give evidence of the same type of thing.[22]

The various results for mica have been mentioned here chiefly to indicate the complications which may arise in the analysis of dielectric data. It is, however, significant that all the evidence for mica is consistent with the constant phase angle characteristic of dielectrics generally.

B. Glass

Voglis has also made measurements on glass, the data again falling on a straight line of slope -0.74 over the major portion of the time range 10^{-2} to 10^3 seconds. The slope increases slightly at the longer times but the departures are so small that it is impossible to estimate from them the value of the relaxation time. It can only be concluded that it is considerably greater than 10^3 seconds. A number of other observers have made measurements over various time intervals for different glasses and find the same sort of behavior. Benedict,[23] for example, finds values $\alpha=0.69-0.75$ for soda lime glass in the range 0.4 to $100\cdot10^{-3}$ second; Tank[24] finds a value 0.70 for times up to 0.2 second.

C. Amber

The absorption current has been measured by a number of observers, the results being in not too good agreement. Seidl[25] finds values $0.88-0.91$ for α in the time range 1–60 minutes, indicating a still larger value of the relaxation time. On the other hand, the data of Neumann[26] plotted in Fig. 5 appear to show a transition between slopes -0.7 and -1.5. These estimates are necessarily rough as the range of times is small and the consistency of the data not very good. If these data constitute an example of the behavior predicted by Eqs. (9), (11), they require the values $\alpha\sim0.7$, $\tau_0\sim30$ minutes. Gnann[27] finds a slope 1.11 on the $\log I-\log t$ plot for times greater than about 15 minutes, which corresponds to $\alpha=0.89$. His data do not extend to sufficiently short times to permit an accurate estimate of the other limiting slope, but it appears from his figure to be of the order 0.9 as it should according to Eqs. (9), (11).

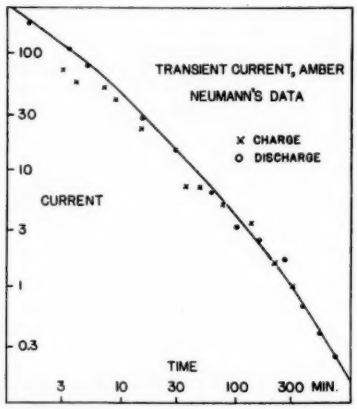

FIG. 5. Transient currents for charge and discharge of amber (from data of H. Neumann).

In view of the disagreements among the various data, they can hardly be said to confirm the results of the present paper. They do, however, give evidence of the transition region for $t\sim\tau_0$

[21] W. A. Yager, Trans. Electrochem. Soc. **74** (preprint), (1938); Bell Telephone Monograph B-1099.

[22] The writers are indebted to Mr. R. F. Field of the General Radio Company for pointing this out and for much helpful discussion of the general subject of this paper, as well as for permission to quote his results for mica.

[23] R. R. Benedict, Trans. A. I. E. E. **49**, 221 (1930).

[24] F. Tank, Ann. d. Physik **48**, 307 (1915).

[25] F. Seidl, Zeits. f. Physik **91**, 318 (1934).

[26] H. Neumann, Zeits. f. Physik **45**, 717 (1927).

[27] W. Gnann, Physik. Zeits. **36**, 222 (1935).

which must occur for any dielectric exhibiting dispersion.

D. Other Data

There are many other data which could be cited here as examples of the $t^{-\alpha}$ time dependence. The majority of these measurements are on such things as various melting point paraffins, impregnated paper for condenser insulation, various waxes and rosins, and other insulation of commercial importance. For the most part, values of α less than one have been observed with little evidence of an increase in negative slope on the $\log I - \log t$ plot. For such materials, it can only be concluded that the times involved were very much less than the relaxation time. An estimate of the static dielectric constant is even less possible, as was the case with the alternating-current data on several solid dielectrics discussed in I.

V. CONCLUSION

The examples discussed above are believed to be representative of experimental results in the literature. The list is by no means complete and it appears probable that the number of examples which could be found to illustrate the $t^{-\alpha}$ time dependence is limited chiefly by one's patience in searching the literature.

The data which have been considered do not give much evidence on the question of the necessary change in time dependence if the total absorption charge is to remain finite. As a consequence, the limiting expression (11) required by the results of alternating-current data cannot as yet be checked from transient current measurements. Such results as do exist are at least not inconsistent with the predictions of the present paper. It is therefore not unreasonable to suppose that the "constant phase angle" characteristic very generally required by alternating-current data will be further substantiated by more complete measurements of absorption currents.

The importance of extending transient current measurements to longer times should be emphasized. Unless this is done one has only a part of the complete picture. These times may extend to the order of hours or even days in some cases, but without such data it is impossible to do more than set lower limits for the values of the relaxation time and static dielectric constant. About all that can be said at present about many solid dielectrics is that both these quantities must be very much larger than is ordinarily supposed. To avoid large errors in correcting for steady-state conduction currents, discharge rather than charging currents should be measured. If these results are to be interpreted without ambiguity, the dielectric must previously have been charged for a time long in comparison with the relaxation time.

It is important to realize that measurements of transient absorption currents in dielectrics give identically the same information as do steady-state alternating-current measurements. Either type of measurement determines the electrical characteristics of a dielectric for which the superposition principle is valid. The choice between the two is then dictated by convenience in measurement and analysis, the transient current method being obviously more suitable if the characteristic relaxation time is of the order of seconds or longer.

The Thermal Decomposition of *n*-Butylamine[1]

HAROLD C. BEACHELL AND H. AUSTIN TAYLOR
New York University, New York, New York

(Received October 29, 1941)

The thermal decomposition of *n*-butylamine proceeds in a manner analogous to that of the lower aliphatic amines. There is no evidence to support the suggestion of a molecular split into ammonia and ethylene. The mechanism appears to involve initially the production of a butylamino radical and a hydrogen atom. The butylamino radical may be the source of the ammonia found, by production of an imine whose presence is indicated. Pressure change rates yield an apparent energy of activation of 89 kcals.

INTRODUCTION

THE pyrolysis of the aliphatic amines, particularly the primary amines, has been shown[2] to be complex. There appears to be some definite evidence that at least in part the mechanisms involve free radicals though the nature of these radicals is not definitely known. Travers and co-workers[2a] present evidence that from methylamine the radicals formed are probably CH_3NH and H rather than CH_3 and NH_2. The former rupture is also that postulated by Emeleus and Jolley[3] for the initial step in methylamine photolysis. The difference in end products of the pyrolysis and photolysis must then be attributed to different subsequent secondary reactions. There is some indication that the radicals lead to chains, the evidence suggesting short chains. In no case so far investigated, has a simple decomposition into stable products molecules been observed. The recent suggestion of Rice and Teller[4] based upon the principle of least motion that butyl derivatives might offer the possibility of simple decomposition by the formation of a ring structure through a hydrogen bond succeeded by rupture and rearrangement into products would require from butylamine the production simply of ammonia and ethylene.

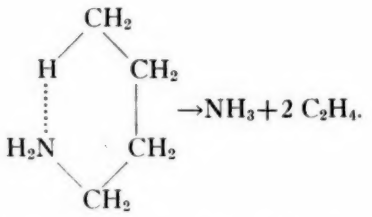

It has recently been shown[5] in the thermal decomposition of methyl butyl ether that the hydrogen bond is too weak to enable the ring structure to form to any extent under pyrolytic conditions and even at room temperature photolysis did not give the products to be expected from the ring rupture and rearrangement. Furthermore in the photolysis of butylamine Bamford[6] has presented evidence that a split into a hydrogen atom and alkylamino radical succeeds the absorption act. If the energy absorbed during illumination should remain in the amine group, such a rupture is to be expected. It is not conclusive proof, however, that the ring structure never exists in this case. The possibility of the formation of ammonia and ethylene, especially at the temperature of a pyrolysis, presents itself on inspection of a model of the butylamine molecule, where, assuming free rotations and relatively small excitation of bending vibrations, the NH_2 group can come quite close to a hydrogen on the gamma-carbon atom in a configuration that would make the formation of ammonia apparently a simple matter, the residual tetramethylene biradical yielding ethylene. This possibility has therefore been examined dynamically under such conditions of high temperature and short contact

[1] Abstract from a thesis submitted by H.C.B. in partial fulfillment of the requirements for the degree of Doctor of Philosophy at New York University, June, 1941.

[2] (a) CH_3NH_2, Carter, Bosanquet, Silcocks, Travers, and Wilshire, J. Chem. Soc. 501 (1939); Travers and Hawkes, *ibid.* 1360 (1939). (b) $C_2H_5NH_2$, Taylor and Ditman, J. Chem. Phys. **4**, 212 (1936). (c) $C_3H_8NH_2$, Sickman and Rice, J. Am. Chem. Soc. **57**, 23 (1935).

[3] Emeleus and Jolley, J. Chem. Soc. 1612 (1935).

[4] Rice and Teller, J. Chem. Phys. **6**, 489 (1938).

[5] Magram and Taylor, J. Chem. Phys. **9**, 755 (1941).

[6] Bamford, J. Chem. Soc. 17 (1939).

time that subsequent reactions might be considered at a minimum. Later, static measurements were made for comparison with pressure change measurements in other amines.

EXPERIMENTAL

Commercial *n*-butylamine with a boiling point range of 76–77°C was fractionally distilled several times to yield a sample boiling completely from 76.5 to 76.6°C. Prior to use the amine, frozen using solid CO_2, was thoroughly evacuated, melted, refrozen and again evacuated to insure complete removal of oxygen and other dissolved gases.

Dynamic Experiments

The dynamic reaction system consisted of a quartz tube, 5-mm internal diameter heated along 30-cm length by an electric furnace capable of reaching 1000°C. The butylamine reservoir was connected through a ground joint at one end of the quartz tube. At the other end were sealed through a Pyrex to quartz graded seal two removal traps connected to a five-liter gas reservoir, a mercury manometer, and the pump system. This latter was twofold, a mercury diffusion pump backed by an oil pump and a Toepler pump connected with the gas analyzer.

In making a run a known weight of butylamine was placed in the reservoir, frozen and evacuated as mentioned. The furnace was raised to the desired temperature and the system shut off from the pump. The dry ice-toluene bath around the butylamine was replaced by a beaker of warm water, the temperature of which was adjusted from experience to give the desired rate of flow of amine vapor. Liquid nitrogen was placed around the traps at the exit end of the furnace to condense everything but the permanent gases which expanded into the evacuated five-liter bulb. At the conclusion of a run the permanent gases were pumped off by means of the Toepler and analyzed. The condensate from the liquid nitrogen traps was then fractionated, first at −131°C using sec-butyl chloride and again at −78°C using dry ice-toluene.

The permanent gases contained only hydrogen and methane and were analyzed by complete combustion in excess oxygen. The second fraction contained saturated and unsaturated hydrocarbons. Acetylenes were estimated from the contraction on passage through ammoniacal silver nitrate solution in a bubbler pipette. The remaining unsaturates were absorbed in fuming sulfuric acid. Saturated hydrocarbons were determined by combustion. In the fraction from dry ice, ammonia was estimated by absorption in dilute sulfuric acid and the remainder was treated as in the last fraction.

Static Experiments

A cylindrical Pyrex reaction vessel 25 cm long and 8 cm in diameter carrying a thermometer well, projecting into the center, was connected through a one-liter storage vessel to the butylamine reservoir and to a constant volume manometer and pump system. Connecting tubing was 2-mm capillary giving a dead space outside the furnace of less than two percent of the reaction volume. This tubing was kept warm to prevent condensation of the amine. The vessel was maintained at a constant temperature in an electrically heated furnace, the temperature being measured by means of a platinum resistance thermometer whose element was placed in the well of the reaction vessel.

The amine reservoir after evacuation as above was warmed to a little above room temperature and opened to contact with the evacuated storage bulb. Amine vapor was drawn from this bulb for experiments. The course of reaction was followed by the pressure change and the products then withdrawn by a Toepler pump for analysis as before.

RESULTS AND DISCUSSION

Analytical Results

The most significant observation in the analyses of products from both dynamic and static runs was the absence of nitrogen. The gases not condensed by liquid nitrogen were completely combustible and analyzed as methane and hydrogen.

The gases drawn from sec-butyl chloride at −131°C consisted of some acetylene, a large amount of ethylene, some ethane and small amounts of propane and methane.

The gas from solid CO_2 at −78°C was essentially ammonia with small amounts of satu-

TABLE I. Products of butylamine pyrolysis.

Temp. °C	Rate of flow cc/min.	Percentage H_2	CH_4	C_2H_2	C_2H_4	C_2H_6	C_3H_8	NH_3	Formula of gas
950	2800	27.8	18.3	3.8	35.0	1.2	0.9	13.0	$C_4H_{12.5}N_{0.51}$
950	4300	24.7	13.7	2.1	41.3	3.7	0.9	13.0	$C_4H_{12.4}N_{0.56}$
950	5600	25.9	17.9	5.1	35.0	2.4	0.3	15.7	$C_4H_{12.6}N_{0.50}$
750	1200	19.1	17.8	1.8	41.5	4.3	1.0	13.6	$C_4H_{12.3}N_{0.47}$
750	4900	17.5	15.4	—	35.0	17.1	—	12.9	$C_4H_{12.8}N_{0.46}$
650	1430	19.3	17.6	—	33.6	16.8	—	13.0	$C_4H_{13.2}N_{0.43}$

rated and unsaturated hydrocarbons. The complete removal of the ammonia necessitated the liquefaction and re-freezing of the residual butylamine.

An attempt was made to analyze the residual liquid fraction. Neutralization of the residual amine with dilute nitric acid followed by treatment with silver nitrate gave a precipitate of silver cyanide. The quantity was not large and would represent only about two percent of the gas phase. This was estimated by weighing the silver produced on ignition of the precipitate at 500° in a nitrogen atmosphere. Distillation of the liquid fraction causing removal of the excess butylamine, gave a substance boiling at about 160°C, which had a somewhat fragrant odor and would reduce ammoniacal silver nitrate in the cold. A micro-Kjeldahl determination gave a value of 30.1 percent nitrogen. The material is thought to be methyl-methyleneimine which has a nitrogen value of 32.6 percent. The difficulty of complete removal of butylamine would tend to give low nitrogen values. There was also some evidence for the presence of dibutylamine in the liquid fraction but it was not isolated or definitely identified.

A summary of the runs made is given in Table I. The last column gives the total formula for the gaseous products which is obtained by calculating the total weight of each element in the various compounds and dividing by the atomic weight. The formula thus obtained is multiplied by a factor to bring the carbon to four for comparison with butylamine.

It may be seen that in general there is no very marked change in the products over rather widely varied conditions of temperature and rate of flow. The formula of the gas shows that only about fifty percent of the original nitrogen is present in the gas phase at the conclusion of a run. This may be judged also from a comparison of the relative amounts of ammonia and ethylene, the former being considerably less than half the ethylene. The variety of products, too, would argue against the ring rupture mechanism and point to a radical mechanism as most probable. The preponderance of hydrogen, even over methane, suggests a mechanism involving hydrogen atoms. The alternative found by Taylor and Ditman[7] in ethylamine pyrolysis, namely, a bimolecular reaction of ethylamine to produce hydrogen and diethylhydrazine, does not appear likely here in view of the absence of nitrogen among the products. Furthermore, the ratio of ammonia to hydrogen is very close to that found by Bamford[6] in the photolysis wherein an initial split of a hydrogen atom was also postulated. The difference of the other products of the pyrolysis from those in the photolysis must be due to the instability of the complex radicals at the high temperatures.

It appears plausible that the following reactions

TABLE II. Rate of pressure change at 530°C.

Time min.	Pressure cm	$k \times 10^3$ sec.$^{-1}$
0	10.8	—
2	12.5	1.23
3	13.3	1.15
4	14.1	1.09
5	14.8	1.05
6	15.5	1.01
7	16.1	0.95
8	16.7	0.91
9	17.3	0.87
15	20.1	0.69
21	21.9	0.56
30	23.5	0.43
40	24.6	0.34
50	25.3	0.29
60	25.8	0.24

[7] Taylor and Ditman, J. Chem. Phys. **4**, 212 (1936).

occur in the photolysis:

$$C_4H_9NH_2 \rightarrow C_4H_9NH- + H, \quad (1)$$

$$H + C_4H_9NH_2 \rightarrow C_4H_9NH- + H_2, \quad (2)$$

$$2C_4H_9NH- \rightarrow C_4H_8=N-C_4H_9 + NH_3. \quad (3a)$$

Since hydrogen always preponderates over ammonia a regeneration of amine by an alternative of reaction is considered by Bamford:

$$2C_4H_9NH \rightarrow C_4H_9NH_2 + C_4H_9N=. \quad (3b)$$

There seems to be no reason why the same scheme should not account for the pyrolysis when the instability of the large radicals and molecules at high temperatures is taken into account. It is well known that the propyl radical dissociates into ethylene and a methyl radical so that the presence of large amounts of ethylene can easily be accounted for. The presence of cyanides may result from decomposition of the butylimine group with consequent production of propane. It would be relatively easy to speculate further on these decompositions but in the absence of direct experimental evidence nothing can be gained by so doing.

Pressure Change Measurements

Pressure change measurements were made over the temperature range 510–530°C and at initial pressures of amine from about 5 to 20 cm. Figure 1 gives a typical series of curves for various initial pressures at 530°C. First-order constants calculated in the usual manner show in all cases a steady decrease throughout a run. One example in Table II will illustrate this.

To surmount this difficulty and at the same time obtain a rate constant more directly related to the initial rate of reaction, the logarithms of the pressures were plotted against the time and the slope at zero time was found. These data are presented in Table III.

The marked decrease even in the initial rate with a decrease in initial pressure is similar to that found with other amines, even to the apparent leveling off in the value of the constant at low pressures.[2c] The reaction is certainly not a straightforward unimolecular decomposition and the static results confirm the complexity suggested by the analytical findings. No satisfactory interpretation of the rate of pressure change can be offered. A plot of the logarithms of the initial rates against the absolute temperatures gave as

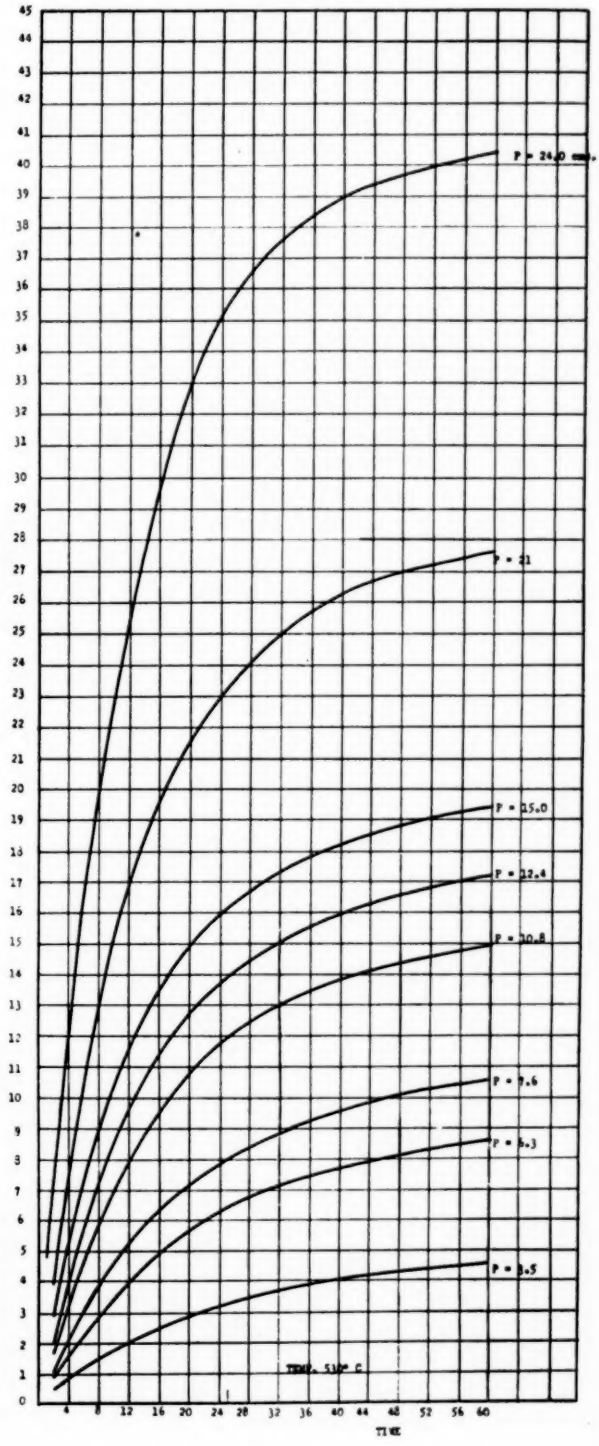

FIG. 1.

TABLE III. Initial rates as function of pressure.

530°C Pressure	530°C $k\times10^3$	520°C Pressure	520°C $k\times10^4$	510°C Pressure	510°C $k\times10^4$
24.0	1.66	22.0	7.66	21.7	4.03
21.0	1.53	20.7	7.31	19.3	3.86
15.0	1.42	16.4	7.31	14.8	3.17
12.4	1.34	15.6	6.56	11.7	2.88
10.8	1.28	12.5	5.64	9.6	2.82
7.6	1.20	10.7	5.58	5.8	2.82
6.3	1.15	6.8	5.58	4.5	2.82
3.5	1.15	4.1	5.58		

an average value for the energy of activation, 89 kcal. This value is much larger than the values found from similar pressure change data for other amines (40–60 kcal.) and would appear to be too large for a single reaction. On the other hand, if the initial split corresponds to rupture of a nitrogen-hydrogen bond the value of 89 kcal. is not an impossible one; reactions subsequent to the initial split, since they involve radicals would be expected to have lower energies of activation and the initial split would be rate controlling.

Analysis of the residual gases from the static runs, though less accurate because of the smallness of the samples, confirms the findings of the dynamic runs. A representative analysis gave 22.0 percent hydrogen, 19.6 percent methane, 30.2 percent ethylene, 15.0 percent ethane and 12.1 percent ammonia. It is evident that the course of the reaction during a contact time of the order of an hour at 500°C is essentially the same as that occurring with a contact time of about 0.1 sec. at 950°C. Coupled with the photochemical data there is thus no evidence for a direct molecular split under any conditions.

FEBRUARY, 1942 JOURNAL OF CHEMICAL PHYSICS VOLUME 10

The Photolysis of Azomethane in the Presence of Hydrogen[1]

H. AUSTIN TAYLOR AND RALPH G. FLOWERS
New York University, New York, New York

(Received November 18, 1941)

The photolysis of azomethane in presence of hydrogen in the temperature range 20–200°C has been shown to yield ethane at a rate which is independent of the hydrogen. At low temperatures methane production is decreased by the presence of hydrogen but the rate increases with temperature faster than from azomethane alone. A mechanism involving CH_5 has been suggested which accounts qualitatively for the observations. Essentially the same mechanism is shown to account for the decomposition of mercury dimethyl, roughly quantitatively. Strong evidence is offered that the reaction producing methane from methyl radicals and hydrogen is not $CH_3+H_2\rightarrow CH_4+H$. This is supported by the absence of hydrogen atoms during the azomethane photolysis studied.

THE reaction of methyl radicals with hydrogen has been studied experimentally by a number of workers[2] and theoretically by Eyring and co-workers.[3] In the former work it was assumed that the products of reaction were methane and a hydrogen atom and the experimental evidence was interpreted as in agreement with this. The theoretical treatment involved the computation of the potential energy surface for the approach of a hydrogen atom to a methane molecule in the direction of one of the C−H bonds to produce a methyl radical and a hydrogen molecule. The most significant feature of this surface is the relatively deep basin corresponding to the complex CH_5 which indicates its stability relative to both CH_4+H and CH_3+H_2. It has been pointed out by one of us[4] that the production of methane from methyl radicals and hydrogen need not necessarily involve the pro-

[1] Abstract from a dissertation submitted in partial fulfillment of the requirements for the degree of Doctor of Philosophy, New York University, November, 1941.

[2] J. P. Cunningham and H. S. Taylor, J. Chem. Phys. **6**, 359 (1938) includes earlier references.

[3] Gorin, Kauzmann, Walter, and Eyring, J. Chem. Phys. **7**, 633 (1939).

[4] H. A. Taylor and M. Burton, J. Chem. Phys. **7**, 679 (1939).

duction of hydrogen atoms but might proceed by the reaction:

$$CH_3+CH_5=2CH_4.$$

The presence or absence of hydrogen atoms becomes crucial as a distinction between these alternatives.

The photolysis of azomethane has been shown[5] to involve the production of methyl radicals and nitrogen. Furthermore, Henkin and Taylor[6] have shown that the simplest reaction of hydrogen atoms with azomethane in presence of hydrogen molecules is an addition reaction producing sym.-dimethylhydrazine even at room temperature. The presence of dimethylhydrazine can be easily proved by the brick-red precipitate which it gives with an acid buffered solution of cupric chloride. The photolysis of azomethane in presence of hydrogen offers, therefore, a means of studying the reaction of methyl radicals with hydrogen while at the same time providing a means of testing for hydrogen atoms.

EXPERIMENTAL

Materials

Azomethane was prepared and purified by the method described by Jahn.[7] It had a vapor pressure at 0°C of 759 mm and was stored as a liquid at −78°C when not in use. The hydrogen used was drawn from a cylinder of commercial hydrogen, was passed over hot platinized asbestos, through a trap immersed in liquid nitrogen and through anhydrous calcium sulfate. The mixtures of azomethane and hydrogen were prepared by measuring the pressure of each gas separately. The azomethane was introduced first into the mixing chamber and its pressure noted. It was then frozen in liquid nitrogen and the hydrogen added. Sufficient quantities of a given mixture were made for a series of runs. The mixing chamber and all connecting tubing in which azomethane could stand exposed to light were covered with black crepe paper to prevent decomposition.

Apparatus and Procedure

The source of illumination was a General Electric H-4 mercury vapor lamp without the glass envelope. The reaction chamber, a cylindrical Pyrex vessel, 433 cc in volume, was located in a furnace with a glass window for illumination purposes and was connected to a manometer, the mixing reservoir and the pump system consisting of a diffusion pump backed by an oil pump. It was also connected to a Toepler pump for transferring the gaseous products to the analytical system.

The procedure for a run involved admission of the reactant, either pure azomethane or a known mixture with hydrogen, to a desired pressure into the reaction chamber. The lamp was allowed to warm up for five minutes before the shutter in front of the reaction vessel was removed and the temperature of the furnace was adjusted. The lamp was then uncovered and the reaction was followed by the pressure change registered on the manometer. When the pressure had increased by an amount approximately one-third of the initial azomethane pressure, the lamp was turned off and the reaction vessel was opened to traps surrounded by liquid nitrogen. Nitrogen, hydrogen, and methane were drawn off with the Toepler pump and analyzed by combustion in excess oxygen. The nitrogen was measured after absorption of residual oxygen and corrected for small amounts of nitrogen in the oxygen. The products condensed in liquid nitrogen were fractionated at −131°C using secondary butyl chloride mush and at −78°C using solid carbon dioxide. Ethane and traces of unsaturates were pumped off at −131°C. At −78°C the gases consisted of undecomposed azomethane and traces of higher hydrocarbons. Their volume having been measured, the azomethane was absorbed in 6*N* sulfuric acid leaving propane or higher hydrocarbons. A condensable liquid, which has been previously reported by many workers, is held back at −78°C. This liquid was tested with an acid buffered solution of cupric chloride to determine the presence or absence of dimethylhydrazine.

EXPERIMENTAL RESULTS

The analytical results for experiments on pure azomethane and on various azomethane-hydro-

[5] Patat, Naturwiss. **23**, 801 (1935); Burton, Davis and Taylor, J. Am. Chem. Soc. **59**, 1989 (1937); Davis, Jahn and Burton, *ibid.* **60**, 10 (1938).

[6] H. Henkin and H. A. Taylor, J. Chem. Phys. **8**, 1 (1940).

[7] F. P. Jahn, J. Am. Chem. Soc. **59**, 1761 (1937).

TABLE I.

T °C	Init. Az.	Init. H_2	CH_4 cc	C_2H_6 cc	C_3H_8 cc	Unsat. cc	H_2 cc	N_2 cc	CH_4/N_2	C_2H_6/N_2
				Pure azomethane						
29.7	57.0		3.5	22.4	0.0	0.3	0.0	26.3	0.14	0.85
31.0	54.9		3.0	19.3	0.5	0.3	0.0	23.4	0.13	0.82
56.9	56.8		2.5	11.9	—	0.2	0.0	15.4	0.16	0.76
77.8	59.6		3.4	—	—	—	0.0	17.1	0.20	—
100.0	56.6		8.2	16.1	0.8	0.2	0.0	31.8	0.26	0.51
131.0	70.5		11.4	7.5	0.3	0.0	0.0	33.5	0.37	0.22
168.0	38.2		9.3	1.5	0.3	0.1	0.3	17.9	0.52	0.09
168.0	37.2		8.3	1.4	0.1	0.1	0.0	16.8	0.50	0.08
196.8	36.8		8.2	0.8	—	0.2	0.0	15.4	0.53	0.05
				Azomethane : hydrogen = 3.3 : 1						
22.2	40.6	11.6	0.3	10.4	—	0.3	7.3	11.4	0.03	0.92
75.5	33.8	10.3	1.0	8.2	—	0.1	6.1	10.6	0.09	0.74
100.0	29.3	8.9	1.8	7.2	0.4	0.2	5.2	12.3	0.14	0.58
201.5	23.1	7.1	5.3	0.6	0.1	0.3	4.1	10.2	0.51	0.06
				Azomethane : hydrogen = 3 : 4						
26.5	32.9	45.2	0.5	13.3	0.3	0.2	40.4	17.9	0.03	0.74
27.0	31.5	42.5	0.5	12.1	0.3	0.2	39.5	15.6	0.03	0.77
73.0	29.8	41.7	1.2	7.8	0.0	0.2	40.1	11.3	0.10	0.69
100.0	19.5	26.5	2.1	6.0	0.0	0.1	25.9	13.2	0.16	0.45
100.0	28.2	37.6	2.6	8.4	0.4	0.0	34.0	16.6	0.16	0.51
112.5	35.6	48.2	3.7	6.7	0.3	0.3	42.7	17.7	0.21	0.38
121.0	22.9	32.2	3.1	4.5	0.3	0.3	31.1	11.8	0.26	0.39
123.5	35.5	47.5	5.4	6.1	0.1	0.1	40.1	20.4	0.27	0.30
131.0	34.6	46.8	5.4	4.6	—	0.0	39.9	18.2	0.30	0.26
142.0	19.1	26.2	4.6	1.7	—	0.1	23.3	10.8	0.40	0.16
167.0	29.7	39.9	8.2	1.0	0.1	0.1	32.0	16.6	0.49	0.06
				Azomethane : hydrogen = 1 : 5						
25.3	42.9	214.0	1.0	11.5	0.2	0.4	211.0	17.2	0.05	0.66
100.0	26.5	132.6	3.3	6.5	0.2	0.1	128.3	14.2	0.23	0.46
100.0	22.9	115.0	2.7	5.4	0.0	0.2	112.0	12.4	0.22	0.44
198.0	23.4	117.0	9.8	0.6	0.2	0.1	113.8	13.1	0.75	0.04

gen mixtures are presented in Table I. The volumes given are for the dry gases at room temperature. Since it has been shown[8] that the nitrogen formed is a good measure of the azomethane decomposed, the last two columns in Table I present the amounts of methane and ethane produced per unit amount of azomethane decomposed. In addition to the data in Table I, it should be noted that the amount of condensable liquid was barely perceptible at room temperature but increased in quantity with increase in temperature. In no case however was the amount sufficient for a macro-analysis and since from previous experience and that of others it seems certain that the liquid is a mixture, no micro-analysis was attempted. The test with cupric chloride was applied in each run but no brick red precipitate, indicative of the presence of a hydrazine, was ever observed.

Figures 1 and 2 show plots of the logarithms of the hydrocarbon-nitrogen ratios taken from Table I against the reciprocal of the absolute temperature.

[8] See C. V. Cannon and O. K. Rice, J. Am. Chem. Soc. **63**, 2900 (1941).

DISCUSSION OF RESULTS

The data for pure azomethane agree well with those of Burton, Davis, and Taylor[5] and show an increase in methane production with temperature but a decrease in ethane. From Fig. 2 it can be seen that within experimental error this decrease in ethane production with temperature rise is unchanged by the presence of hydrogen even in fivefold excess. The production of methane, on the other hand, as seen from Fig. 1, is much *lower* at lower temperatures in the presence of hydrogen than in its absence, but increases at a greater rate with temperature rise than for pure azomethane. This decreased production of methane per unit of azomethane decomposed coupled with an unchanged ethane must mean that methyl radicals produced in the photolysis at lower temperatures are reacting in some manner other than to produce methane or ethane when hydrogen is present. This reaction is

probably the addition of CH_3 to azomethane, indirect evidence for which has previously been adduced[5,6] and direct evidence of the comparable addition of hydrogen definitely proven by Henkin and Taylor.[6] The problem, then, is to account for an increased addition in presence of hydrogen.

The work of Eyring and his co-workers[3] has shown that no potential energy barrier exists to the production of the complex CH_5 from CH_3 and hydrogen; a subsequent collision may be necessary for stabilization, but, depending on the hydrogen concentration, a considerable proportion of the methyl radicals will be present as CH_5. Two additional reactions,

$$CH_3+CH_3N=NCH_3\rightarrow(CH_3)_2N-NCH_3, \quad (1)$$

$$CH_5+CH_3N=NCH_3 \rightarrow(CH_3)_2N-NCH_3+H_2, \quad (2)$$

are thus possible. The formation of hydrogen in (2) would serve, by its removal of excess energy, to stabilize the radical so that there results an effective lower concentration of methyl in presence of hydrogen, thus lowering methane production.

Since the production of ethane is independent of the presence of hydrogen and since as just shown the presence of hydrogen does greatly influence the methyl radical concentration, it again appears evident as in the previous work by one of us,[5] that ethane must be produced by some mechanism other than the association of two methyl radicals. The possibility of a molecular split of azomethane into ethane and nitrogen has already been excluded by the work of Davis, Jahn, and Burton[5] and also Jahn and Taylor[9] who observed no alkane formed in presence of nitric oxide. The addition complex $(CH_3)_2N-NCH_3$ is a possible source of ethane. Simple decomposition of this radical into ethane and nitrogen would reproduce a methyl radical. Since the over-all decomposition of azomethane is not a chain reaction (the quantum yield appears to be unity)[8] this decomposition of the radical is improbable and there remains the possibility of a semi-Walden-inversion reaction of the radical with CH_3 to give ethane. Such a reaction would be analogous to the source of ethane in acetone photolysis:[10]

$$CH_3+CH_3CO\rightarrow C_2H_6+CO.$$

It may be remarked in passing that there are two alternatives for this inversion reaction, one producing ethane and the radical $(CH_3)_2N-N-$, which could yield ethane and nitrogen, or one producing ethane and reforming azomethane. This latter might possibly account for the observed quantum yield being less than unity.

The production of methane from pure azomethane increases with temperature as the ethane decreases, while the amount of condensable liquid increases at a rate comparable to that of methane production. The increase in methane at the apparent expense of the ethane suggests its possible formation by a reaction also involving the same addition radical which

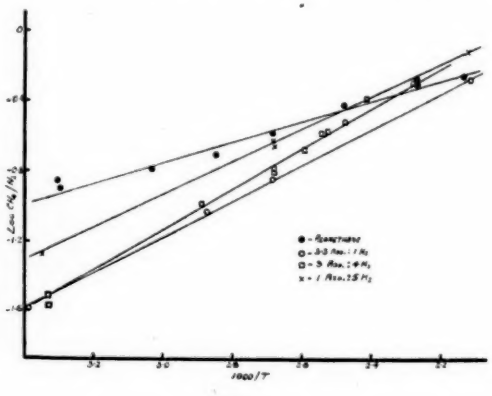

FIG. 1.

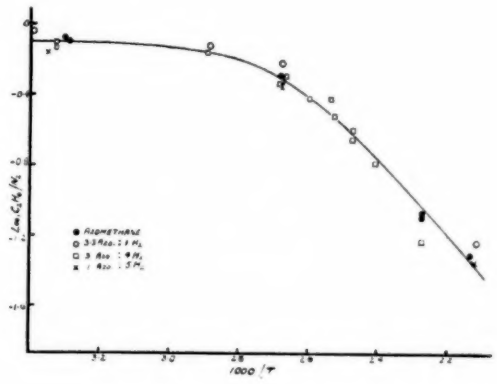

FIG. 2.

[9] F. P. Jahn and H. A. Taylor, J. Chem. Phys. **7**, 474 (1939).

[10] K. W. Saunders and H. A. Taylor, J. Chem. Phys. **9**, 616 (1941).

in over-all might be written:

$$CH_3+(CH_3)_2N-NCH_3\rightarrow CH_4+\text{liquid}.$$

It is not possible with the present evidence to rule out the other alternatives of direct reaction of CH_3 and, in presence of hydrogen, CH_5, with azomethane to produce methane and a product which could also be liquid.

With the radical $(CH_3)_2N-NCH_3$ as a source of both methane and ethane by reaction with CH_3, depending presumably on whether the approach is along a C–H or a C–N bond, the independence of ethane production of the presence of hydrogen is accountable by a balancing of a decreased CH_3 concentration and an increased $(CH_3)_2N-NCH_3$ concentration when hydrogen is present. Furthermore, the increase in the complex radical concentration with the higher hydrogen ratios will favor methane production as observed.

Qualitatively, therefore, the observations are accountable. It is unfortunate that more definite evidence cannot be obtained for the actual reactions producing methane and ethane so that a quantitative interpretation could be made. The slopes of the lines in Fig. 1 are certainly dependent on several activation energies and even the difference of the slopes with and without hydrogen amounting to 2–3 kcal. cannot be interpreted with certainty. It would seem that since the lines of the systems containing hydrogen intersect the pure azomethane line at lower temperatures when the hydrogen concentration is greater, the activation energy for methane production in presence of hydrogen is greater than that in pure azomethane. In presence of hydrogen there are, however, at least two methane producing reactions and probably more.

If the suggested mechanism is correct it should be equally well applicable in other systems which show similar experimental results. The decomposition of mercury dimethyl studied by Cunningham and H. S. Taylor[2] shows great parallelism to the results found here, namely, ethane production is independent of the presence of hydrogen while methane production, which is negligible from mercury dimethyl alone, is increased by hydrogen. The further observation that more mercury dimethyl is decomposed in presence of hydrogen than in its absence was interpreted as indicating a chain mechanism initiated by hydrogen atoms resulting from the interaction of CH_3 and hydrogen. It has already been pointed out by one of us[4] that the authors had neglected to consider the reverse reaction of mercury and methyl. Definite evidence for this has recently been presented by Saunders and H. A. Taylor.[10] On this basis and with the qualitative evidence from the work here reported on azomethane the following scheme for mercury dimethyl decomposition in presence of hydrogen is suggested.

$$Hg(CH_3)_2\rightarrow CH_3+HgCH_3, \quad (1)$$

$$HgCH_3\rightarrow Hg+CH_3, \quad (2)$$

$$CH_3+H_2\rightarrow CH_5, \quad (3)$$

$$CH_5+Hg\rightarrow HgCH_3+H_2, \quad (4)$$

$$CH_3+HgCH_3\rightarrow C_2H_6+Hg, \quad (5)$$

$$CH_5+Hg(CH_3)_2\rightarrow 2CH_4+HgCH_3. \quad (6)$$

Evaluating the stationary concentrations of the radicals involved, yields:

$$d[C_2H_6]/dt=k_1I$$

and

$$\frac{d[CH_4]}{dt}=\frac{2}{(k_4[Hg]/k_6[Hg(CH_3)_2])+1}\times\left(\frac{k_1Ik_2k_3[H_2]}{k_5}\right)^{\frac{1}{2}}.$$

These equations show the rate of ethane production to be independent of hydrogen and of mercury dimethyl, so long as the light absorption is strong, as is found experimentally. The rate of methane production is proportional to the square root of the hydrogen. Since the rate of decomposition of mercury dimethyl is equal to the rate of ethane production plus half the rate of methane production, mercury dimethyl will decompose faster in presence of hydrogen. Cunningham and Taylor claim that methane production is independent of the concentration of mercury dimethyl at a given temperature, while from the above it should decrease as the mercury alkyl decreases. Actually the methane decrease will depend on the mercury concentration as well as that of the alkyl and will thus not be too sensi-

tive. At the same time the data do show evidence of a small decrease in methane production although it may be within the limits of experimental error.

The temperature dependence of methane production judged by the above scheme should involve principally the energies of activation of reactions (5) and (6) since those of the other reactions are probably very small. To a rough approximation then $E_M = E_6 - \frac{1}{2}E_5$. Saunders and Taylor have shown that for the reaction of methyl and mercury dimethyl the activation energy is probably 13–14 kcal.; a value of 13 kcal. for (6) is not improbable. A Walden inversion calculation following Eyring[3] for reaction (5) using 35 kcal. as the bond strength in $HgCH_3$ gives an energy of activation of about 10 kcal. This may be compared with the 6–7 kcal. value for ethane production in acetone. Hence $E_6 - \frac{1}{2}E_5 = 13 - 5 = 8$ in excellent agreement with the 8.1 kcal. observed by Cunningham and Taylor.

It is necessary to add to the above scheme the reactions:

$$CH_5 + CH_3 = 2CH_4, \qquad (7)$$

$$CH_5 + HgCH_3 = 2CH_4 + Hg, \qquad (8)$$

and possibly

$$CH_3 + Hg(CH_3)_2 = C_2H_6 + HgCH_3. \qquad (9)$$

The methane producing reactions (7) and (8) will compete with (6) and would tend to counteract the decrease in methane with decrease in mercury dimethyl. Their inclusion in the general scheme leads, however, to complexity in the evaluation of the stationary concentration terms which cannot easily be resolved.

Ethane production though independent of the presence of hydrogen was found to have a small temperature coefficient equivalent to 1.5 kcal. This was interpreted as indicating a chain mechanism. To include reaction (9) above, which would provide this chain mechanism, with the scheme (1) to (6) leads again to too great complexity However, in absence of hydrogen some simplification is possible, as in the following scheme, since no methane is then observed:

$$Hg(CH_3)_2 = CH_3 + HgCH_3, \qquad (1)$$

$$HgCH_3 = Hg + CH_3, \qquad (2)$$

$$Hg + CH_3 = HgCH_3, \qquad (3)$$

$$CH_3 + HgCH_3 = C_2H_6 + Hg, \qquad (4)$$

$$CH_3 + Hg(CH_3)_2 = C_2H_6 + HgCH_3. \qquad (5)$$

Reactions (1) to (4) alone yield as before $d[C_2H_6]/dt = k_1 I$ but the inclusion of (5) adds a further term

$$+k_5[Hg(CH_3)_2] \times \left(\frac{k_1 k_2 I}{k_3 k_4 [Hg] + k_4 k_5 [Hg(CH_3)_2]}\right)^{\frac{1}{2}}.$$

This latter term, less in importance than the first term, $k_1 I$, will give a temperature dependence to ethane production and also a small dependence on substrate concentration. The data show a small concentration dependence though again it may be within the limits of accuracy. The analysis of the temperature dependence is not simple. However, once again reactions (4) and (5) will be the major ones involved. Neglecting other factors, to a first approximate $E_E = E_5 - \frac{1}{2}(E_4 + E_5)$. Assigning to E_5 and E_4 the probable values 13 and 10 kcal., respectively, $E_E = 1.5$ kcal. as is experimentally observed. The decomposition of mercury dimethyl is thus adequately explained and the similarity of the azomethane scheme lends credence to the suggested mechanism. The reaction of methyl radicals with hydrogen would not appear to involve hydrogen atoms and the *observed*[2] value 9 ± 2 kcal. is complex and in no way specific of methane production from methyl and hydrogen.

Systematics in the Vibrational Spectra of the Halogen Derivatives of Methane

TA-YOU WU
Department of Physics, National University of Peking, Kun-ming, China
(Received August 12, 1940)

On considerations of the symmetry and the approximate nature of the vibrations, the observed infra-red and Raman frequencies of the halogen derivatives of methane are classified and their transitions in passing from one molecule to another in the series $CH_4-CH_3X-CH_2XY-CH_2X_2-CHX_2Y-CHX_3-CX_4$ are given. A potential function of the valence force type containing six constants is suggested for CH_2X_2 and the frequency equations given.

KOHLRAUSCH and Wagner have given recently the genealogical relations of the vibrational frequencies in the series of molecules $CH_4-CH_3X-CH_2XY-CH_2X_2-CHX_2Y-CHX_3-CX_4$, where X, Y are halogen atoms.[1] These relations can be found by first examining the symmetry classes to which the various normal vibrations of the different molecules belong, or, what is the same thing, examining the coordinates involved in the equations of motion for the various vibrations. This by itself is not sufficient for tracing the transitions in the frequencies when in a molecule there is more than one vibration belonging to one symmetry class. It is then necessary to consider the nature of the vibrations in the different molecules by examining the equations giving the various normal vibrations in detail. It appears that the transition curves given by Kohlrausch and Wagner do not satisfy all these considerations. Since the Raman spectrum data for a number of halogen derivatives of methane are now available, we shall reexamine the classification of the observed frequencies of these molecules and their genealogical relations.

TRANSITION RELATIONS

Table I summarizes the symmetry properties and the approximate nature of the normal vibrations of the CH_3X, CH_2X_2, CH_2XY, CHX_2Y molecules.

The descriptions given in Table I for the nature of vibrations are only approximate because of the coupling between the motions of the various atoms. They serve to guide us, however, in estimating the spectral regions in which the frequencies will lie. Now the next problem is to find the relation between the vibrations of one molecule and those of another of a different symmetry class. For the transition CH_4-CH_3X where X is a halogen atom, it has been shown by Wagner from a calculation of the frequencies of CH_3X in which the mass of X is varied from small to large values that $\nu_1(1)$ of CH_4 goes over to $\nu_3(\|)$ of CH_3X, while $\nu_3(3)$ splits into $\nu_1(\|)$ and $\nu_2(\perp)$.[2] For the transition from CH_3X to CH_2X_2, it follows from the calculations of Rosenthal on the isotopic molecule YX_2X_2* that the $4A_1$ vibrations are derived from 3 $\perp$ and one $\|$ vibrations of CH_3X; the $2B_1$ (or B_2) vibrations from 2 $\perp$ vibrations; the $2B_2$ (or B_1) from 2 $\|$ vibrations; and the A_2 from a $\perp$ vibration.[3] For the transition $CHX_3-CH_2X_2$, the same holds after interchanging B_1 and B_2. In passing from CH_2X_2 to CH_2XY, it is evident that the $4A_1$ and the $2B_2$ vibrations pass over into the $6A$ vibrations while the A_2 and the $2B_1$ pass into the $3B$ vibrations. On the other hand, for the transition $CH_2X_2-CHX_2Y$, the $4A_1$ and the $2B_1$ vibrations pass over into the $6A'$ while the A_2 and the $2B_2$ pass into the $3B'$ vibrations.[4]

Now the exact relations of the frequencies in the transitions $CH_3X-CH_2XY-CH_2X_2-CHX_2Y-CHX_3$ must be obtained from a

[1] K. W. F. Kohlrausch and J. Wagner, Zeits. f. physik. Chemie **B45**, 93 (1939).

[2] J. Wagner, Zeits. f. physik. Chemie **B40**, 36 (1938). This calculation is interesting since according to Dennison, Rev. Mod. Phys. **3**, 280 (1931), one would expect $\nu_1(1)\rightarrow\nu_1(\|)$ and $\nu_3(3)\rightarrow\nu_2(\perp)$ and $\nu_3(\|)$; or according to the tables of frequencies for the deuteromethanes given by Johnston and Dennison, Phys. Rev. **47**, 94 (1935) and by Benedict *et al*, J. Chem. Phys. **5**, 1 (1937), $\nu_1(1)\rightarrow\nu_1(\|)$ and $\nu_3(3)\rightarrow\nu_2(\perp)$ and $\nu_5(\|)$.

[3] J. Rosenthal, Phys. Rev. **45**, 538, 766; **46**, 730 (1934).

[4] Kohlrausch and Wagner, reference 1, connected 2 of the A_1 vibrations of CH_2X_2 to the parallel vibrations in CH_3X. This is obviously not correct according to the equations of motion of Rosenthal.

calculation of the frequencies of CH_2XY in which the mass of Y is varied from that of H to that of X, and at the same time appropriate account is taken of the variations in the force constants. Such a calculation would be very lengthy as the $6A$ and the $3B$ vibrations are given by equations of the sixth and the third degrees, respectively. Without going through such a calculation, it is still possible to arrive at the correct transition relations in the following manner. When the assignments of the fundamental frequencies in CH_3X and CHX_3 are known, we seek to arrange the $4A_1$, $2B_1$, $2B_2$ and the A_2 frequencies of CH_2X_2 in such an order that in addition to satisfying all the above symmetry requirements, we further require that the 6 transition lines through the A vibrations of CH_2XY must not cross one another, and similarly for the 3 lines through the B vibrations, although the lines in one group may cross those of the other. Similarly for the transition $CH_2X_2-CHX_2Y-CHX_3$. This, however, is not sufficient for uniquely determining the order of the 9 vibrations of CH_2X_2. Of the many possible orders the correct one is that which must in addition agree with the order of magnitude of the frequencies expected from the nature of the vibrations. Thus the correct tracing of the frequency transitions depends on the correct assignments of the observed frequencies which in turn necessitate adequate polarization data for the Raman spectra and a knowledge of the contours of the infra-red absorption bands. On these considerations, the frequency transitions for the series $CH_4-CH_3X-CH_2XY-CH_2X_2-CHX_2Y-CHX_3-CX_4$ are given in Table II and Figs. 3 and 4.

ASSIGNMENTS OF FREQUENCIES

The observed infra-red and Raman frequencies of the halogen derivatives of methane are summarized in Table II and Fig. 2.[5] The assignments of the fundamental frequencies of the CH_3X, CHX_3, CX_4, CX_3Y, CX_2Y_2 molecules are quite certain on the basis of the polarization data and the trend of the frequencies in passing through

TABLE I. Normal vibrations in CH_3X, CH_2X_2, CH_2XY, CHX_2Y type molecules. s=sym., a=antisym., d=degenerate, $\sigma(CH_2)$=plane of CH_2, etc.

Molecule	Symmetry		Notation	Approximate nature of vibration
	Axis			
CH_3X (or CHX_3)	s		$A\ \nu_1(\parallel)$	$\parallel$ valence vib. in CH_3 (or CX_3)
	s		$A\ \nu_3(\parallel)$	$\parallel$ deformation vib. in CH_3 (or CX_3)
	s		$A\ \nu_5(\parallel)$	valence vib. in C−X (or C−H)
	d		$E\ \nu_2(\perp)$	$\perp$ valence vib. in CH_3 (or CX_3)
	d		$E\ \nu_4(\perp)$	$\perp$ deformation vib. in CH_3 (or CX_3)
	d		$E\ \nu_6(\perp)$	deformation vib. of X−CH_3 (or H−CX_3)
	$\sigma(CH_2)$	$\sigma(CX_2)$		
CH_2X_2	s	s	$A_1\ \nu_1(s)$	sym. valence vib. in CH_2
	s	s	$A_1\ \nu_2(s)$	sym. valence vib. in CX_2
	s	s	$A_1\ \delta_1(s)$	sym. deformation vib. in CH_2
	s	s	$A_1\ \delta_2(s)$	sym. deformation vib. in CX_2
	s	a	$B_1\ \nu_1(a)$	antisym. valence vib. in CH_2
	s	a	$B_1\ \delta_1(a)$	bending of CH_2 group in its plane
	a	s	$B_2\ \nu_2(a)$	antisym. valence vib. in CX_2
	a	s	$B_2\ \delta_2(a)$	bending of CX_2 group in its plane
	a	a	$A_2\ \delta$	torsional vib. about sym. axis
	σ(CXY)			
CH_2XY	s		$A\ \nu_1(s),\ \nu_2(s),\ \nu_3(s)$,	valence vib. in CH_2, C−X, C−Y, respectively
	s		$A\ \delta_1(s),\ \delta_2(s),\ \delta_3(s)$,	deformation vib. in CH_2, CXY, and bending of CXY in its plane, respectively
	a		$B\ \nu_1(a)$	antisym. valence vib. in CH_2
	a		$B\ \delta_1(a)$	bending of CH_2 in its plane
	a		$B\ \delta$	torsional vib.
	σ(CHY)			
CHX_2Y	s		$A'\ \nu_1(s),\ \nu_2(s),\ \nu_3(s)$,	valence vib. in CX_2, C−H, C−Y, respectively
	s		$A'\ \delta_1(s),\ \delta_2(s),\ \delta_3(s)$,	deformation vib. in CX_2, CHY, and bending of CHY in its plane, respectively
	a		$B'\ \nu_1(a)$	antisym. valence vib. in CX_2
	a		$B'\ \delta_1(a)$	bending of CX_2 in its plane
	a		$B'\ \delta$	torsional vib.

[5] The sources of the observed data are the following:
CH_2F_2, Glockler and Leader, J. Chem. Phys. **7**, 382 (1939).
CH_2FCl, Glockler and Bachmann, Phys. Rev. **55**, 1273 (1939).
CH_2Cl_2, Cabannes et Rousset, Ann. de physique **19**, 229 (1933); Trumpy, Zeits. f. Physik **88**, 226 (1934); Kohlrausch and Ypsilanti, Zeits. f. physik. Chemie **B29**, 274 (1935); infra-red data from Corin and Sutherland, Proc. Roy. Soc. **A165**, 43 (1938).
CH_2Br_2, Cabannes et Rousset, *ibid.*; Trumpy, Zeits. f. Physik **90**, 133 (1934); **100**, 250 (1936); Kohlrausch and Ypsilanti, *ibid.*
CH_2ClBr, CH_2BrI, CH_2I_2, Bacher and Wagner, Zeits. f. physik. Chemie **B43**, 191 (1939); polarization data from Kohlrausch and Wagner, reference 1.
CHF_3, Glockler and Edgell, J. Chem. Phys. **9**, 224 (1941).
$CHFCl_2$, CF_2Cl_2, Bradley, Phys. Rev. **40**, 908 (1932); Glockler, Edgell and Leader, J. Chem. Phys. **8**, 897 (1940); Glockler and Edgell, *ibid.* **9**, 224 (1941).
CHF_2Cl, Glockler and Bachmann, Phys. Rev. **55**, 669 (1939); Glockler and Leader, J. Chem. Phys. **8**, 125, 669 (1940).
$CHFClBr$, $CHFBr_2$, Glockler and Leader, J. Chem. Phys. **8**, 125, 669 (1940).
$CHCl_2Br$, Emschwiller and Lecomte, J. de phys. et rad. **8**, 130 (1937).
$CHClBr_2$, Glockler and Leader, J. Chem. Phys. **7**, 553 (1939).
$CFCl_3$, Glockler and Leader, *ibid.* **7**, 278 (1939).
CCl_3Br, $CClBr_3$, Lecomte, Volkringer and Tchakirian, Comptes rendus **204**, 1927 (1937).
CCl_2Br_2, Lecomte, Volkringer and Tchakirian, J. de phys. et rad. **9**, 105 (1938).
For other molecules see Kohlrausch's *Smekal-Raman Effekt* and the paper of Cabannes and Rousset.

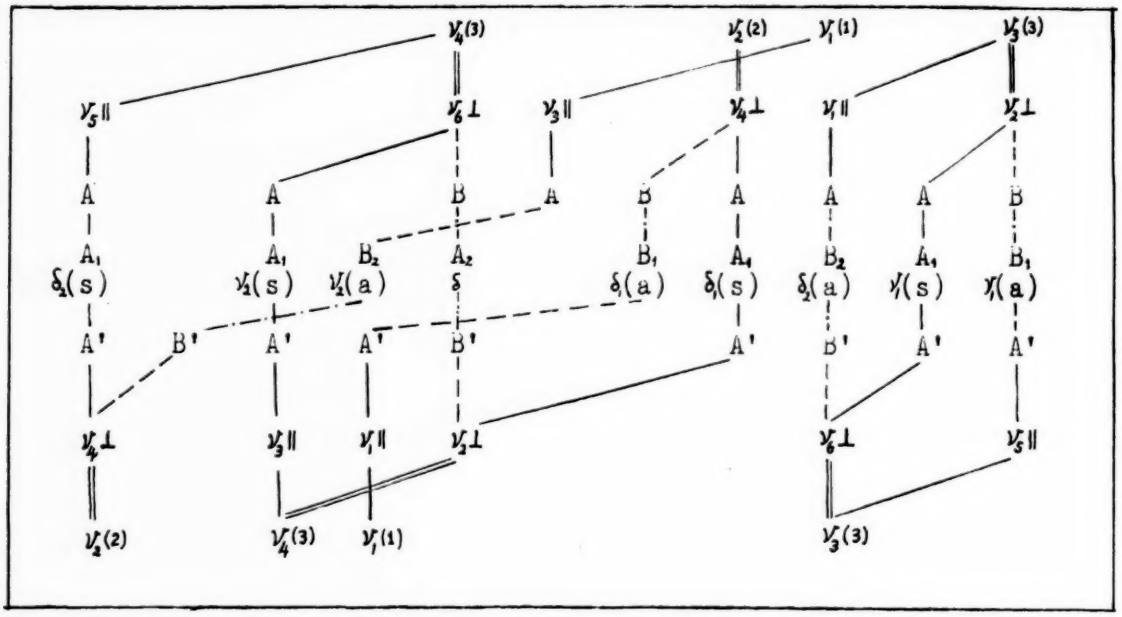

FIG. 1. Frequency transitions in $CH_4-CH_3X-CH_2XY-CH_2X_2-CHX_2Y-CHX_3-CX_4$; doubled lines connect doubly degenerate vibrations, see Table I.

each series of molecules. The major uncertainties are in the assignments in the group of dihalogen derivatives. Previous discussions of the fundamental frequencies of these molecules by various authors[6] do not seem satisfactory in view of the polarization data and of the more recent observations on CH_2F_2, CH_2FCl, CH_2ClBr, CH_2BrI and CH_2I_2. The situation can now be summarized as follows: There is little doubt as to the correctness of the assignments of the $\nu_1(s)$, $\nu_1(a)$, $\nu_2(s)$ and $\delta_1(s)$ frequencies in CH_2X_2 on consideration of both their order of magnitude and their polarization characters. One expects $\nu_2(a)$ to be slightly higher than $\nu_2(s)$. The assignments of the 5 lines in $CH_2Cl_2-CH_2I_2$ in Table II and Fig. 2 to $\nu_2(a)$ are based on this consideration and the fact that the line is polarized in CH_2ClBr and depolarized in CH_2Cl_2 and CH_2Br_2, in agreement with the symmetry requirement as seen in Table I and Fig. 1. That the $\nu_2(s)$ and $\nu_2(a)$ are more widely separated in CH_2ClBr than in CH_2Cl_2 and CH_2Br_2 is understandable since in CH_2ClBr they become $\nu_2(s)$ and $\nu_3(s)$ and are more nearly the valence vibrations in C−Cl and C−Br. That the corresponding lines in CH_2FCl and CH_2F_2 are not observed may be due to low intensities. For the $\delta_1(a)$ frequencies, we take the series of lines shown in Fig. 2 and Table II for the following reasons: (1) $\delta_1(a)$, being a B_1 vibration as $\nu_1(a)$ in CH_2X_2, should appear depolarized in CH_2XY and this is now the case with CH_2ClBr. (2) The $\delta_1(a)$ involves essentially changes in the angle between the C−H bond and the CX_2 plane and may be compared with the similar vibrations in $C_2H_2Cl_2$, etc., which are of the order 1050 cm^{-1}.[7] Also the deformation vibration of the CHCl radical is of the order 1200 cm^{-1}.[8] $\delta_1(s)$ should be polarized. The strong line at 1261 cm^{-1} in CH_2F_2, the polarized lines at 1060 cm^{-1} in CH_2Cl_2 and 1030 cm^{-1} in CH_2ClBr and the very weak line at 944 cm^{-1} in CH_2BrI seem to be in the correct positions. The objection to this

[6] For CH_2Cl_2, Corin and Sutherland, reference 5. For CH_2Cl_2, CH_2Br_2, CH_2I_2, Emschwiller and Lecomte, reference 5; Barchewitz and Parodi, J. de phys. et rad. **10**, 143 (1939). The assignment given in the last paper does not even satisfy the symmetry requirements. Assignments for CH_2Cl_2, CH_2Br_2, CH_2ClBr are also given by Kohlrausch and Wagner, reference 1. See footnotes 4 and 10. The assignments given by Wu in *Vibrational Spectra and Structure of Polyatomic Molecules* (Prentice-Hall, New York, 1939), must also be partly modified as shown in this paper.

[7] T.-Y. Wu, J. Chem. Phys. **7**, 965 (1939), there denoted as $\delta(CH_2)$.

[8] T.-Y. Wu, J. Chem. Phys. **5**, 392 (1937).

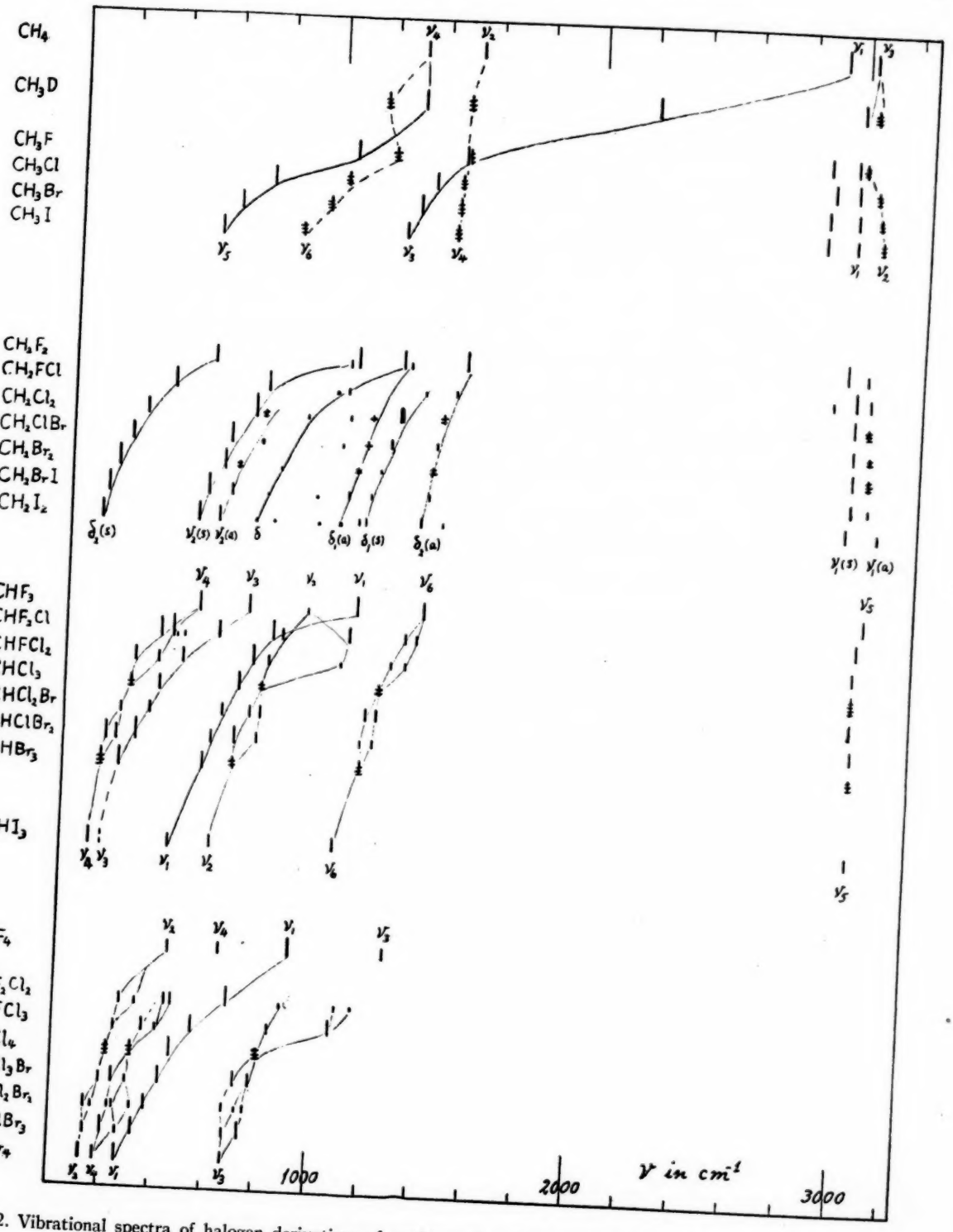

FIG. 2. Vibrational spectra of halogen derivatives of methane. For those molecules for which polarization data are available, depolarized lines are crossed with bars while polarized ones are not.

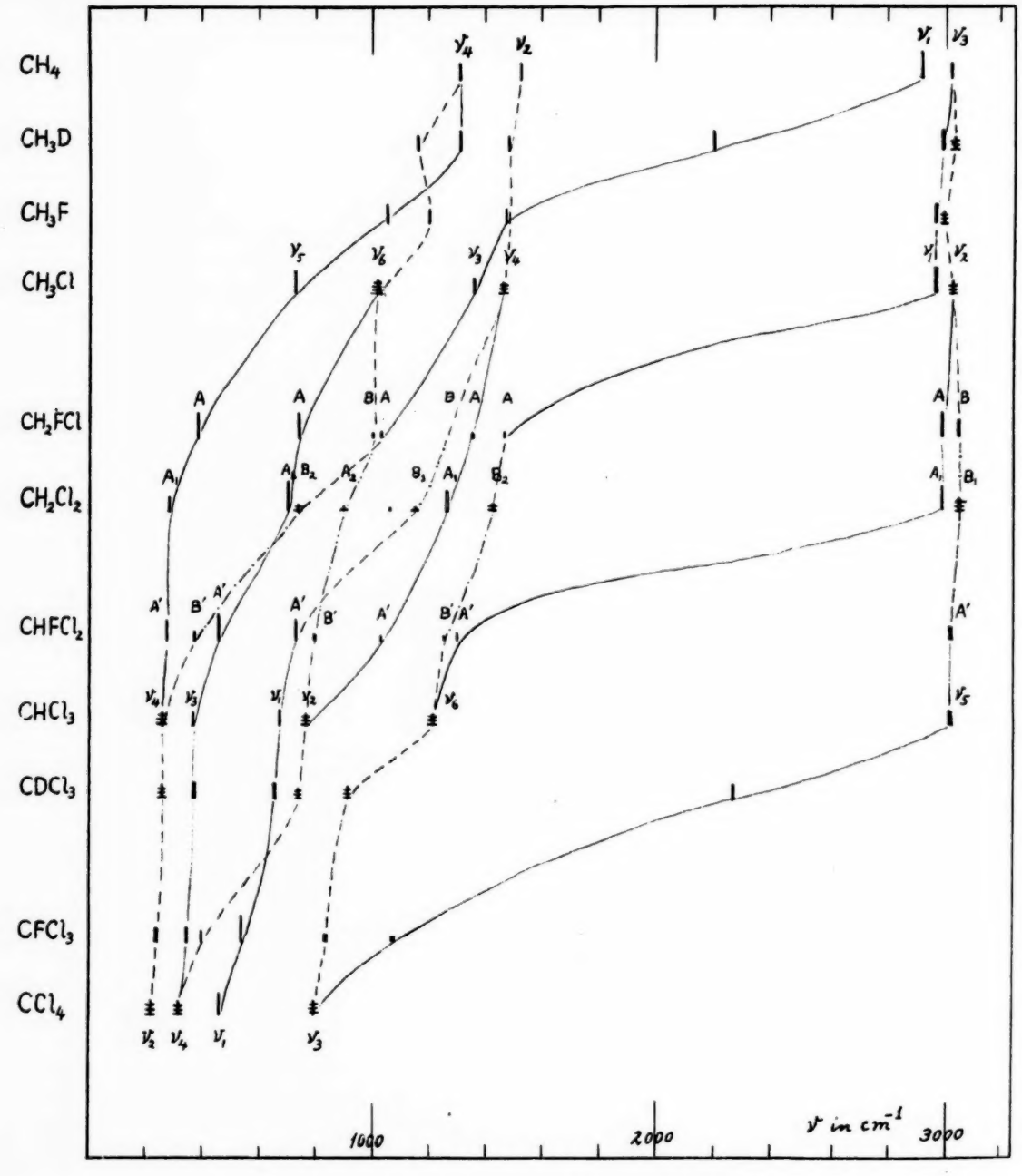

FIG. 3. Frequency transitions in $CH_4-CH_3Cl-CH_2Cl_2-CHCl_3-CCl_4$.

assignment is that the last 3 lines are all very weak and the corresponding lines in the other molecules have not been observed. Perhaps the more satisfactory alternative is to take as $\delta_1(s)$ the series of lines corresponding to the infra-red 1266 cm^{-1} band in CH_2Cl_2. The arguments in favor of this choice are: (1) the corresponding lines in CH_2ClBr and CH_2Br_2 are polarized, and (2) the 1266 cm^{-1} band appears by far more intense than the other bands in the infra-red.[9]

[9] Corin and Sutherland, reference 5. They explain the 1149 cm^{-1} line of CH_2Cl_2 as the difference frequency

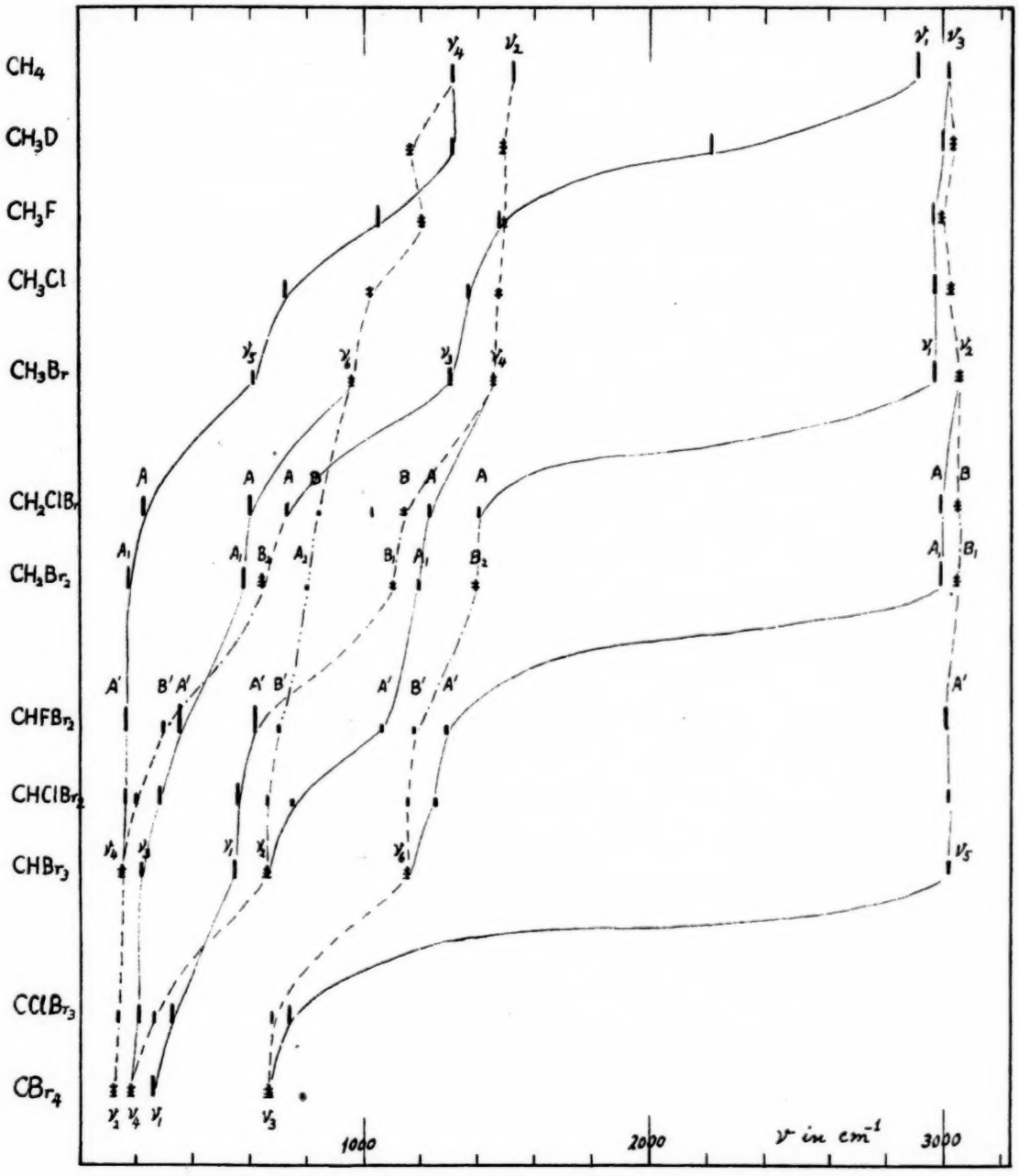

FIG. 4. Frequency transitions in $CH_4-CH_3Br-CH_2Br_2-CHBr_3-CBr_4$.

The objection is that it has not been observed in the Raman spectrum.

We are then left with 3 unassigned series of lines (Fig. 2) and 2 series of vibrations $\delta_2(a)$ and δ. $\delta_2(a)$, being a B_2 vibration in CH_2X_2 and an A vibration in CH_2XY, should be depolarized in the former and polarized in the latter. The series of lines at *ca.* 1400 cm^{-1} would fit in very well with the selection rules if the 1403 cm^{-1} line of CH_2ClBr is polarized, as indicated in the diagram

1425–283. Although the assignments of some 20 infra-red bands on this assumption are satisfactory, the existence in the other dihalogen methanes of frequencies corresponding to it seems to favor its being a fundamental rather than a difference frequency.

TABLE II. Fundamental frequencies of halogen derivatives of methane. The frequencies for CH_3D, CH_3Cl, CH_3F, CH_3Br, CH_3I are from the infra-red absorption spectra; the rest are Raman effect data, reference 5.

CH_4									ν_4	1306			ν_2	1520			ν_1	2915			ν_3	3020
CH_3D		1307								1156		2205		1477				2983				3031
CH_3F	ν_5	1049							ν_6	1200	ν_3	1476	ν_4	1476			ν_1	2965			ν_2	2987
CH_3Cl		732								1020		1355		1460				2967				3047
CH_3Br		610								957		1306		1450				2973				3061
CH_3I		532								885		1252		1445				2971				3074
CH_2F_2		532		1078		?				1261		1294		?				1508		2964		3029
CH_2FCl	A	385	A	743	A	?			B	1004	B	?	A	1352			A	1468	A	2993	B	3048
CH_2Cl_2	A_1	284p	A_1	700p	B_2	736d			A_2	896	B_1	1149d	A_1	1266			B_2	1425d	A_1	2985p	B_1	3046d
CH_2ClBr		226p		603p		726p				?		1130d		1224p				1403p?		2986p		3054d
CH_2Br_2		173p		576p		638d				806		1090d		1183p?				1390d		2988p		3054d
CH_2BrI		144		517		616				754		1065		1150				1374		2978		3053
CH_2I_2		120		487		565				713		1027		1130				1350		2970		3091
CHF_3			508			697					937			1116					1376			3062
CHF_2Cl	A'	369	B'	416	A'	596			B'	831	A'	1099	A'	800			B'	1310	A'	1355	A'	3032
$CHFCl_2$		277		366		457				796		1065		730				1255		1309		3019
$CHCl_3$			262			366					761			668					1215			3019
$CHCl_2Br$		?		217		329				719		760		602				1170		1214		3020
$CHBr_2Cl$		168		201		279				658		749		569				1145		1194		3022
$CHBr_3$			154			222					655			539					1144			3021
CHI_3			ν_4	112	ν_3	?					ν_2	576	ν_1	416					ν_6	1053	ν_5	3020
CF_4			437							630				904						1265		
CF_3Cl			?			?				?				?				?		?		
CF_2Cl_2		260		320		433				455		—		664				877		1083		1147
$CFCl_3$			244							349		387		535						833		1067
CCl_4			217							313				459						790		
CCl_3Br			187			243				289				418				710		765		
CCl_2Br_2		141		164		230				250		318		370				670		720		750
$CClBr_3$			139							210		266		326						674		734
CBr_4			125							183				265						667		
			ν_2 (2)						ν_4 (3)				ν_1 (1)						ν_3 (3)			

of Kohlrausch and Wagner.[10] If it is depolarized, then this assignment must be abandoned. Hence the polarization character of this line is of the greatest importance in deciding the assignment.

The δ vibration should be depolarized in all the molecules CH_2X_2 and CH_2XY and inactive in absorption in CH_2X_2. Here we meet with a difficulty that all the 3 series of unassigned lines have been observed also in the infra-red.[5] Assigning tentatively either one of the two remaining series to δ, we find it difficult to account for the other in a simple manner. Here we have assigned the series of weak lines corresponding to the 896 cm^{-1} in CH_2Cl_2 as δ rather than the series corresponding to 1060 cm^{-1} in CH_2Cl_2, for the reason that the transition curve from ν_6 of CH_3X through δ of CH_2X_2 to ν_2 of CHX_3 is smoother with the former choice than with the latter, as seen in Fig. 3.

[10] The Raman lines at *ca.* 1400 cm^{-1} in CH_2Cl_2 and CH_2Br_2 are given as polarized in Kohlrausch and Wagner's diagrams and are taken as one of the A_1 vibrations in each molecule. That these lines are depolarized has been shown by Cabannes and Rousset, by Trumpy and by Kohlrausch and Ypsilanti (see reference 5). Since no new measurements are mentioned, it appears that these are due to some slips in Kohlrausch and Wagner's work. The 1403 cm^{-1} line of CH_2ClBr is also drawn as polarized in their diagrams; but in view of the discrepancies in the case of CH_2Cl_2 and CH_2Br_2 we must regard the polarization character of this line as questionable.

In Figs. 3 and 4, we give the transition curves for the two series CH_4-CCl_4 and CH_4-CBr_4 on the basis of the assignments discussed above. It is seen that the transition curves satisfy all the symmetry requirements discussed earlier. All the polarization data available and the intensity data are consistent with our scheme. It can be shown, however, that changing the assignments of the CH_2Cl_2 frequencies to the following order

A_1	A_1	B_2	B_1	A_1	B_2	A_2	A_1	B_1
$\delta_2(s)$	$\nu_2(s)$	$\nu_2(a)$	$\delta_1(a)$	$\delta_1(s)$	$\delta_2(a)$	δ	$\nu_1(s)$	$\nu_1(a)$
284p	700p	736d	896d	1060p	1266Inf	1425d	2985p	3046d

also satisfies the same symmetry requirements but leads to a different set of transition curves. It does not seem possible to rule out entirely this and other possible schemes on the basis of the data now available. More detailed study of the polarization of the Raman lines, especially in the case of CH_2F_2, CH_2FCl, CH_2ClBr, CH_2BrI, CH_2I_2, would be necessary. An investigation of the infra-red spectra of CH_2F_2, CH_2Cl_2, etc., under higher dispersion would be very useful, since from the contours of the absorption bands it would be possible to distinguish between vibrations with changes of the electric moment of inertia along the axes of greatest intermediate and smallest moments of inertia corresponding to the B_1, A_1, B_2 vibrations, respectively.

VALENCE FORCE TREATMENT OF CH_2X_2 TYPE MOLECULES

For the purpose of studying the motion of the CH_2X_2 type molecules, it is desirable to have a normal coordinate treatment with a potential containing only a few constants. General functions of the type employed by Rosenthal and Voge for the CH_3X type molecules would be quite complicated. Since the methyl halides can be satisfactorily described by a potential of the valence force type and since the CClH radical can also be approximately described by a valence potential,[8] we propose the following potential for the dihalogen methanes.

$$\begin{aligned}2V&=2k_1(\delta r_1)^2+k_{\theta 1}(r_1\delta\theta_1)^2+2k_{\varphi 1}(s_1\delta\varphi_1)^2\\&\quad+2k_2(\delta r_2)^2+k_{\theta 2}(r_2\delta\theta_2)^2+2k_{\varphi 2}(s_2\delta\varphi_2)^2\\&=2k_1(\delta r_1)^2+k_{\alpha 1}(r_1\delta\theta_1)^2+2k_2(\delta r_1)^2+k_{\alpha 2}(r_2\delta\theta_2)^2\end{aligned}$$

where

$$k_{\alpha 1}=k_{\theta 1}+\tfrac{1}{2}(s_1/r_1)^2k_{\varphi 1},\quad k_{\alpha 2}=k_{\theta 2}+\tfrac{1}{2}(s_2/r_2)^2k_{\varphi 2}.$$

Here r_1, r_2 are the $M-m_1$ and $M-m_2$ bond distances, and ϑ_1, ϑ_2 the $\angle m_1Mm_1$ and $\angle m_2Mm_2$ bond angles, respectively; φ_1 is the angle which $M-m_1$ makes with the m_1-M-m_1 plane, φ_2 that which $M-m_2$ makes with the m_2-M-m_2 plane, so that $\vartheta_1+2\varphi_1=2\pi$, $\vartheta_2+2\varphi_2=2\pi$. s_1, s_2 are quantities having the dimensions of length. For brevity the two terms for the two $M-m_1$ (and $M-m_2$) valence bonds have been written together. It can be shown that for the 4 totally symmetrical A_1 vibrations, the determinantal equation reduces to

$$\begin{vmatrix} P_1\lambda-2k_1 & Q_1\lambda-2k_1\sin\dfrac{\vartheta}{2} & W\cos\dfrac{\vartheta_1}{2}\cos\dfrac{\vartheta_2}{2}\lambda & 0 \\ & R_1\lambda-2k_1\sin^2\dfrac{\vartheta_1}{2}-4k_{\alpha 1}\cos^2\dfrac{\vartheta_1}{2} & 0 & 0 \\ & & P_2\lambda-2k_2 & Q_2\lambda-2k_2\sin\dfrac{\vartheta_2}{2} \\ & & & R_2\lambda-2k_2\sin^2\dfrac{\vartheta_2}{2}-4k_{\alpha 2}\cos^2\dfrac{\vartheta_2}{2}\end{vmatrix}=0$$

which is symmetrical with respect to the diagonal and where

$$P_i=2m_i\left(1+\frac{2m_i}{S}\sin^2\frac{\vartheta_i}{2}\right),$$

$$Q_i=P_i\sin\frac{\vartheta_i}{2}+\frac{4m_i^2}{S}\cos\frac{\vartheta_i}{2},$$

$$R_i=2m_i+\frac{2m_i^2}{S}(1+\cos^2\vartheta_i+2\sin\vartheta_i),\quad i=1,2,$$

$$W=4m_1m_2(2M+S)/S^2,\quad S=M+2m_1+2m_2.$$

For the B_1 vibrations in which the change of the electric moment is parallel to the axis in the m_1-M-m_1 plane, the determinantal equation gives[11]

$$\lambda_5+\lambda_6=C_1k_1+\left(\frac{B_1}{a_1^2}+\frac{2A_1}{b_1^2}+\frac{2L_1}{a_1b_1}\right)k_{\varphi 1}s_1^2,$$

$$\lambda_5\lambda_6=\left(\frac{G_1}{a_1^2}+\frac{2F_1}{b_1^2}+\frac{2L_1}{m_1a_1b_1}\right)k_1k_{\varphi 1}s_1^2$$

where

$$A_1=(M+2m_2)/2Mm_2,\quad B_1=\frac{1}{m_1}+\frac{2}{M}\cos^2\frac{\vartheta_1}{2},$$

[11] The two B_1 vibrations can be regarded as the two perpendicular planar vibrations ν_4, ν_5 of the formaldehyde type molecule $X_2C-(Y_2)$ and the B_2 vibrations are those of $Y_2C-(X_2)$. See Wu, reference 6, pp. 244–5. The frequency equations are hence directly obtainable from those for the formaldehyde molecule, see Lechner, Wien. Ber. **141**, 633 (1932), after making a proper change in the masses of the particles.

$$C_1=\frac{1}{m_1}+\frac{2}{M}\sin^2\frac{\vartheta_1}{2}, \qquad F_1=C_1/2m_2+1/Mm_1,$$

$$G_1=(M+2m_1)/Mm_1^2, \qquad L_1=\frac{2}{M}\cos\frac{\vartheta_1}{2},$$

a_1 = equilibrium value of r_1,

$$b_1=r_2\cos\frac{\vartheta_2}{2}.$$

For the B_2 vibrations in which the change of the electric moment is parallel to the axis in the m_2-M-m_2 plane, the frequency equations are the same as above but with the subscripts 1 and 2 interchanged throughout. All the above equations simplify somewhat on assuming tetrahedral angles so that

$$\cos^2\frac{\vartheta_1}{2}=\cos^2\frac{\vartheta_2}{2}=\frac{1}{3}.$$

From the eight frequencies ($4A_1$, $2B_1$, $2B_2$), it should be possible to determine the six constants in V and still have two relations as a check. It is proposed to apply these results to the CH_2F_2, etc., molecules when the final assignments of the fundamental frequencies are available.

FEBRUARY, 1942 JOURNAL OF CHEMICAL PHYSICS VOLUME 10

The Variation of the Transference Numbers of Sodium Chloride in Aqueous Solution with Temperature. II

R. W. ALLGOOD AND A. R. GORDON
Chemistry Department, University of Toronto, Toronto, Canada
(Received November 18, 1941)

The transference numbers of sodium chloride in aqueous solution at temperatures from 15° to 45° for concentrations up to 0.1N have been determined by the moving boundary method; both anion and cation boundaries were employed. The results for 25° are in close agreement with those of Longsworth. The Longsworth function $t_+^{0\prime}$ is linear in the concentration for the more dilute range at all temperatures, thus permitting a satisfactory extrapolation to infinite dilution, but shows definite deviations from linearity for the more concentrated. The transference numbers for sodium chloride and those previously obtained for potassium chloride, combined with the conductance data reported in the accompanying paper, yield values of the ionic mobilities for the whole temperature range.

AN earlier paper[1] from this laboratory reported the transference numbers for potassium chloride in aqueous solution for concentrations from 0.01 to 0.10N at temperatures from 15° to 45°C; here we give similar data for sodium chloride. By combining the transference numbers for the two salts with the conductance measurements reported in the accompanying paper,[2] it is possible to obtain mobilities for the three ions involved for the whole range of temperature.

The experimental procedure was the same as that for potassium chloride. Ascending autogenic cation boundaries with cadmium chloride as indicator, ascending anion boundaries with sodium bromate or iodate as indicator, and descending anion boundaries with sodium acetate as indicator were employed. The measurements with descending boundaries were carried out in a sheared junction cell similar to cell III (see Fig. 1 of reference 1) but with the hollow stopcock S at the top instead of at the bottom of the graduated tube T. The sodium chloride was B.D.H. Analar, precipitated by hydrogen chloride, twice recrystallized from conductivity water, and rapidly fused in platinum in an atmosphere of dry nitrogen; the solutions were made up gravimetrically using a good grade of conductivity water. The sodium bromate and

[1] R. W. Allgood, D. J. LeRoy, and A. R. Gordon, J. Chem. Phys. **8**, 418 (1940).
[2] H. E. Gunning and A. R. Gordon, J. Chem. Phys. **10**, 126 (1942).

iodate were B.D.H. Analar twice recrystallized, while the sodium acetate solutions were made by the method of MacInnes and Shedlovsky.[3] The cadmium serving as anode was found by spectroscopic analysis to contain not more than 0.01 percent of any impurity. All weights are corrected to vacuum, and in computing volume from mass concentrations, the density data of *International Critical Tables* were employed.[4]

TABLE I.

Cell	C	$t_{\pm}$obs.	Sol.+Vol. Corr.	t_+
		15° centigrade		
II	0.014950	0.3872	+0.0003	0.3875
II	.015081	.3875	+0.0003	.3878
II	.019990	.3866	+0.0003	.3869
II	.020186	.3867	+0.0003	.3870
IIIi	.040046	.6146	+0.0002	.3852
II	.040090	.3851	+0.0002	.3853
II	.040299	.3851	+0.0002	.3853
IIIi	.065324	.6162	0.0000	.3838
IIIi	.065324	.6164	0.0000	.3836
II	.065324	.3839	+0.0001	.3840
II	.066162	.3838	+0.0001	.3839
II	.09944	.3817	+0.0001	.3818
II	.09994	.3816	+0.0001	.3817
II	.10034	.3819	+0.0001	.3820
		25° centigrade		
II	.015024	.3908	+0.0002	.3910
II	.015024	.3909	+0.0002	.3911
II	.019965	.3898	+0.0002	.3900
II	.019965	.3899	+0.0002	.3901
II	.029132	.3892	+0.0002	.3894
II	.029132	.3890	+0.0002	.3892
II	.059853	.3873	+0.0001	.3874
IIIb	.059853	.6126	0.0000	.3874
IIIb	.059853	.6127	0.0000	.3873
II	.09975	.3852	+0.0001	.3853
II	.09975	.3853	+0.0001	.3854
IIIb	.10028	.6149	−0.0001	.3852
IIIi	.10028	.6146	−0.0001	.3855
		35° centigrade		
II	.014973	0.3944	+0.0004	0.3948
II	.014984	.3945	+0.0004	.3949
II	.019870	.3938	+0.0003	.3941
II	.019904	.3940	+0.0003	.3943
II	.032643	.3933	+0.0001	.3934
II	.033180	.3931	+0.0001	.3932
II	.040225	.3925	+0.0001	.3926
IV	.059196	.6086	+0.0001	.3913
IV	.059196	.6085	+0.0001	.3914
II	.059823	.3914	+0.0001	.3915
II	.064984	.3911	+0.0001	.3912
II	.098166	.3892	+0.0000	.3892
IV	.10045	.6109	0.0000	.3891
IV	.10806	.6116	0.0000	.3884
IV	.10806	.6118	0.0000	.3882
		45° centigrade		
II	.014926	.3985	+0.0003	.3988
II	.015020	.3985	+0.0003	.3988
II	.018089	.3981	+0.0002	.3983
II	.019856	.3979	+0.0002	.3981
II	.032514	.3969	+0.0001	.3970
II	.033162	.3968	+0.0001	.3969
II	.059600	.3950	+0.0001	.3951
II	.060296	.3950	+0.0001	.3951
II	.09905	.3932	0.0000	.3932
II	.09932	.3934	0.0000	.3934

[3] D. A. MacInnes and T. Shedlovsky, J. Am. Chem. Soc. **54**, 1429 (1932).

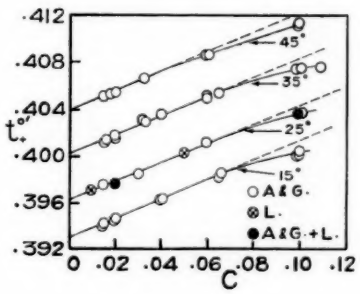

FIG. 1.

Table I gives the results. In the first column, II indicates the autogenic cell for cation boundaries, IIIb and IIIi the sheared cell with ascending anion boundary, employing sodium bromate or iodate, respectively, as indicator; IV means the cell with descending anion boundary and sodium acetate as indicator. In all measurements with anion boundaries, the cadmium anode served as the closed side of the cell so that the volume correction ΔV is given by

$$\Delta V = t_+ \cdot \bar{V}_{NaCl} + \tfrac{1}{2} V_{Cd} - \tfrac{1}{2} \bar{V}_{CdCl_2}.$$

For cell II, ΔV is given by a similar expression but with all the signs changed. Owing to a fortuitous cancelation, $-C\Delta V/1000$ amounts to only 0.0001 in the measured transport number at $0.1N$ for 15° and 25°, and is negligible for other temperatures and for lower concentrations; it has therefore been included in the solvent correction[5] in the fourth column of the tables. As was the case with potassium chloride, it was found impossible at 45° to determine anion transport numbers, since the measured value of t_- was found to vary with indicator ion concentration in a manner analogous to that shown in Fig. 2 of reference 1.

Figure 1 shows the plots of the Longsworth function $t_+^{\circ\prime}$ computed from the last column of Table I; the curve for 25° includes the data obtained by Longsworth[6] for this temperature; the solid black circle indicates that Longsworth's value and ours cannot be distinguished on the

[4] *International Critical Tables*, Vol. 3, p. 79.

[5] For a discussion of these corrections, see D. J. MacInnes and L. G. Longsworth, Chem. Rev. **11**, 171 (1932); also reference 1.

[6] L. G. Longsworth, J. Am. Chem. Soc. **54**, 2741 (1932).

TABLE II. t_+ for sodium chloride solutions as a function of temperature and concentration.

C	15°	25°	35°	45°
0	0.3929	0.3962	0.4002	0.4039
0.0005	.3918	.3951	.3992	.4028
.001	.3914	.3947	.3987	.4023
.002	.3908	.3941	.3981	.4018
.005	.3897	.3930	.3970	.4008
.01	.3885	.3918	.3958	.3996
.02	.3870	.3903	.3943	.3982
.05	.3846	.3878	.3919	.3957
.07	.3837	.3869	.3909	.3947
.10	.3820	.3853	.3892	.3932

plot. Here $t_+^{o\prime}$ is given by

$$t_+^{o\prime}=(t_+\cdot\Lambda'+\sigma\sqrt{C})/(\Lambda'+2\sigma\sqrt{C}),$$

where $\Lambda'=\Lambda_0-(\vartheta\Lambda_0+2\sigma)\sqrt{C}$, Λ_0 is the equivalent conductance at infinite dilution, and ϑ and σ have their theoretical values (see Table III of reference 2). It is evident that while the plots are linear in concentration for the more dilute range and thus permit a satisfactory extrapolation to infinite dilution, there are definite deviations from linearity for the higher concentrations. The slopes of the linear parts of the curves are moreover much greater than for potassium chloride and are almost independent of temperature, *viz.*, 0.084, 0.082, 0.082 and 0.085 for 15, 25, 35 and 45°, respectively. It is also evident that in distinction from potassium chloride, sodium chloride shows a normal variation of transference number with temperature, i.e., the transference number for a given concentration approaches one-half with rising temperature.

A discussion of the correlation of the transference data with the conductance for the two salts is reserved for the accompanying paper;[2] it is sufficient to say here that the results for sodium chloride are entirely consistent with those previously reported for potassium chloride and with the results of the conductance measurements. Table II gives for round concentrations values of t_+ corresponding to the smooth curves of Fig. 1.

In conclusion we wish to express our thanks to Mr. A. G. Keenan for his assistance in some of the measurements.

FEBRUARY, 1942 JOURNAL OF CHEMICAL PHYSICS VOLUME 10

The Conductance and Ionic Mobilities for Aqueous Solutions of Potassium and Sodium Chloride at Temperatures from 15° to 45°C

H. E. GUNNING AND A. R. GORDON
Chemistry Department, University of Toronto, Toronto, Canada

(Received November 18, 1941)

The conductance of aqueous solutions of potassium and sodium chloride has been determined at 15, 25, 35 and 45°C for concentrations from 0.0005N to 0.01N by a modified direct-current method of high precision. At 15° and 25°, the results are in highly satisfactory agreement with the best of the existing data obtained by the a.c. bridge method. For all temperatures, the conductance can be represented within a few hundredths of a percent by the extended Onsager-Shedlovsky equation. A calculation of the mobility of chloride ion from the conductance and the transference numbers obtained in this laboratory shows that for all temperatures the Kohlrausch rule of independent ionic mobilities is obeyed at infinite dilution within the apparent limit of error of the measurements—0.02 to 0.03 percent. The conductance and ionic mobilities for round values of the concentration, and the temperature coefficients of the ionic mobilities at infinite dilution are tabulated.

THE work reported in this paper was undertaken primarily to provide conductance data for use in conjunction with transference numbers determined in this laboratory.[1,2] In modern theories of electrolytes, it is the ionic mobilities that play the leading rôle, and while there has been accumulated in recent years a great mass of accurate information for 25°C, precise values for temperatures less than 25° are still rather sparse and for temperatures greater than 25° are practically non-existent.

[1] R. W. Allgood, D. J. Le Roy, and A. R. Gordon, J. Chem. Phys. **8**, 418 (1940).
[2] R. W. Allgood and A. R. Gordon, J. Chem. Phys. **10**, 124 (1942).

A second purpose of this work was to investigate the use of the direct-current method of determining electrolytic conductance. While this method has been known since the time of Kohlrausch, it has never been considered a serious rival to the a.c. bridge, particularly since the development of the bridge to its present perfection. Newberry[3] and Eastman[4] made careful investigations of the possibilities of the d.c. method but only for relatively concentrated solutions. Brönsted and Nielsen[5] used it for solutions as dilute as $0.002N$ and obtained in most cases agreement with the a.c. data within one- or two-tenths of a percent. Recently, Andrews and Martin[6] studied with it the conductance of potassium chloride solutions down to $0.0005N$; their technique, however, is open to criticism and their results are of doubtful accuracy according to modern standards (see below).

For all its apparent simplicity, the reason for the comparative neglect of the d.c. method is not hard to find. Essentially, what must be determined is the difference in potential between two points in a liquid conductor through which a known current is passing, and such a difference can only be measured by using some form of reversible electrode. If the electrodes also serve as the means by which the current enters and leaves the solution, they must be non-polarizable —a condition difficult if not impossible to fulfil in practice. On the other hand, if the electrodes serve merely as probes between which the potential difference is measured, they should (theoretically at any rate) be points, since if they are of appreciable size, there will be a sensible ohmic drop across each of them, and the measured P.D. will not bear any direct relation to the true resistance of the conductor. This becomes at once apparent in practice, since the apparent resistance of the conductor, determined from voltage-current measurements, will be found to vary with the current.

After numerous trials, the cell described below has proven satisfactory, at any rate for the concentrations studied here. It is shown in plan

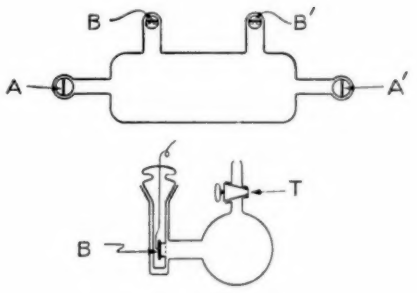

FIG. 1.

and cross section in Fig. 1. A and A' are the electrodes through which the current enters and leaves the solution, B and B' are the probes connected to the potentiometer; all four electrodes are mounted in ground glass joints, and their positions are accurately fixed in the cell by fine lines etched on the male and female parts of the joints. The large center section of the cell is approximately 5 cm in diameter, while B and B' are 10 cm apart. The detail of the probe electrodes is shown in the cross section. B is a disk of platinum 8 mm in diameter and 1.5 mm thick, mounted vertically and at right angles to the plane of the paper in the male part of the joint; the whole of the outer platinum surface is covered with fused glass except for a vertical slit 1 mm in width and 6 mm high; this narrow strip of platinum, after being silver-plated and chloridized after the method of Brown and MacInnes[7] serves as the probe electrode. This design possesses several obvious advantages: its position is rigidly fixed in the cell; its area and rigidity ensure reproducible potential readings; owing to its narrow width and position in the side arm of the cell, there is a negligibly small ohmic drop from side to side of its active surface; finally, the electrolytic resistance in the galvanometer circuit is not inconveniently great.

The current electrodes A and A' are of heavy platinum foil, silver-plated and dipped in fused silver chloride; they are in deep wells, opening into the narrow collimating tubes which lead to the large central portion of the cell. The cell itself is of Pyrex glass, and after construction was boiled in concentrated hydrochloric acid. The cell, in series with a calibrated 500-ohm

[3] E. Newberry, J. Chem. Soc. **113**, 701 (1918).
[4] E. D. Eastman, J. Am. Chem. Soc. **42**, 1648 (1920).
[5] J. N. Brönsted and R. F. Nielsen, Trans. Faraday Soc. **31**, 1478 (1935).
[6] L. V. Andrews and W. E. Martin, J. Am. Chem. Soc. **60**, 871 (1938).
[7] A. S. Brown and D. J. MacInnes, J. Am. Chem. Soc. **57**, 1356 (1935).

TABLE I.

E_s	E_c	E_s/E_c
0.91985 v	+1.15299 v	0.79784
	−1.15284	
.91985	+1.15291	0.79789
	−1.15281	
.73632	+0.92290	0.79786
	−0.92283	
.44970	+0.56367	0.79786
	−0.56359	
.18431	+0.23105	0.7978_8
	−0.23095	
	Mean	0.79786±0.00002

resistance, is connected to the "constant current" circuit of LeRoy and Gordon.[8] After setting the current, the potential difference across the standard resistance E_s is read, then the potential difference between the probes E_c, the direction of the current through the cell is then reversed, E_c is again measured, and finally (as a check) E_s. By taking the average for a given E_s of the two values of E_c, any static bias potential between the probes is eliminated.

It is obvious that for a given cell, the ratio E_s/E_c should be proportional to the specific conductance of the solution. Just how reproducible this is in practice, and how independent it is of the actual current passing through the solution, may be illustrated by a typical set of readings on a 0.0051996N potassium chloride solution at 35°C (Table I). All measurements of potential difference were determined on a calibrated Leeds and Northrup Type K_2 potentiometer by means of a galvanometer of sensitivity 2×10^{-10} amp./mm scale deflection.

Since with the most dilute solutions studied here, the solvent conductance may be as great as 2 percent of the observed specific conductance of the solution, the former quantity must be determined to 0.5 percent if the equivalent conductance is to be known to 0.01 percent. To determine the solvent conductance, a cell similar

[8] D. J. Le Roy and A. R. Gordon, J. Chem. Phys. **6**, 398 (1938).

TABLE II. Potassium chloride.

$10^4 \cdot C$	15°C Λ	$10^4 \cdot C$	25°C Λ
5.1235	119.41 (−1)	5.0382	147.79 (0)
9.8576	118.74 (+2)	10.1948	146.91 (+1)
21.835	117.65 (+2)	19.442	145.84 (0)
32.758	116.97 (−2)	38.072	144.35 (−2)
48.898	116.11 (0)	47.744	143.73 (−1)
71.938	115.19 (0)	73.215	142.42 (−1)
97.148	114.40 (+1)	100.615	141.27 (+1)
	35°C		45°C
4.9106	177.95 (0)	5.1736	209.33 (0)
10.8290	176.76 (−1)	10.3639	208.05 (+1)
20.465	175.37 (+4)	20.766	206.31 (−2)
33.684	174.07 (−2)	32.670	204.82 (−0)
51.996	172.62 (−1)	46.675	203.43 (0)
75.455	171.17 (+1)	74.584	201.24 (+3)
103.282	169.75 (+2)	98.546	199.75 (+2)

TABLE III. Sodium chloride.

$10^4 \cdot C$	15°C Λ	$10^4 \cdot C$	25°C Λ
3.7551	99.86 (−2)	5.4593	124.44 (+1)
9.1558	99.09 (0)	14.3010	123.24 (+2)
21.697	97.96 (+4)	27.434	122.05 (+3)
33.405	97.30 (−2)	34.974	121.57 (−2)
49.972	96.52 (−2)	48.156	120.79 (−2)
74.105	95.64 (−2)	71.368	119.66 (−1)
99.987	94.85 (+3)	98.243	118.60 (+2)
	35°C		45°C
4.9401	151.47 (−2)	5.1845	179.75 (−2)
9.7942	150.49 (+2)	10.8316	178.46 (0)
20.616	149.10 (−3)	21.023	176.87 (0)
32.966	147.90 (−1)	34.916	175.27 (+5)
50.007	146.64 (0)	49.475	174.08 (−4)
74.013	145.21 (+3)	73.163	172.36 (−2)
98.781	144.03 (0)	100.832	170.73 (0)

to that just described was used but with all electrodes bright platinum; the potential difference between the probes (usually of the order of 50 to 100 volts) was measured by means of a calibrated galvanometer of current sensitivity 10^{-7} amp./scale division in series with a 21.6-megohm resistance; since the characteristics of the galvanometer circuit are known, it is a simple matter to calculate for a given current through the standard resistance, what are the true current through the cell and the potential difference for that current between the probes. The results for solvent conductance obtained in this way are reproducible to better than 0.5 percent. It might be added, that the relatively large volumes of solution and solvent in the cells (approx. 400 cc) are a positive advantage since contamination from the glass on standing in the cells is negligible in the average experiment; for example, a 0.001N

KCl solution left by accident in the cell over night showed an increase in conductance in the morning of only 0.02 percent.

The cells were immersed in an oil bath regulated to ±0.002°, the oil level coming just below tap T, i.e., to the level of the ground glass joints of the electrodes; bath temperature was read on Beckman thermometers which had been set by means of a platinum resistance thermometer with National Bureau of Standards certificate. The cells were calibrated with Jones and Prendergast's 0.01N potassium chloride solution[9] at 25°C, *viz.*, 0.746558 g KCl/kg solution (all weights reduced to vacuum), specific conductance (corrected for conductance of the solvent) 0.00141145. The cells were recalibrated after they had been used at other temperatures, and no significant change in cell factor was observed. The cell factor thus obtained for 25°C was increased by 0.003 percent for 15°, and was decreased by 0.003 percent and 0.006 percent for 35° and 45°, respectively.

The potassium and sodium chloride were prepared as previously described.[1,2] The solutions were made by gravimetric dilution with conductivity water of gravimetrically prepared stock solutions. In converting from mass to volume concentrations, all weights were corrected to vacuum, and the density data in *International Critical Tables*[10] were employed. The conductivity water had a specific conductance at 25°C of 1.0 to 1.5×10^{-6}; see reference 9.

The solution (or conductivity water) after being swept with water-saturated CO_2-free air, was forced from its reservoir into the cell by air pressure with the tap T open; the probe electrodes, which had been standing in a sample of the solution to be used, and the current electrodes were adjusted in position, more solution was forced into the cell until the level stood just above T, and the cell was then placed in the bath and allowed to come to thermal equilibrium; T was then closed.

Tables II and III give the observed values of the equivalent conductance Λ as a function of the concentration C expressed in moles per liter. In correlating conductance data for strong electrolytes, probably the most convenient method is to employ the extended Onsager-Shedlovsky equation[11,12]

$$(\Lambda+2\sigma\sqrt{C})/(1-\vartheta\sqrt{C})=\Lambda'_0 =\Lambda_0+BC+DC\log C \quad (1)$$

where ϑ and σ have their theoretical values (see Table IV), Λ_0 is the conductance at infinite dilution, and B and D are disposable constants.[13] The result of a calculation of Λ by means of Eq. (1) with the values of Λ_0, B and D given in Table IV is indicated by the numbers in brackets after the entries of Tables II and III; these give in hundredths of a reciprocal ohm the difference between the observed value of Λ and that calculated by Eq. (1); if the difference is positive, it means that the calculated value is greater than the observed, e.g., the first entry in Table II

TABLE IV.

	15°	25°	35°	45°
ϑ	0.2249	0.2289	0.2335	0.2387
σ	23.38	30.09	37.60	45.72
Λ_0, KCl	121.09	149.88	180.50	212.49
B, KCl	217.1	153.7	150.2	157.0
D, KCl	76.0	32.1	16.0	6.1
Λ_0, NaCl	101.20	126.48	153.85	182.73
B, NaCl	210.2	107.4	136.9	159.3
D, NaCl	72.7	3.1	2.0	0

TABLE V.

$10^4\cdot C$	0	5	10	20	50	100
			Λ for potassium chloride.			
15°	121.09	119.42	118.74	117.80	116.06	114.33
25°	149.88	147.79	146.95	145.79	143.59	141.30
35°	180.50	177.93	176.89	175.46	172.76	169.92
45°	212.49	209.38	208.13	206.40	203.14	199.69
			Λ for sodium chloride			
15°	101.20	99.63	99.00	98.12	96.49	94.88
25°	126.48	124.54	123.77	122.69	120.67	118.55
35°	153.85	151.43	150.47	149.14	146.64	144.03
45°	182.73	179.79	178.62	177.00	173.96	170.78

[9] Grinnell Jones and M. J. Prendergast, J. Am. Chem. Soc. **59**, 731 (1937).

[10] *International Critical Tables*, Vol. 3, p. 79, 87.

[11] T. Shedlovsky and A. S. Brown, J. Am. Chem. Soc. **56**, 1066 (1934).

[12] T. Shedlovsky, A. S. Brown and D. A. MacInnes, Trans. Electrochem. Soc. **66**, 165 (1934).

[13] In computing the values of ϑ and σ entered in Table IV, e was taken to be 4.802×10^{-10} e.s.u. instead of 4.774×10^{-10} as given in *International Critical Tables* [R. T. Birge, Phys. Rev. **58**, 658 (1940)]. This has the effect of decreasing the Avogadro number by 0.6 percent from the value given in the *Tables*, and of increasing the Boltzmann constant by the same percentage. The dielectric constants employed were those of Wyman [Phys. Rev. **35**, 623 (1930)], while the viscosities were from *International Critical Tables*, Vol. 6, p. 234.

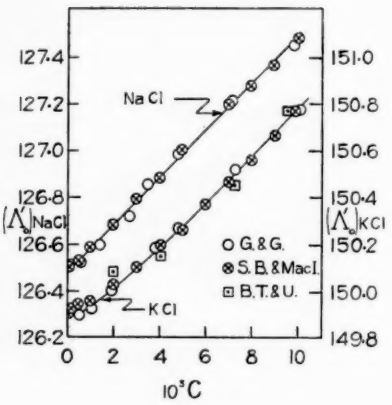

FIG. 2.

indicates 119.40 for the calculated value as compared with 119.41 observed. It is at once apparent that the agreement is excellent—in the majority of cases to 0.02 percent or better. It is, however, of interest to note the steady decrease in importance of the logarithmic term in Eq. (1) with rising temperature. Table V gives Λ, calculated by Eq. (1), for a few round values of the concentration.

Of the a.c. measurements on potassium and sodium chlorides at 25°, by far the most extensive and accurate are those of Shedlovsky, Brown, and MacInnes,[12] which are now generally recognized as definitive. Figure 2 shows Λ'_0 for 25° calculated from our Tables II and III and from their observed values of Λ; these latter have been increased by 0.021 percent to bring them into conformity with Jones and Prendergast's calibration.[14] It is apparent that the agreement is satisfactory, in general within 0.02 or 0.03 reciprocal ohms; this is within the apparent precision of either set of measurements. The figure also shows values of Λ'_0 calculated from Bremner, Thompson, and Utterback's measurements;[15] for consistency, these have also been increased by 0.021 percent to bring them in conformity with Jones and Prendergast's standards. The continuous curves of the figure correspond to Eq. (1) with the constants of Table IV.

Bremner and Thompson[16] have determined for 15°C the conductance of Jones and Bradshaw's 0.01 Demal solution;[14] Eq. (1) predicts $\Lambda = 114.33$ for this solution at this temperature, which may be compared with 114.31—their observed value (after being increased by 0.021 percent). Bremner, Thompson, and Utterback's results for 15° are also in good agreement with Eq. (1); the equation gives for the four solutions in their table 114.44, 115.19, 116.53 and 117.89; their observed values (after correction to Jones and Prendergast's calibration) are 114.48, 115.22, 116.54, and 117.91. Thus a plot of the potassium chloride data for 15°C, similar to Fig. 2, would show Bremner and Thompson's result slightly below our curve, and Bremner, Thompson, and Utterback's slightly above.

We believe the agreement between our measurements and the best existing a.c. data amply demonstrates the possibilities of the d.c. method when properly employed. Moreover, since the errors of the electrical measurements in the two methods are radically different, we believe that the slight uncertainty (of the order of a few hundredths of a percent) still existing in conductance values does not arise from design of cell or circuit, but comes from unavoidable contamination of the solution. On the other hand, Andrews and Martin's[6] d.c. measurements on potassium chloride solutions at 25° lead to a roughly constant value of 150.8 for Λ'_0; thus their result for their most dilute solution ($0.0005N$) must be in error by half a percent.

[14] Shedlovsky, Brown, and MacInnes' original results are based on Jones and Bradshaw's "Demal" standards [Grinnell Jones and B. C. Bradshaw, J. Am. Chem. Soc. **55**, 1780 (1933)]. That the "Demal" standards are not entirely consistent with the "normal" standards of Jones and Prendergast is evident from the following table.

	"0.01N"	"0.1N"	"0.01D"	"0.1D"
g KCl per kg solution	0.746558	7.43344	0.745263	7.41913
Density (25°C)	0.99754	1.00179	0.99754	1.00178
Moles per liter (KCl = 74.553)	0.0099892	0.099885	0.0099718	0.099692
Specific Cond.	0.00141145	0.0128862	0.00140877	0.0128560
Λ	141.298	129.010	141.275	128.957

Thus in each case, the "Demal" solution, although it is slightly weaker than the corresponding "normal," has the lower equivalent conductance. From Shedlovsky, Brown, and MacInnes' results, $d\Lambda/dC$ is -380 and -68 at $0.01N$ and $0.1N$, respectively; hence Λ for the two "Demal" solutions, to be consistent with the "normal" solutions, should be 141.305 and 129.021, respectively. The discrepancy is thus 0.021 percent at $0.01N$ and 0.050 percent at $0.1N$. Shedlovsky, Brown, and MacInnes' Eq. (7), after being increased by 0.021 percent, predicts $\Lambda = 141.310$ for the 0.01 Demal and $\Lambda = 129.004$ for the 0.1 Demal, results which differ only by 0.003 percent and 0.013 percent from those computed above from the "normal" calibrations.

[15] R. W. Bremner, T. G. Thompson, and C. L. Utterback, J. Am. Chem. Soc. **61**, 1219 (1939).

[16] R. W. Bremner and T. G. Thompson, J. Am. Chem. Soc. **59**, 2372 (1937).

From Table V and the transference data[1,2] one obtains at once values of the ionic mobilities; these are listed for chloride ion in Table VI; those for potassium and sodium ions may be obtained by subtracting the corresponding entries in Tables V and VI. If one remembers that the transference numbers are probably accurate to not much better than a part in three thousand, a glance at the table shows that at infinite dilution the Kohlrausch rule of independent ionic mobility is obeyed for all the temperatures—an excellent check on the self-consistency of all the data. The same is true within the limit of error of the experiments for the whole range of concentrations at 15°, but for the other temperatures, for the higher concentrations, there are definite deviations greater than the apparent precision of the experiments; moreover, chloride ion has the greater mobility with sodium as cation than potassium. This is surprising, since one would have expected that if there were any deviation at all for the concentrations studied here, it would have been in the opposite direction.[17] It is just for 25°, however, that there are the most complete and concordant data for the two salts not only for conductance but for transference, so the effect, slight as it is, would seem to be a real one.

Recently, Owen and Sweeton[18] have reported values of the mobility of chloride ion based on their conductance measurements of hydrochloric acid solutions and on Harned and Dreby's values[19] of the HCl transference numbers; they give 61.2, 76.3, 92.5, and 109.5 as the mobility at infinite dilution for 15°, 25°, 35°, and 45°, respectively. Harned and Dreby's numbers, however, were obtained from a comparison of e.m.f. measurements on cells with and without transference, and are only quoted to three significant figures; hence their values of t_-° and the resulting λ_-°, are at best known only to 0.5 percent; thus their results agree with our Table VI as closely as can be expected.

TABLE VI. Values of λ_- for potassium and sodium chloride.

$10^4 \cdot C$	0	5	10	20	50	100
15°, KCl	61.42	60.58	60.24	59.76	58.89	58.02
15°, NaCl	61.44	60.59	60.25	59.77	58.89	58.02
25°, KCl	76.36	75.31	74.89	74.31	73.19	72.03
25°, NaCl	76.37	75.33	74.91	74.34	73.25	72.10
35°, KCl	92.25	90.96	90.43	89.71	88.33	86.90
35°, NaCl	92.28	90.98	90.48	89.77	88.43	87.02
45°, KCl	108.96	107.39	106.77	105.88	104.22	102.48
45°, NaCl	108.94	107.38	106.77	105.90	104.25	102.54

TABLE VII. Values of $d \ln \lambda^\circ/dT$.

	15°	25°	35°	45°
K_+	0.02235	0.01950	0.01705	0.01500
Na_+	0.02430	0.02185	0.01935	0.01680
Cl_-	0.02345	0.02030	0.01770	0.01565

From Tables V and VI, it is possible to obtain values of $d \ln \lambda^\circ/dT$, the temperature coefficient of the ionic mobility at infinite dilution—quantities which are of interest in the light of modern theories of solutions.[20,21] To effect the differentiation, two different empirical forms were fitted to the values of $\ln \lambda^\circ$ for the four temperatures:

$$\ln \lambda^\circ = -A/T + B + C \log T + DT, \qquad (2)$$

$$\ln \lambda^\circ = A + BT + CT^2 + DT^3. \qquad (3)$$

As might be expected, differentiation of the resulting equations led to values of $d \ln \lambda^\circ/dT$ which differed slightly (by a few units in the fifth decimal place); the results from the two equations for a given temperature were therefore averaged and rounded to the nearest 0.00005; they are recorded in Table VII. For 25°, they correspond to activation energies of transport of 3445, 3860, and 3585 cal. per gram ion for potassium, sodium and chloride ions, respectively.

[17] The table of D. A. MacInnes [J. Frank. Inst. **225**, 661 (1938)] which shows the mobility of chloride ion at 25° as greater at 0.01*N* in potassium chloride than in sodium chloride, is based apparently on Shedlovsky's earlier conductance measurements (J. Am. Chem. Soc. **54**, 1411 (1932)] corrected to Jones and Bradshaw's calibration.

[18] B. B. Owen and F. H. Sweeton, J. Am. Chem. Soc. **63**, 2811 (1941).

[19] H. S. Harned and E. C. Dreby, J. Am. Chem. Soc. **61**, 3113 (1939).

[20] H. S. Taylor, J. Chem. Phys. **6**, 331 (1938).

[21] H. Eyring, J. Chem. Phys. **4**, 283 (1936).

Statistical Thermodynamics of Rubber

FREDERICK T. WALL
Noyes Chemical Laboratory, University of Illinois, Urbana, Illinois
(Received November 29, 1941)

The entropy change for the stretching of rubber is calculated by statistical methods, neglecting intermolecular attractions and deformation of bonds and bond angles. The calculation involves the probability of finding the system with a given distribution of molecular configurations. An equation of state relating the tension, length, and temperature of a rubber band is then derived. Following this a discussion of the applicability and the limitations of the theory is presented.

INTRODUCTION

IT has been proposed that when a piece of unvulcanized rubber is stretched, the forces involved arise principally from straightening the long rubber molecules rather than from intermolecular attractions or from deformation of chemical bonds and bond angles.[1] Assuming free rotation is possible about the various bonds of a long molecule, it is recognized that such a molecule can assume any of a great many configurations when left to itself. It is improbable, however, that a molecule will be found in a straightened condition,* because only a few configurations are compatible with such a condition. By associating the idea of configuration probability with entropy, it becomes possible to calculate some thermodynamic properties of rubber.

Several investigators, including Guth and Mark,[2] Kuhn[3] and Pelzer[4] have contributed to the statistical theory of rubber. Although these workers took cognizance of the statistical nature of the problem, some parts of their treatments require modification. Their procedure consisted essentially of calculating the entropy of a single molecule, then relating the changes taking place in that molecule to the macroscopic behavior of rubber. In the treatment which follows here no attempt will be made to calculate individual molecular entropies, but instead the system will be considered in its entirety. At the same time the macroscopic behavior of the rubber will be related statistically to the individual molecules in a plausible way.

THEORETICAL CALCULATIONS

Let us assume that the piece of rubber we are dealing with has the shape of a cylinder with a cross-sectional area A and a length l_0 in its unstretched condition. When the rubber is at its equilibrium length, the individual molecules will have various shapes and orientations such as are illustrated in Fig. 1. Let x equal the component of the distance between the ends of a given molecule along the direction in which stretching takes place. It is then clear that the probability of a given molecule having a value of x in the range x to $x+dx$ will be given by the normal probability distribution function:

$$p(x)dx=\frac{\beta}{\sqrt{\pi}}\exp(-\beta^2x^2)dx. \qquad (1)$$

In this expression β is a constant depending upon the number of units in the molecule chain and the length of each unit. Equation (1) is valid, of course, only if the chains are uniformly long; for large values of x it is subject to the usual

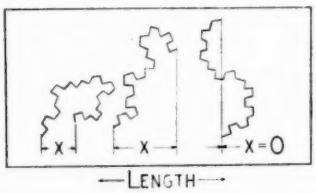

FIG. 1. Plane projections for rubber-like molecules.

[1] See H. Mark, *High Polymers* (Interscience Publishers, New York, 1940), pp. 69–78 for a discussion of this subject.

* By a "straight" molecule we shall mean one for which the line of atoms is as close to a straight line as possible without any distortion of bonds or bond angles.

[2] Guth and Mark, Monats. F. Chem. **65**, 93 (1934); Naturwiss. **25**, 353 (1937).

[3] Kuhn, Kolloid-Zeits. **68**, 2 (1934); **76**, 258 (1936); **87**, 3 (1939).

[4] Pelzer, Monats. F. Chem. **71**, 444 (1938).

limitations encountered in problems of this type.[5] A graph of $p(x)$ plotted against x appears as curve S in Fig. 2.

Now let the macroscopic piece of rubber be stretched from a length l_0 to l. It is then reasonable to suppose that all of the x's will change in the same ratio† as the over-all length, giving rise to the distribution curve S' of Fig. 2. If $\alpha=l/l_0$, then the new distribution will be given by

$$p'(x)dx=\frac{\beta}{\alpha\sqrt{\pi}}\exp(-\beta^2x^2/\alpha^2)dx. \quad (2)$$

If S corresponds to the most probable (equilibrium) distribution, then S' will have a lower probability meaning that the stretched rubber will have a lower entropy. Our problem then resolves itself into calculating the relative probabilities of finding the system in the states S and S'.

Let us divide the x space into a number of cells, the ith of which is located in the neighborhood of x_i and has the size Δx_i. Also let p_i be the probability that a given molecule will be in the ith cell and let s_i be the number of molecules in that cell. Then the probability P of finding the system characterized by $s_1, s_2, s_3, \cdots$ etc., will be given by

$$P=N!\prod_i p_i^{s_i}/s_i! \quad (3)$$

where N is the total number of molecules. The probability P_0 of finding the molecules in their most probable distribution will be

$$P_0=N!\prod_i p_i^{n_i}/n_i!, \quad (4)$$

where $n_i=Np_i$. The ratio of the two probabilities will then be

$$\frac{P}{P_0}=\prod_i\frac{n_i!}{s_i!}p_i^{s_i-n_i}. \quad (5)$$

Introducing Stirling's approximation, $n!=(n/e)^n$, it is found upon simplification that

$$\frac{P}{P_0}=\prod_i\left(\frac{n_i}{s_i}\right)^{s_i} \quad (6)$$

or

$$\ln\frac{P}{P_0}=\sum_i s_i\ln\frac{n_i}{s_i}. \quad (7)$$

But if P and P_0 refer, respectively, to the states S' and S represented in Fig. 2, then it

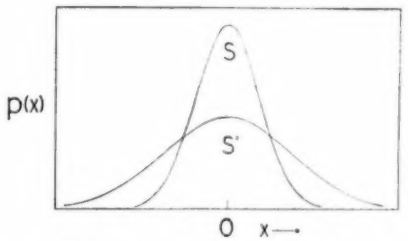

FIG. 2. S—distribution function for unstretched rubber ($\alpha=1$); S'—distribution function for stretched rubber with 100 percent elongation ($\alpha=2$).

follows by Eqs. (1) and (2) that

$$n_i=\frac{N\beta}{\sqrt{\pi}}\exp(-\beta^2x_i^2)\Delta x_i \quad (8)$$

and

$$s_i=\frac{N\beta}{\alpha\sqrt{\pi}}\exp(-\beta^2x_i^2/\alpha^2)\Delta x_i. \quad (9)$$

Hence

$$\frac{n_i}{s_i}=\alpha\exp[-\beta^2x_i^2(\alpha^2-1)/\alpha^2] \quad (10)$$

and

$$\ln\frac{P}{P_0}=\sum_i s_i\ln\alpha-\frac{\beta^2(\alpha^2-1)}{\alpha^2}\sum_i s_ix_i^2. \quad (11)$$

But $\sum_i s_i=N$ and $\sum_i s_ix_i^2=N\overline{x^2}$ where $\overline{x^2}$ is the average value of x^2 for the distribution S'. By use of Eq. (2) it is found that $\overline{x^2}=\alpha^2/2\beta^2$. Therefore

$$\ln\frac{P}{P_0}=N\ln\alpha-N(\alpha^2-1)/2 \quad (12)$$

or

$$P=P_0\alpha^N\exp[-N(\alpha^2-1)/2]. \quad (13)$$

It can readily be established from Eq. (13) that P has its maximum value (equal to P_0) when $\alpha=1$, thus providing a check on the work so far.

The entropy change upon stretching can now

[5] M. L. Huggins has considered the question of the most probable shape of a long chain hydrocarbon. See J. Chem. Phys. **8**, 181 (1940); J. Phys. Chem. **42**, 911 (1938); J. App. Phys. **10**, 700 (1939).

† A few molecules will of course have x values near the maximum possible value. These molecules cannot undergo appreciable extension without distortion of bonds or angles. If the chains are long, such molecules will be few in number, so no appreciable error is introduced by neglecting them. See reference 1 for a discussion of this point.

be calculated immediately. Evidently

$$S-S_0=k\ln\frac{P}{P_0}=Nk\ln\alpha-Nk(\alpha^2-1)/2. \quad (14)$$

Replacing α by l/l_0 and differentiating, it is found that

$$\left(\frac{\partial S}{\partial l}\right)_E=-\frac{Nk}{l_0}\left(\frac{l}{l_0}-\frac{l_0}{l}\right). \quad (15)$$

The partial derivative in (15) is taken to be at constant energy (E) because only free rotation effects have been utilized. But from thermodynamics we know that

$$dE=TdS+\tau dl \quad (16)$$

where τ is the tension in the rubber. Accordingly

$$\tau=-T\left(\frac{\partial S}{\partial l}\right)_E=\frac{NkT}{l_0}\left(\frac{l}{l_0}-\frac{l_0}{l}\right). \quad (17)$$

If ρ is the density of the rubber in its unstretched condition and M the molecular weight, it follows that

$$\tau=\frac{\rho ART}{M}\left(\frac{l}{l_0}-\frac{l_0}{l}\right). \quad (18)$$

From this we deduce the elastic constant or Young's modulus to be

$$\epsilon=\frac{\rho RT(l+l_0)}{Ml}\approx\frac{2\rho RT}{M}. \quad (19)$$

The approximate form of Eq. (19) holds for small relative stretchings, but it is interesting to note that the more exact form does not predict a constant value for the elastic constant. Assuming $\rho=1$ g/cm^3, $T=300$°K and $\epsilon=10^6$ dynes/cm^2, M is calculated to be about 50,000. This value for the molecular weight is not unreasonable for it would imply that the molecules consist of approximately 730 isoprene units, which is of the correct order of magnitude.

DISCUSSION

The principal difference between the present calculation and previous ones lies in the manner of relating the macroscopic stretching to the straightening of the individual molecules. The fact that all of the molecules do not undergo the same displacement is automatically taken care of in the present treatment and no uncertain assumptions relative to this fact are necessary. The final results of the calculations do not involve individual bond lengths or bond angles, but depend only on the molecular weight and on externally measurable physical properties.

The dependence of τ on l as shown in Eq. (18) is the same as in an equation derived by Pelzer,[4] but with a different coefficient. Pelzer showed that this dependence is in better agreement with experiment than is an equation with τ directly proportional to $l-l_0$. The tension is found, as before, to be proportional to the absolute temperature, a point which has been verified experimentally by Meyer and Ferri.[6]

The theory here developed is not limited to stretching of rubber, but can be applied equally well to compression. It will be seen that Eq. (18) has the proper limiting behavior as l approaches zero. A formula which predicts τ to be proportional to $l-l_0$, obviously would fail for compression. It is accordingly recommended that the equation of state for an ideal piece of rubber be taken as $\tau=\text{const.}\ T(l/l_0-l_0/l)$ instead of $\tau=\text{const.}\ T(l-l_0)$, even though the latter is a little simpler.

In view of the assumptions made, the theory cannot be expected to hold well for all polymeric substances, since no account was taken of intermolecular forces or of deformations other than free rotation effects. The fact that rubber has such a large extensibility makes the picture assumed here appear valid when applied to that substance. Other polymeric substances which exhibit extensibility to a much lesser extent are more or less in crystalline form with the various chains bearing ordered relationships to each other. Rubber-like substances are in a class by themselves and cannot be regarded as (crystalline) solids.

[6] Meyer and Ferri, Helv. Chim. Acta **18**, 570 (1935).

Absorption of Polysubstituted Benzene Derivatives*

A. L. SKLAR
Chemical Laboratory, Catholic University of America, Washington, D. C.
(Received October 29, 1941)

The intensification, by nonchromophoric substitutions, of the forbidden, $^1A_{1g} \rightarrow {}^1B_{2u}$, transition in benzene is due, on the one hand, to the unsymmetrical distortion of the ring by the normal vibrations and, on the other hand, to the transition moment produced at the equilibrium position by the migration of charge from the substitution into the ring or vice versa. The latter effect is treated by the method of antisymmetrical molecular orbitals, all calculations being limited to the first order. The rules for combining transition moments due to the various groups in a polysubstituted benzene are calculated. It is shown that, for weak nonchromophoric substitutions, the intensity ratios (except for the less important variation in the normal vibrations) are for C_6H_5X : $oC_6H_4X_2$: $mC_6H_4X_2$: $pC_6H_4X_2$: 1,3,5 $C_6H_3X_3$: 1,2,3 $C_6H_3X_3$: 1,2,4 $C_6H_3X_3$ = 1 : 1 : 1 : 4 : 0 : 0 : 3. It is further shown that if one substitutes benzene by a meta-directing group, M, and by an ortho-para-directing group, P, of the same intensifying power, the ratios for the mono : ortho : meta : para-derivatives should be 1 : 3 : 3 : 0. These ratios are shown to be in good qualitative agreement with experimental data.

INTRODUCTION

THE effect of substitutions upon the intensity of the characteristic absorption bands of a chromophoric nucleus depends both upon the nature of the substituting group and upon the nature of the electronic transition associated with the absorption. The various substituting radicals may be first subdivided into chromophoric and non-chromophoric classes. The former (e.g., $-NO_2$) possesses a resonating system independent of the chromophore to which they are attached and cause new long wave-length electronic bands in the derivative. The effect of such radicals will be considered in a later paper. Here we will be concerned with those groups which in themselves do not have a resonating system either because the group is saturated or because one of the structures has a considerably lower energy than all others. Each class of radicals may now be further broken up into weak and strong types, depending upon the magnitude of the interaction between the radical and the nucleus on which it is substituted. There is, of course, no sharp dividing line between these classes. We shall consider only those radicals whose effect on the electronic states is sufficiently small to be handled as a first-order correction only.

The nature of the electronic transition in the chromophore nucleus also plays an essential role in determining the effect of the substitution. The intensity of a strong band associated with an allowed transition will not be much affected percentually by a weak substitution which does not form an enlarged chromophore. However, the intensity of a weak band whose weakness is due to the geometrical symmetry of the molecular nucleus will in general be greatly enhanced percentually by substitutions which destroy symmetry.

The long wave-length electronic band of benzene at 2600A has been shown to be due to a transition of the latter type,[1] appearing weakly in benzene itself only through the distortion of the ring by unsymmetrical vibrations. The intensification of this band by a monosubstitution has been attributed[2] to the migration of unsaturation electrons[3] into or out from the aromatic nucleus. It was shown that such a migration produces a transition moment in the plane of the ring at right angles to the ring-substituent axis.[2]

This transition moment alone determines the entire intensity of the band only if the nuclei are held fast in their equilibrium position. The interaction of unsymmetrical vibrations, just as in the case of unsubstituted benzene, will cause

* Presented in part before the Physical Section of the American Chemical Society at the April, 1941, meeting at St. Louis, Missouri.

[1] A. L. Sklar, J. Chem. Phys. **5**, 669 (1937); M. Goeppert-Mayer and A. L. Sklar, J. Chem. Phys. **6**, 645 (1938); H. Sponer, G. Nordheim, A. L. Sklar, and E. Teller, J. Chem. Phys. **7**, 207 (1939).
[2] A. L. Sklar, J. Chem. Phys. **7**, 984 (1939).
[3] R. S. Mulliken, J. Chem. Phys. **7**, 123 (1939); **7**, 353 (1939).

additional bands.[4] The occurrence of two such superimposed spectra, one having the appearance of an allowed transition (migration moment) and one that of a forbidden transition (vibration moment) has recently been discussed for the case of monochlorobenzene.[5]

From a chemical point of view one can separate the various substitutions into two classes,[6] meta-directing (e.g., NO_2, COOH) and ortho-para-directing (e.g., CH_3, Cl, OH, NH_2). It has been shown[7] that (except for a few unimportant cases) the ortho-para-directing groups send charge into the benzene ring whereas the meta-directing groups attract charge from the ring. One must accordingly consider separately the transition moment caused by ortho-para-(P) and meta-(M) directing groups.

In the following we will consider the combined effects of several groups in various positions upon the intensity of the 2600A band of benzene.

INTENSITIES IN $C_6H_{6-n}P_n$

Group Theoretical Discussion

The combined effect of a number of identical weak non-chromophoric substitutions (P or M) can be most quickly seen from a group theoretical point of view. The 2600A band of benzene (D_{6h} group) has been shown[1] to be a ${}^1A_{1g} \rightarrow {}^1B_{2u}$ transition. The coordinate perpendicular to the plane of the ring[2] transforms like A_{2u} while the two coordinates in the plane (x, y) transform like the degenerate representation E^-_u. Since neither $A_{1g}A_{2u}B_{2u}(=B_{1g})$ nor $A_{1g}E^-_uB_{2u}(=E^+_g)$ contain A_{1g} the transition in benzene is forbidden. Now it is clear that a perturbation symmetrical to a reflection in the plane of the ring cannot give a transition moment in the Z direction since both the ground and excited state contain the same number of P_Z electrons and no others. Since the induction effect,[8] which is the only perturbation in the plane molecule in its equilibrium position not necessarily symmetrical to a reflection in the plane, has only a negligible

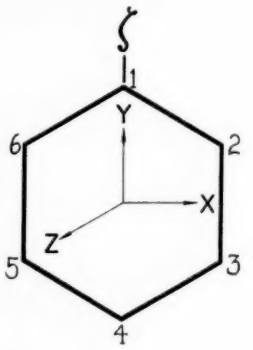

FIG. 1. Orientation of coordinate system in a monosubstituted benzene and notation for positions of substitution.

effect[2] on the intensity we need consider only the transition moment in the plane of the ring. Now in order to have a first order transition moment in the plane of the ring it is both necessary and sufficient that the perturbation either mix an E^+_g component into the ground (A_{1g}) state or an E^-_u component into the excited (B_{2u}) state. Now both of these admixtures can be brought about only by a perturbation which transforms like E^+_g. If we now consider any perturbation, say that of a single substitution which has only axial symmetry, as expanded into a series in the normal coordinates of D_{6h} symmetry, it is clear that only the E^+_g term can affect the transition moment. Now a perturbation of symmetry E^+_g transforms under rotations in the plane like $e^{2i\varphi}$. Since the transition moment is proportional, in the first order, to the perturbation, the relative intensity of

$$C_6H_5P_2 : o\text{-}C_6H_4P_2 : m\text{-}C_6H_4P_2 : p\text{-}C_6H_4P_2$$

will be

$$1 : \left|1+\exp\left(2i\frac{\pi}{3}\right)\right|^2 : \left|1+\exp\left(4i\frac{\pi}{3}\right)\right|^2 : \left|1+\exp\left(6i\frac{\pi}{3}\right)\right|^2 \quad \text{or} \quad 1:1:1:4.$$

That is, one can find the combined action of two or more identical weak non-chromophoric substituents by adding the perturbations as vectors whose angular displacement is twice as great as that of the substitutions.

Non-Group Theoretical

The above results may also be obtained by a less general argument which, however has the compensating merit of being able to yield more

[4] G. Herzberg and E. Teller, Zeits. f. physik. Chemie **B21**, 410 (1933).
[5] H. Sponer and S. A. Wollman, Phys. Rev. **57**, 1078 (1941).
[6] E. Emmet Reid, *College Organic Chemistry* (D. Van Nostrand), p. 498.
[7] G. W. Wheland and L. Pauling, J. Am. Chem. Soc., **57**, 2086 (1935).
[8] E. Hückel, Zeits. f. Physik **72**, 310 (1931).

detailed information such as the difference between the effect of an ortho-para-directing group and that of a meta-directing group. Group theory can only tell us that the transition moments for both types of substitutions will be collinear,* but not whether they will reinforce or interfere.

We will first treat the case of two identical ortho-para-directing (P) substitutions whose relative orientation is either ortho, meta, or para. It is known[7] that such substituents send charge into the ring. The effect of a single P group on the intensity of absorption has been treated in a previous paper[2] in the following manner. One writes a molecular orbital including not only the six P_z (unsaturation) electrons in the ring but also a pair of P_z electrons on the substitution. The atomic orbitals for the six P_z ring electrons are the same as in unsubstituted benzene while the atomic orbitals for the pair of electrons on the radical are linear combinations of radical functions and benzene orbitals.

If one writes $K(\nu)$ for the P_z atomic function of the kth carbon atom in the ring, the benzene orbitals may be written in the following real form:

$$\left.\begin{aligned}\varphi_o(\nu)&=\frac{1}{\sqrt{6}}\sum_k K(\nu),\\ \varphi_l(\nu)&=\frac{1}{\sqrt{3}}\sum_k \cos\left(\frac{2\pi}{6}lk\right)\cdot K(\nu)\\ \varphi_{-l}(\nu)&=\frac{1}{\sqrt{3}}\sum_k \sin\left(\frac{2\pi}{6}lk\right)\cdot K(\nu)\end{aligned}\right\} l=1,2, \quad (1)$$

$$\varphi_3(\nu)=\frac{1}{\sqrt{6}}\sum_k (-1)^k K(\nu),$$

where $k=0, 1, 2, \cdots, 5$.

The orbitals for the pair of radical electrons on a substituent attached to carbon atom zero is then:

$$\psi(\nu)=\sum_{j=1}^{3} a_j\varphi_j(\nu)+b\zeta(\nu) \quad (2)$$

where ζ is the atomic orbital of the radical and $\lambda_j=a_j/b$ is determined by minimizing the energy.[2] In Eq. (2) the summation runs over the positive values of j only since ζ and φ_{-j} are, respectively, even and odd with respect to a rotation by π about the ring-radical axes and hence do not interact.

The antisymmetrized molecular orbitals for the ground, Ψ_0 and excited state, Ψ', corresponding to the 2600A band[1] become,[9] after neglecting terms containing squares of λ_j:

$$\begin{aligned}\Psi_0&=(8!\mu_0)^{-\frac{1}{2}}\sum_P(-1)^P P\varphi_0(1)\varphi_0(2)\varphi_1(3)\varphi_1(4)\varphi_{-1}(5)\varphi_{-1}(6)\\ &\qquad\times\{\zeta(7)\zeta(8)+\textstyle\sum_j\lambda_j[\varphi_j(7)\zeta(8)+\zeta(7)\varphi_j(8)]\}\chi_0,\\ \Psi'&=(8!2\mu')^{-\frac{1}{2}}\sum_P(-1)^P P\varphi_0(1)\varphi_0(2)[\varphi_1(3)\varphi_1(4)\varphi_{-1}(5)\varphi_2(6)+\varphi_{-1}(3)\varphi_{-1}(4)\varphi_1(5)\varphi_{-2}(6)]\\ &\qquad\times\{\zeta(7)\zeta(8)+\textstyle\sum_j\lambda_j[\varphi_j(7)\zeta(8)+\zeta(7)\varphi_j(8)]\}\chi',\end{aligned} \quad (3)$$

where μ is the normalization factor and the spin functions χ are:

$$\chi_0=\alpha_1\beta_2\alpha_3\beta_4\alpha_5\beta_6\alpha_7\beta_8,$$
$$\chi'=\alpha_1\beta_2\alpha_3\beta_4\frac{1}{\sqrt{2}}(\alpha_5\beta_6-\beta_5\alpha_6)\alpha_7\beta_8.$$

The transition moment, $e\int\Psi_0\mathbf{x}\Psi'd\tau$, may then be evaluated directly, yielding the oscillator strength, f.[2,10]

* It is easily seen that the transition moment induced in the $A_{1g}\rightarrow B_{2u}$ transition by a monosubstitution, whether ortho-para- or meta-directing, is along the X axis (cf. Fig. 1). This follows from the fact that both the reflection in the plane (σ_h) and the rotation by π about the Y axis (C'_2) are symmetry operations of the substituted molecule. The former operation shows that there is no component of the transition moment along the Z axis since

$$\sigma_h\times[A_{1g}ZB_{2u}]=-[A_{1g}ZB_{2u}].$$

The Y component is likewise zero since $C'_2\times(A_{1g}YB_{2u})=-(A_{1g}YB_{2u})$. One can accordingly say that the transition moment is along the X axis for any type of group S; one cannot, however, say in this manner whether both types of group will give a moment in the positive direction.

[9] In the previous paper (reference 2) the minus sign in Eq. (9) should be a plus sign.

[10] R. S. Mulliken, J. Chem. Phys. **7**, 14 (1939).

If ζ is the atomic orbital of a radial attached to carbon atom $k=0$ and ξ that of a second radical oriented either ortho, meta, or para with respect to the first, one can write one-electron functions for the P_z electrons of the two substituents.

$$\psi(\nu)=\sum_j a_j\varphi_j(\nu)+b\zeta(\nu), \quad j=1, 2, 3,$$
$$\bar{\psi}(\nu)=\sum_j \bar{a}_j\varphi_j(\nu)+\bar{b}\xi(\nu), \quad j=\pm1, \pm2, 3. \tag{2'}$$

If one writes the variation function for $\bar{\psi}(\nu)$ as a linear combination of φ_j, the summation runs over negative as well as positive values of j, since the ring-radical axis to ξ is not a symmetry axis for the degenerate φ_j's. It is, however, no loss of generality to write the function $\bar{\psi}(\nu)$ in terms of the rotated orbitals, $\bar{\varphi}_j$, which do have the ring-ξ radical axis as a symmetry axis, since the $\varphi_{\pm j}$ are linear combinations of the $\bar{\varphi}_{\pm j}$. In this case the summation runs only over positive values of j, as in the case of $\psi_j(\nu)$, and the coefficients a_j are exactly the same in $\bar{\psi}$ as in ψ if the substitutions are identical. Hence:

$$\bar{\psi}(\nu)=\sum_j a_j\bar{\varphi}_j(\nu)+b\xi(\nu), \quad j=1, 2, 3. \tag{2''}$$

One can now form the molecular orbitals [3'] for the six ring and two pairs of radical electrons, again neglecting higher powers of λ.

$$\begin{aligned}\Psi_0&=[10!\mu_0]^{-\frac{1}{2}}\sum_P(-1)^P P\varphi_0(1)\varphi_0(2)\varphi_1(3)\varphi_1(4)\varphi_{-1}(5)\varphi_{-1}(6)\{\zeta(7)\zeta(8)\xi(9)\xi(10)\\&\quad+\sum_j\lambda_j[\zeta(7)\varphi_j(8)+\varphi_j(7)\zeta(8)]\xi(9)\xi(10)+\zeta(7)\zeta(8)\sum_j\lambda_j[\xi(9)\bar{\varphi}_j(10)+\bar{\varphi}_j(9)\xi(10)\}\chi_0,\\\Psi'&=[10!2\mu']^{-\frac{1}{2}}\sum_P(-1)^P P\varphi_0(1)\varphi_0(2)\{\varphi_1(3)\varphi_1(4)\varphi_{-1}(5)\varphi_2(6)+\varphi_{-1}(3)\varphi_{-1}(4)\varphi_1(5)\varphi_{-2}(6)\}\\&\quad\times\{\zeta(7)\zeta(8)\xi(9)\xi(10)+\sum_j\lambda_j[\zeta(7)\varphi_j(8)+\varphi_j(7)\zeta(8)]\xi(9)\xi(10)\\&\quad+\zeta(7)\zeta(8)\sum_j\bar{\lambda}_j[\xi(9)\bar{\varphi}_j(10)+\bar{\varphi}_j(9)\xi(10)]\}\chi',\end{aligned} \tag{3'}$$

where $\varphi_{\pm j}$ and $\bar{\varphi}_{\pm j}$ are the benzene orbitals, and the spin functions χ_0, χ' are the product of $\alpha_9\beta_{10}$ and the corresponding χ_0, χ' of Eq. (3).

One can now proceed to form the transition moment

$$\mathbf{M}=e\int\Psi_0\mathbf{r}\Psi'd\tau,$$

which may be done in two parts. Let us first form the moment $\mathbf{M}_\zeta$ which is obtained by deleting from Eqs. (3') the summation over j which has $\zeta(j)\zeta(j+1)$ as a factor;[11] and separately form $\mathbf{M}_\xi$ which is similarly obtained by deleting the summation over j having $\xi(j)\xi(j+1)$ as a factor. Since the overlap function $\int\zeta(\nu)\xi(\nu)d\tau$ is completely negligible and since the unperturbed transition is forbidden we may write $\mathbf{M}=\mathbf{M}_\zeta+\mathbf{M}_\xi$.

Before considering separately the vectors $\mathbf{M}_\zeta$ and $\mathbf{M}_\xi$ it is first necessary to notice the behavior of Ψ_0 and Ψ', Eqs. (3'), under symmetry operations. Each of the functions $\varphi_{\pm j}(\nu)$, $\zeta(\nu)$, and $\xi(\nu)$ are P_z orbitals and hence change sign under a reflection in the plane of the ring (σ_h). Ψ_0 and Ψ', being homogeneous functions of an even degree in $\varphi_{\pm j}(\nu)$, $\zeta(\nu)$, and $\xi(\nu)$, are both symmetrical to σ_h. It is accordingly clear that both $\mathbf{M}_\zeta$ and $\mathbf{M}_\xi$ contain no component along the Z axis.

Let us consider, for the moment, only $\mathbf{M}_\zeta$ which is formed by deleting from Eqs. (3') those terms containing $\zeta(j)\zeta(j+1)$ as factor of a sum. Both Ψ_0 and Ψ' then contain as a factor $\xi(l)\xi(l+1)$ which does not affect the transition moment $\mathbf{M}_\zeta$. Now the $\varphi_{+j}(\nu)$ and $\zeta(\nu)$ are even with respect to a rotation by π about the Y axis (C'_2), whereas the $\varphi_{-j}(\nu)$ are odd with respect to C'_2, which is a symmetry operation of the deleted Ψ's without the inactive factor $[\xi(j)\xi(j+1)]$. Ψ_0, being homogeneous of the second degree in φ_{-j}, is symmetrical with respect to C'_2. Ψ', however, contains the φ_{-j} only singly or as triple products and is accordingly antisymmetrical with respect to C'_2. It follows, then, that $\mathbf{M}_\zeta$ contains no component along the Y axis. Accordingly, $\mathbf{M}_\zeta$ is parallel to the X axis. Whether it is directed along the positive or

[11] The wave function so obtained is one in which the substituent ζ sends an electron into the ring while the substituent ξ keeps its P_z electrons to itself. The latter, therefore, do not influence the moment $\mathbf{M}_\zeta$, which comes out the same as if ζ had been the only substituent.

negative X axis depends[12] on the arbitrary choice of the sign of the $\varphi_{\pm j}(\nu)$ in Eq. (1).

Let us now consider $\mathbf{M}_\xi$ which is obtained by deleting in Eq. (3′) the terms containing the factor $\xi(j)\xi(j+1)$ in front of a summation over j. The moment $\mathbf{M}_\xi$ is complicated only by the occurrence of both $\varphi_j(\nu)$ and $\bar{\varphi}_j(\nu)$ functions; the φ_j and $\bar{\varphi}_j$ differing in that k is counted from the carbon atom joined to ζ and ξ, respectively. The moment $\mathbf{M}_\xi$ is, however, easily obtained if one expresses the $\varphi_{\pm j}(\nu)$ in terms of the $\bar{\varphi}_{\pm j}(\nu)$. If one introduces the complex $\phi_{\pm j}$

$$\varphi_j=\frac{1}{\sqrt{2}}(\phi_j+\phi_{-j}),\quad \varphi_{-j}=\frac{-i}{\sqrt{2}}(\phi_j-\phi_{-j}),\qquad (4)$$

the transformation is easily made since

$$\bar{\phi}_{\pm j}(\nu)=\exp\left[i(\pm j)(\zeta,\xi)\right]\cdot\phi_{\pm j},\qquad (5)$$

where (ζ,ξ) is the angle between the radius vectors from the center of the benzene ring to ζ and ξ. It is thus easily checked that[13]

$$\Psi_0=\bar{\Psi}_0\quad\text{and}\quad\Psi'=\bar{\Psi}'\exp\left[3i(\zeta,\xi)\right],\qquad (6)$$

where the Ψ's are the $\mathbf{\Psi}$'s without the terms in λ; that is, without migration. The moment $\mathbf{M}_\xi$, then, differs from $\mathbf{M}_\zeta$ in only two respects. First it has a factor $\exp\left[3i(\zeta,\xi)\right]$ and second $\bar{\varphi}_{\pm j}$ functions appear uniformly instead of $\varphi_{\pm j}$. The latter causes the vector moment $\mathbf{M}_\xi$ to be turned through an angle (ζ,ξ) with respect to $\mathbf{M}_\zeta$ and the former causes it to be reversed every sixty degrees, that is, to be reversed in sign for ortho- and para- but not for meta-orientated groups. Since the intensity depends on the square of the vector sum of the moments the intensity ratios for $C_6H_5P : C_6H_4P_2 : m$-$C_6H_4P_2 : p$-$C_6H_4P_2$ is 1 : 1 : 1 : 4, in agreement with the result obtained group theoretically. One can in this way also form intensity ratios for polysubstituted products, $C_6H_{6-n}P_n$. If the substituted radicals are not all the same, that is in $C_6H_{6-m-n}P_nP_m'$, the ratios will differ from the above but are easily obtained by adding unequal vectors whose lengths may be estimated from C_6H_5P and C_6H_5P', as will be discussed later. These ratios will be discussed and compared with experimental data in a later section.

INTENSITIES IN $C_6H_{6-n}M_n$

It is immediately clear from a group theoretical point of view that the relative intensity ratios for $C_6H_{6-n}M_n$ are the same as for $C_6H_{6-n}P_n$ since the arguments depended only on the symmetry and not upon the nature of the interaction. The general theory, however, does not tell us how to combine moments due to ortho-para-directing groups with those due to meta-directing ones. In order to find the effect of a meta-directing group (M) let us consider an M-monosubstituted benzene. We cannot use the orbitals of Eq. (3) since they consider only migration into the benzene ring and we are now concerned with migration of charge out from the ring into the radical.[7] One can form an appropriate variation function which permits migration out from the ring by replacing the benzene orbitals in the function for unsubstituted benzene by linear combinations[14] of benzene functions and radical function, that is,

$$\phi_j=\varphi_j+\lambda_j\zeta.\qquad (7)$$

The variation function for the ground and excited state after neglecting higher powers of λ becomes

$$\begin{aligned}\Xi_0&=[6!\mu_0]^{-\frac{1}{2}}\sum_P(-1)^P P\{\varphi_0(1)\varphi_0(2)\varphi_1(3)\varphi_1(4)\varphi_{-1}(5)\varphi_{-1}(6)+\lambda_0(\varphi_0(1)\zeta(2)+\zeta(1)\varphi_0(2))\\&\quad\times\varphi_1(3)\varphi_1(4)\varphi_{-1}(5)\varphi_{-1}(6)+\lambda_1\varphi_0(1)\varphi_0(2)(\varphi_1(3)\zeta(4)+\zeta(3)\varphi_1(4))\varphi_{-1}(5)\varphi_{-1}(6)\}\chi_0,\\\Xi'&=[6!2\mu']^{-\frac{1}{2}}\sum_P(-1)^P P\{(\varphi_0(1)\varphi_0(2)+\lambda_0[\varphi_0(1)\zeta(2)+\zeta(1)\varphi_0(2)])(\varphi_1(3)\varphi_1(4)\varphi_{-1}(5)\varphi_2(6)\\&\quad+\varphi_{-1}(3)\varphi_{-1}(4)\varphi_1(5)\varphi_{-2}(6))+\lambda_1\varphi_0(1)\varphi_0(2)([\varphi_1(3)\zeta(4)+\zeta(3)\varphi_1(4)]\varphi_{-1}(5)\varphi_2(6)\\&\quad+\varphi_{-1}(3)\varphi_{-1}(4)\zeta(5)\varphi_{-2}(6))+\lambda_2\varphi_0(1)\varphi_0(2)\varphi_1(3)\varphi_1(4)\varphi_{-1}(5)\zeta(6)\}\chi',\end{aligned}\qquad (8)$$

[12] The choice made in Eq. (1) leads, as can be shown, to an $\mathbf{M}_\zeta$ along the positive X axis, but that is not essential to the argument. Only the relative orientations of the transition moments are important.

[13] Ψ° and Ψ' contain products of ϕ_j's in which the sum of the j values over all factors in the product is zero for Ψ° and three for Ψ'.

[14] ψ is used for a one-electron function; Ψ is a molecular orbital without migration; $\mathbf{\Psi}$ is a molecular orbital with migration into the ring; and $\mathbf{\Xi}$ is used to represent migration out from the ring.

where

$$\chi_0 = \alpha_1\beta_2\alpha_3\beta_4\alpha_5\beta_6,$$

$$\chi' = \alpha_1\beta_2\alpha_3\beta_4\frac{1}{\sqrt{2}}(\alpha_5\beta_6 - \beta_5\alpha_6).$$

One can now calculate the transition moment for the meta-directing substitution

$$\mathbf{M}_m = \int \Xi_0 \mathbf{r} \Xi' d\tau.$$

The result easily follows that the transition moment is in the X direction (Fig. 1) and its magnitude is:

$$\mathbf{M}_m = (2\lambda_1 T_1 + \lambda_1^2) \int \varphi_{-1}\chi\varphi_2 d\tau, \tag{9}$$

where

$$T_j = \int \varphi_j(\nu)\zeta(\nu) d\tau.$$

The transition moment for an ortho-para-directing group has been discussed earlier.[2] Using the orbitals of Eq. (3) one finds that the transition moment M_{op} for an ortho-para-directing group is:[15]

$$\mathbf{M}_{op} = (\lambda_1 T_1 + \lambda_2 T_2 + \lambda_2^2) \int \varphi_{-1}\chi\varphi_2 d\tau - \lambda_3 T_1 \int \varphi_3\chi\varphi_{-2} d\tau. \tag{10}$$

Now it is easily checked that:

$$\int \varphi_1\chi\varphi_{-2} d\tau = -\int \varphi_{-1}\chi\varphi_2 d\tau,$$

and further that $\int \varphi_3\chi\varphi_{-2} d\tau$ has the same sign as $\int \varphi_{-1}\chi\varphi_2 d\tau$. It is accordingly clear that $\mathbf{M}_m$ is exactly antiparallel to $\mathbf{M}_{op}$.

Although this result is important in discussing $C_6H_{6-n-m}P_nM_m$ compounds, it does not in itself imply that $C_6H_{6-n}M_n$ obey the same combination rule as the $C_6H_{6-n}P_n$ compounds. This, however, is clear from the group theoretical discussion and should follow from extending Eqs. (8) to poly-substitutions in the same way that Eqs. (3) were extended.

INTENSITIES IN $C_6H_{6-n-m}P_nM_m$

As previously discussed the transition moment due to an ortho-para-directing radical ζ attached to the carbon atom on the positive Y axis is directed along the X axis. We may summarize the rules for combining transition moments as follows:

I. The transition moment of a second ortho-para-directing radical in the position ξ is rotated from the X axis by an angle $\tau = (\zeta 0 \xi)$ and multiplied by $(-1)^{3\tau/\pi}$.

II. The transition moment of a meta-directing radical is 180° out of phase from the moment of a para-group located at the same place in the ring.

If the monosubstituted benzenes C_6H_5P and C_6H_5M have nearly the same intensity of absorption, then the ratio of intensity of the monosubstituted : ortho-C_6H_4PM : meta-C_6H_4PM : para-C_6H_4PM is, accordingly, 1 : 3 : 3 : 0. The previously discussed ratio of C_6H_5P : o-$C_6H_4P_2$: m-$C_6H_4P_2$: p-$C_6H_4P_2$ was 1 : 1 : 1 : 4 as is also the ratio of C_6H_5M : o-$C_6H_4M_2$: m-$C_6H_4M_2$: p-$C_6H_4M_2$. The transition in the symmetrical trisubstituted benzene $C_6H_3P_3$, as might be expected, is still forbidden by symmetry and the increase in intensity should be zero. The 1 : 2 : 4 $C_6H_3P_3$ should have three times the intensity of the monosubstituted derivatives. In 1 : 2 : 3 $C_6H_3P_3$, although the transition is

[15] Formula (10) is an intermediate formula used in obtaining formula (13) of reference 2.

no longer forbidden by symmetry, the intensification should still be zero since the contributions annul one another in the first order. Before one can compare these statements with empirical data the effect of the normal vibrations, which also contribute to the intensity, must be discussed.

EFFECT OF NORMAL VIBRATIONS

Until now we have, in effect, been considering the transition moments of substituted benzenes which are constrained to their equilibrium position in both the ground and excited electronic states. In addition to the previously discussed transition moment, there is also the moment which arises from the distortion of the molecule by certain unsymmetrical vibrations. In order to decide how to combine the effect of a migration of charge and that of a vibrational distortion we may proceed as follows.

During a vibration the electronic wave functions will be functions of the normal coordinates. Neglecting, for the moment, the migration of charge, one may expand the $\Psi(q)$ into a series in terms of the $\Psi(q_0)$, q_0 being the equilibrium position:

$$\Psi^k(q) = a_0{}^k\Psi^k(q_0) + \sum_j a_j{}^k(q)\Psi^j(q_0). \quad (11)$$

If one now makes a first-order perturbation calculation for $a_j{}^k$ the perturbing potential (4) is clearly a periodic function of the time whose frequency is the same as that of the vibration. We may accordingly write:

$$a_j{}^k(q) = \sum_l \overset{0k}{a}_{jl} \exp(2\pi i \nu_l t), \quad (12)$$

where $\overset{0k}{a}_{jl}$ is independent of q, the summation over l meaning a possible summation over different normal vibrations.

We can include the effect of the migration of charge into Eq. (11) by replacing the $\Psi(q_0)$ by the $\mathbf{\Psi}(q_0)$ given in Eqs. (3′). Equation (11), after neglecting higher powers in λ_s and $\overset{0k}{a}_{jl}$, becomes:

$$\mathbf{\Psi}^k(q) = a_0{}^k[\Psi^k(q_0) + \sum_s \lambda_s \mathbf{\Phi}(q_0)] + \sum_j \sum_l \overset{0k}{a}_{jl} \exp(2\pi i \nu_l t)\Psi^j(q_0). \quad (13)$$

in which the boldface functions are those which express, as before, a migration of charge, and λ_k is independent of t.

We can now form the transition moments

$$\int \mathbf{\Psi}_0(q)\{\mathbf{x}, \mathbf{y}, \mathbf{z}\}\mathbf{\Psi}'(q)d\tau.$$

$$M_{\{x,y,z\}} = \sum_s \lambda_s M^s_{\{x,y,z\}} + \sum_l M^l_{\{x,y,z\}} \exp(2\pi i \nu_e t), \quad (14)$$

in which the quadratic terms in the λ_s and $\overset{0k}{a}_{jl}$ have been neglected. The first sum is the moment due to migration of charge and the second sum is that due to vibrational distortion.

Since the intensity of absorption is proportional to the time average of MM^* we may write:

$$I \sim \overline{MM^*} = [\sum_s \lambda_s M^s_{\{x,y,z\}}]^2 + \sum_l [M^l_{\{x,y,z\}}]^2, \quad (15)$$

the cross products vanish on averaging over time.

It is accordingly clear that, at least to a first order, the intensity of absorption produced by the migration of charge and that caused by vibrations are additive.[16]

The vibrational intensity is not small enough to be neglected in comparison with the intensity produced by weak non-chromophoric substitutions. This can be seen from the comparison of the intensities of benzene and C_6X_6, which have no migrational intensity. In order to obtain quantitative data on the migration intensity it would be necessary to investigate theoretically the effect of substitution on the vibrational intensity, both as regards the mass and the orientation of the substituents. In the absence of a theoretical analysis of the effect of substitution on the vibrational intensity, one might anticipate that the relative orientation of the substitutions does not sensitively affect the vibrational intensity. Which particular vibrations appear in the spectrum should depend on the orientation but the total effect might be expected to depend predominantly on the kind and number of substituents, since the latter determine the amplitudes of vibration. This is,

[16] In expressing the dependence of the electronic wave function on the normal coordinates (Eq. (13)) it was assumed that one could write the total wave function as a product of an electronic and of a vibrational function. It is, however, clear that the inclusion of terms into Eq. (13) which represent the deviation from the product representation will not affect the argument for Eq. (15) in the first order, since the coefficients of these new terms will be periodic functions with vibrational frequencies.

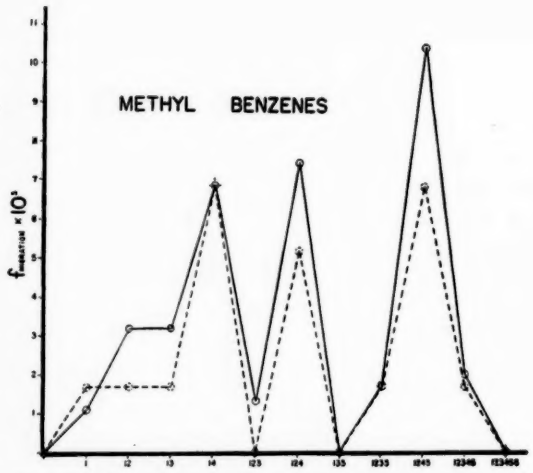

FIG. 2. Migrational oscillator strengths of the methyl benzenes. The experimental f values (reference 17) are plotted against the various positions (cf. Fig. 1) of substitution as a solid line; the theoretical values by a dashed line.

indeed, borne out by the fact that, in both the halogen and methyl benzene series, the 1, 3, 5 trisubstituted benzene is intermediate in intensity to benzene and the hexa-substituted product. In all these cases the symmetry is such that electron migration will not affect the intensity, so that the whole effect is due to vibration. But the symmetry of the vibrations in the 135 trisubstituted compound is lowered, so that more vibrations make the transition allowed than in benzene or the hexa-derivatives. Nonetheless, the intensity of the trisubstituted compounds lies between those of benzene and the hexa-derivatives.

That the vibrational intensity is not the sensitive factor in determining the relative intensities in isomeric substituted benzenes can furthermore be seen by comparing the effects of inserting a methyl group into the para positions in toluene and benzo-nitrile. The total absorption intensity of para-xylene is double that of toluene whereas the total intensity of para-toluo-nitrile is less than that of benzo-nitrile. That *P–P* derivatives are consistently found to follow different intensity rules than *M–P* derivatives, as is shown below, indicates clearly that the qualitative features, at least, are to be sought in the migrational effect on the intensity.

One can either apply the intensity rules for migrational intensity in a qualitative way or one can make a semi-quantitative comparison by estimating the vibrational intensity from symmetrical molecules, where the vibrations alone are responsible for the intensity. The zero-zero transition is forbidden by symmetry for benzene, 1, 3, 5 $C_6H_3X_3$, and for C_6X_6. One can make a crude estimate of the vibrational intensity by plotting the oscillator strengths of these three compounds against molecular weight and interpolating for the other members of the same series. For each substituent **X**, a separate curve is drawn, one for the chlorobenzenes and one for the methylbenzenes. The f values found by this interpolation are given in the tables as "vibrational f_v"; subtracting these f_v's from the total f values gives the "migrational f_m" in the table.

COMPARISON WITH EXPERIMENT

We can first test the intensity rules in a qualitative manner by the total oscillator strength. We must limit our qualitative comparisons to isomeric molecules, that is molecules which differ only in that the substitutions are shuffled.

For the *P–P* disubstituted benzenes, we should expect from the foregoing that the ortho- and meta-derivatives be equally intense and that the para-derivative be considerably more intense than both. That this is indeed so for the dichlorobenzenes and for the xylenes may be seen from Table I and also from Figs. 2 and 3. In *M–P* disubstituted derivatives, on the other hand,

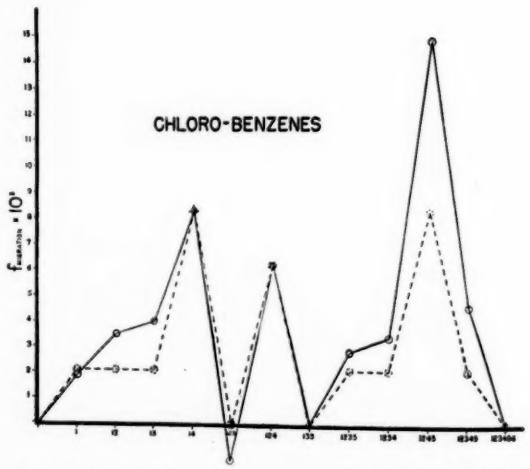

FIG. 3. Migrational oscillator strengths of the chlorobenzenes. The experimental f values (reference 17) are plotted against the various positions (cf. Fig. 1) of substitution as a solid line; the theoretical values by a dashed line.

the para-compound should be very much weaker than the ortho- or meta-isomers; the latter should again be equally intense. This is indeed the case, as is borne out by the chloronitriles, toluonitriles, chloroisonitriles and toluoisonitriles (cf Figs. 4 and 5).

Striking confirmation of the rules is also afforded by the three trisubstituted derivatives. That 1, 3, 5, $C_6H_3X_3$ has a very weak absorption is clear independently of these rules since the electronic transition is forbidden by symmetry. However, the transition in 1, 2, 3, $C_6H_3X_3$ is not forbidden by symmetry but is forbidden, in the first order, by these rules and is indeed found to be of the same order of intensity as the 1, 3, 5 isomer, slightly less in the trichloro series and slightly more in its trimethyl series. This is perhaps the most striking evidence for these rules. The 1, 2, 4 derivative is, of course, quite strong and of the expected intensity.

TABLE I.*

	Experimental $f\times10^3$	$f_v\times10^3$	$f_m\times10^3$	Theoretical estimate $f_m\times10^3$
Benzene	2.7	2.7	(0)	0
Toluene	5.3	4.2	1.1	1.7
O-xylene	8.8	5.6	3.2	1.7
M-xylene	8.8	5.6	3.2	1.7
P-xylene	12.5	5.6	6.9	(6.9)
123 trimethylbenzene	8.4	7.1	1.3	0
124 trimethylbenzene	14.6	7.1	7.5	5.2
135 trimethylbenzene	7.1	7.1	(0)	0
1235 tetramethylbenzene	8.8	7.1	1.7	1.7
1245 tetramethylbenzene	17.6	7.1	10.5	6.9
penta methylbenzene	9.2	7.2	2.0	1.7
hexa methylbenzene	7.3	7.3	(0)	0
chlorobenzene	4.9	3.0	1.9	2.1
O-dichlorobenzene	6.8	3.2	3.5	2.1
M-dichlorobenzene	7.2	3.2	4.0	2.1
P-dichlorobenzene	11.5	3.2	8.3	(8.3)
123 trichlorobenzene	2.1	3.5	−1.4	0
124 trichlorobenzene	9.7	3.5	6.2	6.2
135 trichlorobenzene	3.5	3.5	(0)	0
1235 tetrachlorobenzene	6.3	3.5	2.8	2.1
1234 tetrachlorobenzene	6.9	3.5	3.4	2.1
1245 tetrachlorobenzene	18.3	3.5	14.8	8.3
pentachlorobenzene	8.2	3.6	4.6	2.1
hexachlorobenzene	3.7	3.7	(0)	0

* The experimental data for this table were taken from reference 17.

TABLE II.*

	Experimental $f\times10^3$	$f_v\times10^3$	$f_m\times10^3$	Theoretical estimate $f_m\times10^3$
Benzene	2.4	2.4	(0)	0
Toluene	4.7	3.1	1.6	1.2
O-xylene	5.7	3.9	1.8	1.2
M-xylene	6.0	3.9	2.1	1.2
P-xylene	8.6	3.9	4.7	(4.7)
Chlorobenzene	4.3	2.7	1.6	1.3
O-dichlorobenzene	5.5	2.8	2.6	1.3
M-dichlorobenzene	5.4	2.8	2.6	1.3
P-dichlorobenzene	8.0	2.8	5.2	(5.2)
Benzonitrile	10.4	2.9	7.5	(7.5)
O methyl benzonitrile	21.7	3.7	18.0	11.6
M methyl benzonitrile	18.7	3.7	15.0	11.6
P methyl benzonitrile	9.7	3.7	6.0	2.8
O chloro benzonitrile	20.7	3.0	17.7	11.9
M chloro benzonitrile	15.9	3.0	12.9	11.9
P chloro benzonitrile	8.0	3.0	5.0	2.6
Benzoisonitrile	6.5	2.9	3.6	(3.6)
O methyl benzoisonitrile	20.7	3.7	17.0	6.8
P methyl benzoisonitrile	7.2	3.7	3.5	.7
O chloro benzoisonitrile	10.7	3.0	7.7	7.1
M chloro benzoisonitrile	10.3	3.0	7.3	7.1
P chloro benzoisonitrile	6.4	3.0	3.4	1.2

* The experimental data for this table was taken from reference 18.

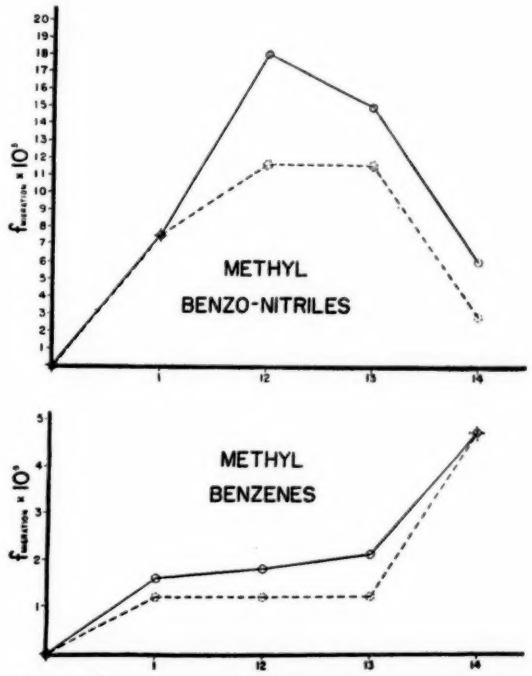

FIG. 4. The migrational oscillator strengths of the methyl benzenes ($C_6H_4P_2$) are contrasted with those of the methyl benzo-nitriles (C_6H_4MP). The experimental values (reference 18) are plotted against the various positions of substitution as a solid line; the theoretical values by a dashed line.

The tetra- and penta-substitution products are also in agreement with the rules but, of course, add nothing new qualitatively.

Table I contains the oscillator strengths of a number of substituted benzene derivatives with weak auxochromes of the type $C_6H_{6-m}P_m$. The most complete series of this type are the methylbenzenes and chlorobenzenes investigated by Conrad-Billroth;[17] the f values calculated from his measurements are given in the first column of Table I. Some scattered measurements on the compounds of this series were also made by Wolf and co-workers[18] and are given in Table II for comparison. The vibrational f_v in the second

[17] H. Conrad-Billroth, Zeits f. physik. Chemie **B19**, 76 (1932); **B29**, 170 (1935).

[18] K. L. Wolf and W. Herold, Zeits f. physik. Chemie **B13**, 201 (1931); K. L. Wolf and O. Strasser, *ibid.* **B21**, 389 (1933).

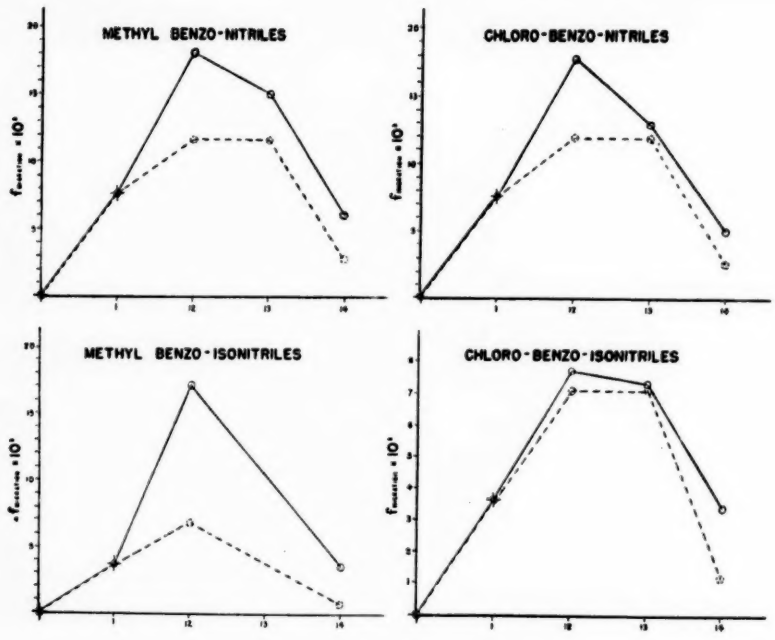

FIG. 5. Oscillator strengths of C_6H_4MP. The experimental values (reference 18) are plotted against the various positions of substitution as a solid line; the theoretical values by a dashed line.

column is obtained, as discussed before, by interpolating between the f's (in column 1) of those compounds which owe their entire intensity to vibration. The experimentally estimated migration effects f_m are the differences between the first and second column, and are plotted as solid lines in Fig. 2 for the various methyl benzenes and in Fig. 3 for the chlorobenzenes. Those points which have been used to calculate the vibrational f_v are marked with a cross. To calculate the theoretical curves in Figs. 2 to 5 one needs the value of the migrational effects for CH_3 and for Cl. This is obtained from the f_m of the para-disubstituted derivative. This compound is selected since it should have the largest f_m and a smaller f_v than the 1245 substituted derivative which is the only other compound having as large a predicted f_m. Half the square root of the f_m of para $C_6H_4P_2$ is taken as a measure of the magnitude of the transition moment induced by the migration of charge from group P.

The experimental oscillator strengths for compounds of the type $C_6H_{6-2}MP$ are given in Table II. Since a complete series of this type is not available, the vibrational f had to be estimated from other series. The mean of the interpolated f_v value for the monomethyl and monochloro derivatives was taken as the f_v for benzonitrile and isonitrile, since the mass of the nitrile group is the mean of the masses of the methyl and chloro groups. The f_v for the disubstitutions was obtained by adding to the f_v of the nitrile the difference between the interpolated f_v of $C_6H_4P_2$ and that of C_6H_5P. The f_m's so obtained are plotted in Fig. 5 as a solid line. The square root of the f_m for C_6H_5M is taken as the transition moment due to M. This moment and the one of the para-directing group obtained previously are combined according to the rules developed and the intensities plotted in Fig. 5 as dashed lines.

The large difference between the effect of an ortho-para-directing group, (P), on the absorption intensity of C_6H_5P as compared with its effect on the intensity of C_6H_5M is brought out in Fig. 4, in which the oscillator strengths of the xylenes, $[C_6H_4 \cdot CH_3 \cdot CH_3]$ are contrasted with those of the methyl benzonitriles, $[C_6H_4 \cdot CH_3 \cdot CN]$.

In conclusion the author would like to express his indebtedness to Professor K. F. Herzfeld for continued inspiration and discussion and also to Sister M. Ann Elizabeth Waters C.S.C. for assistance in computing the experimental oscillator strengths.

Letters to the Editor

Effects of Heat Capacity Lag in Gas Dynamics

ARTHUR KANTROWITZ
National Advisory Committee for Aeronautics, Langley Field, Virginia.
December 8, 1941

RECENT measurements of the velocity and absorption of sound have shown that gases absorb their vibrational heat content exponentially with a measurable relaxation time. The object of this letter is to point out, first, the significance of this for gas dynamics and, secondly, that methods of gas dynamics provide simple and flexible means of measuring heat capacity lag.

In the flow of gases, compressions and expansions occur in which the temperature of the gas changes. It has usually been assumed that these pressure and temperature changes occur reversibly in actual gases (apart from the effects of viscosity, heat conduction, and compression shocks). However, in problems involving the flow of a gas with vibrational heat capacity, one would expect that the vibrational heat energy would lag behind translational energy changes in the gas. This lag would lead to dissipation of energy in the gas in the same way as it produces a high absorption of sound.

Consider the compression at the nose of a total head tube in a uniform stream as an example. Let us first consider the case where the tube is very small, i.e., small enough so that the gas is brought to rest (or more precisely, loses the greatest part of its kinetic energy) in a time short compared with the relaxation time of the gas. In this case the vibrational energy is unchanged during the compression, i.e., effectively the gas has a reduced heat capacity during the compression. This results in an impact pressure *lower* (by several percent for CO_2, for example) than that which would have been obtained in a compression slow enough so that the vibrational energy would not lag appreciably behind the translational energy of the molecules.

In the more general case some of the changes in temperature occur in times comparable with the relaxation time of the gas. An approximate solution of this problem can be found by calculating the excess vibrational energy H in a fluid particle at all times during its passage along a streamline, assuming the flow pattern to be unaffected by the heat capacity lag. In this case H at any point along a streamline can be expressed as an integral involving the time history of the fluid particle up to that point. The change in entropy of the fluid particle can then be found from an integral of a function of H along a streamline. In this way it is, in principle, possible to find the total entropy change and thus the energy dissipation in a general flow problem. For example, the pressure at the nose of an impact tube in the case where the relaxation time is comparable to the time of compression at the nose can be obtained since the energy, entropy, and velocity at the nose are now known.

An apparatus with which one can readily detect these energy dissipations consists of a small chamber with arrangements to permit gas to enter the chamber and escape through a $\frac{1}{8}$-inch diameter faired orifice in a $\frac{1}{2}$-inch plate. A small glass impact tube is placed axially in the center of the mouth of the orifice, and the difference in pressure between the impact tube and the chamber is measured. This pressure difference is nearly zero for gases without vibrational heat capacity. The total head defects anticipated were easily found for air and CO_2 and agreed with expectations from sonic experiments.

Gas dynamical methods appear in principle capable of measuring relaxation times as short as 10^{-8} second. It is intended to develop these methods and to report them in a later paper.

Spectra of Lipoid Fractions from Human Non-Cancerous and Cancerous Tissue

H. S. PENN
Los Angeles, California
December 20, 1941

THE object of this communication is to report on the spectra of fluorescent lipoid fractions obtained from human non-cancerous and cancerous livers, and cancerous tissue. All tissues were treated under identical conditions, and a report of the preparation of the lipoids will be given elsewhere. The fluorescence was excited with the light of a mercury arc. The non-cancerous lipoid fractions showed much weaker fluorescence than did the cancerous fractions under identical experimental conditions. Although the fluorescence spectrum of the non-cancerous fractions lies in the same general region as that of the cancerous fractions we are not yet prepared to say that the two spectra are identical. The strong and easily identifiable fluorescence of the cancerous fraction lies on the long wave-length side of the 4047–4077 pair and with increasing deproteinization

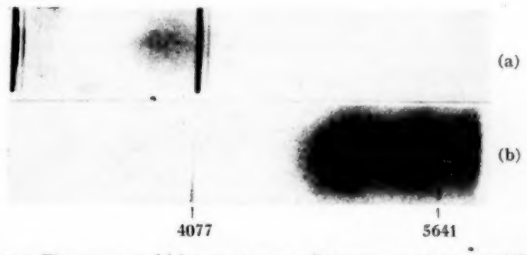

FIG. 1. Fluorescence of (a) non-cancerous, (b) cancerous tissue, partially deproteinized.

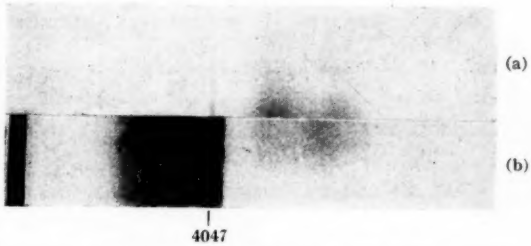

FIG. 2. (a) Fluorescence of methyl cholanthrene. (b) Fluorescence of cancerous tissue, maximum deproteinization.

approaches the characteristic fluorescence spectrum of methyl cholanthrene. The best sample indicates an identity between the fluorescence spectra of methyl cholanthrene and the cancerous fraction. The possibility that many forms of cancer may originate in the metabolic production of methyl cholanthrene or related substances from the bile acids, or perhaps from the sterol or sex hormones of the body, has been mentioned elsewhere. The spectrographic work has been done with the aid of Dr. S. M. Rubens and Professor J. Kaplan of the University of California at Los Angeles.

The Low Frequency Fundamental Band of Ethane at 12μ

RALPH G. OWENS* AND E. F. BARKER
Harrison M. Randall Laboratory of Physics, University of Michigan, Ann Arbor, Michigan
December 29, 1941

IN preparing for a study, now under way, of the infra-red spectra of deuterium bearing ethanes we have re-examined the low frequency fundamental absorption band of C_2H_6. This band was first resolved by Levin and Meyer,[1] with a spectrometer somewhat less effective than the best now available. They showed that it is of the degenerate perpendicular type, consisting of a family of Q branches spaced at intervals of approximately 2.6 cm^{-1}. The significance of this and other details of the ethane spectrum has been discussed more recently by Crawford, Avery, and Linnett.[2]

The pattern of this band as obtained with our present instrument is shown in Fig. 1, and the wave numbers

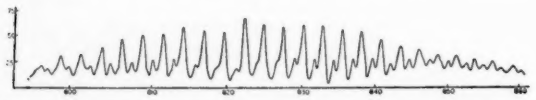

FIG. 1. The 12μ band of ethane; percent absorption *vs.* wave number.

(reduced to vacuum) for the various maxima are listed in Table I. These measurements reveal two features worthy of remark. (1) The spin effect, which slightly accentuates every third line, is clearly revealed. Since the band center must lie one-half interval toward lower frequencies from the strongest line, its position may be definitely fixed. We obtain for it the value 820.82 cm^{-1}. The high frequency side of the band is the more intense because of lower initial K values. (2) Approximately midway between the major peaks a series of minor absorption maxima are observed. These appear to be relatively stronger near both limits of the band, and less intense in the neighborhood of the center, suggesting two subsidiary transitions. They probably arise from the change 1→2 in the same vibrational quantum number for which the transition 0→1 yields the principal band. The first excited state involves an internal angular momentum which, for the upper transitions, may either increase or decrease, with resulting bands at frequencies above and below that of the fundamental. From the present measurements we are not able to determine the centers for these low intensity bands.

TABLE I. Observed line positions in wave numbers reduced to vacuum.

Major peaks	Minor peaks	Major peaks	Minor peaks
859.54	857.72	822.20	
856.70	855.23	819.52	
853.95	852.76	816.79	815.78
851.34	850.08	814.22	812.96
848.59	847.58	811.60	810.35
846.06	844.60	808.94	807.60
843.36	842.06	806.39	805.00
840.75	839.50	803.84	802.36
838.08	836.81	801.24	798.98
835.39	834.12	798.69	797.18
832.67	831.53	796.39	
830.05	829.02		
827.40			
824.76			

* Now at Colorado School of Mines.

[1] A. Levin and C. F. Meyer, J. Opt. Soc. Am. and Rev. Sci. Inst. 16, 137 (1928).
[2] B. L. Crawford, W. H. Avery and J. W. Linnett, J. Chem. Phys. 6, 682 (1938).

Erratum: Chain Length and Chain-Ending Processes in Acetaldehyde Decomposition

(J. Chem. Phys. 7, 1080 (1939))

MILTON BURTON, H. AUSTIN TAYLOR AND THOMAS W. DAVIS
New York University, University Heights, New York, New York
January 3, 1942

In a paper under the above title,[1] the chain lengths in the azomethane-induced decomposition and in the photolysis of acetaldehyde at equal rates of free radical production and equal aldehyde concentrations were calculated from the available data. It has been called to our attention by Professor O. K. Rice that the calculation for the induced decomposition is in error. The chain length per free radical should have the value ~220. Comparison of this value with that for the photolysis given by us as 844 vitiates our conclusions drawn in the paper cited relative to the chain-ending processes and would necessitate a new analysis of the possible reactions involved. It is our understanding that Professor Rice plans to discuss such possibilities in a forthcoming paper.

[1] J. Chem. Phys. 7, 1080 (1939).

Erratum: Ethylene-Ethane and Propylene-Propane Equilibria

(J. Chem. Phys. 10, 78 (1942))

G. B. KISTIAKOWSKY AND A. GORDON NICKLE
Department of Chemistry, Harvard University, Cambridge, Massachusetts

THROUGH an error Dr. Nickle's name was omitted from this Letter to the Editor. The authors should have been listed as above.